DOKUZ EYLÜL UNIVERSITY
GRADUATE SCHOOL OF NATURAL AND APPLIED SCIENCES

ANTIFOULING PERFORMANCES OF ECO-FRIENDLY SECONDARY METABOLITE COCKTAILS FROM MARINE PLANTS

by
Hakan ALYÜRÜK

June, 2012
İZMİR

ANTIFOULING PERFORMANCES OF ECO-FRIENDLY SECONDARY METABOLITE COCKTAILS FROM MARINE PLANTS

A Thesis Submitted to the
Graduate School of Natural and Applied Sciences of Dokuz Eylül University
In Partial Fulfillment of the Requirements for the Degree of Master of Science
in Chemistry Program

by
Hakan ALYÜRÜK

June, 2012
İZMİR

M.Sc THESIS EXAMINATION RESULT FORM

We have read the thesis entitled **"ANTIFOULING PERFORMANCES OF ECO-FRIENDLY SECONDARY METABOLITE COCKTAILS FROM MARINE PLANTS"** completed by **HAKAN ALYÜRÜK** under supervision of **ASSOC.PROF.DR. LEVENT ÇAVAŞ** and we certify that in our opinion it is fully adequate, in scope and in quality, as a thesis for the degree of Master of Science.

Assoc.Prof.Dr. Levent ÇAVAŞ

Supervisor

Prof.Dr. İlgi Kapdan

(Jury Member)

Doç.Dr. Yoldaş SELİ

(Jury Member)

Prof.Dr. Mustafa SABUNCU

Director

Graduate School of Natural and Applied Sciences

ACKNOWLEDGEMENTS

I am very grateful to my supervisor Assoc.Prof.Dr.Levent ÇAVAŞ for his guidance and support. I am thankful to Asst.Prof.Dr.Güleser KALAYCI-DEMİR from Department of Electrical & Electronics Engineering for her helps in video processing and microscope imaging. I thank to The Scientific and Technological Research Council of Turkey for supporting our research group with national research project grant (Grant no: 111T166) and scholarship (TÜBİTAK-BİDEB 2228). I also thank to Moravia Paint and Chemical Industry Trading Limited Company, Istanbul for providing raw materials and biocides for paint preparation. I am also grateful to my family because they have always supported and encouraged me.

Hakan ALYÜRÜK

ANTIFOULING PERFORMANCES OF ECO-FRIENDLY SECONDARY METABOLITE COCKTAILS FROM MARINE PLANTS

ABSTRACT

Attachment of micro and macro marine organisms onto an artificial surface is called as biofouling. Biofouling is a natural process and it can take place on any substrate surface. However, biofouling is a serious problem for the ships. As fouling organisms cover the hulls of the ships, they cause to increase of weight, reduction of speed, limitations in maneuverability, corrosion and high fuel consumption. In order to prevent biofouling, ship's hulls are painted with special marine paints called as antifouling paints. Tributyltin (TBT) based self-polishing copolymer type antifouling paints were successfully used for prevention of fouling; but after their ban, a need for an eco-friendly and effective antifouling paint has been emerged. With respect to above mentioned needs, development of an eco-friendly biocide alternative to booster biocides was aimed based on secondary metabolite cocktails of marine plants both in laboratory and field tests in this thesis. According to results of acute toxicity tests, zosteric acid was not toxic to *A. salina* compared to other compounds tested. However, booster biocides (irgarol, diuron, copper and zinc pyrithione) and extracts of *Zostera noltii* and *Cymodocea nodosa* were decreased survival percentage of *A. salina* more than 50 percent at 185 ppm concentration. In the first field test, the surfaces of test panels were covered by micro-slime layer mostly composed of diatoms. In the second field test, macro-fouling organisms like serpulidae, bryozoans and tube worms were observed on paint free and primer coated test panels. Zosteric acid containing paint was covered by micro-slime layer but it was resistant against macro-fouling organisms for 90 days of test period. In conclusion, zosteric acid could be used in rosin based self-polishing antifouling paints not only solely but also as co-biocide or it could be modified to provide prolonged protection from fouling organisms.

Keywords: acute toxicity, antifouling, diuron, irgarol, zosteric acid.

DENİZ BİTKİLERİNDEN ELDE EDİLEN ÇEVRE DOSTU SEKONDER METABOLİT KOKTEYLLERİNİN ANTİFOULİNG PERFORMANSLARI

ÖZ

Mikro ve makro deniz organizmalarının yapay bir yüzeye tutunmaları olayına biyofouling adı verilir. Biyofouling doğal bir olaydır ve herhangi bir substrat yüzeyinde meydana gelebilir. Fakat biyofouling gemiler için ciddi bir problemdir. Fouling organizmalar gemilerin yüzeyini kapladıkça, ağırlığın artmasına, hızın azalmasına, manevra kabiliyetinin sınırlanmasına, korozyona ve yüksek yakıt sarfiyatına neden olurlar. Biyofouling'i önlemek için, gemilerin karina kısımları antifouling boyalar adı verilen özel deniz boyaları ile boyanır. Tribütil kalay (TBT) tabanlı kendini temizleyen kopolimer (SPC) tip antifouling boyalar, fouling olayının önlenmesi için başarıyla kullanılmıştır; ancak bu boyaların yasaklanmasından sonra çevre dostu ve etkili bir antifouling boya ihtiyacı açığa çıkmıştır. Yukarıda sözü edilen ihtiyaçlar kapsamında, bu tezde hem laboratuar hem saha çalışmalarıyla deniz bitkilerinin sekonder metabolit kokteylleri vasıtasıyla yardımcı biyositlere alternatif bir çevre dostu biyositin geliştirilmesi hedeflenmiştir. Akut toksisite testlerinin sonuçlarına göre, test edilen diğer bileşiklerle karşılaştırıldığında zosterik asitin *A. salina*'ya karşı toksik olmadığı bulunmuştur. Fakat yardımcı biyositler (irgarol, diuron, bakır ve çinko prityon) ve *Z. noltii* ile *C. nodosa* ekstraktları 185 ppm'de *A. salina*'nın hayatta kalma yüzdesini yüzde 50'den daha fazla düşürmüştür. İki sezon boyunca gerçekleştirilen saha çalışmalarında, test panellerinin yüzeyleri genellikle diatomlardan oluşan mikro-film tabakasıyla kaplanmıştır. İkinci saha çalışmasında, boyasız ve astar ile kaplı test panellerinin üzerinde serpulidae, bryozoan ve boru kurtları gibi makro-fouling organizmalar gözlenmiştir. Zosterik asit içeren boya mikro-balçık tabakası ile kaplanmış olmasına rağmen 90 günlik test periyodu boyunca makro-fouling organizmalara karşı dayanıklılığını korumuştur. Sonuç olarak, zosterik asit çam reçinesi tabanlı kendini temizleyen antifouling boyalarda sadece tek başına değil aynı zamanda yardımcı biyosit olarak da kullanılabilir veya fouling organizmalardan daha uzun süreli koruma sağlamak üzere modifiye edilebilir.

Anahtar Kelimeler: akut toksisite, antifouling, diuron, irgarol, zosterik asit.

CONTENTS

Page

CHAPTER ONE
INTRODUCTION

1.1 What is Biofouling?

Biofouling can be defined as attachment of micro and macro marine organisms onto a surface (Clare, 1996; Wahl, 1989). As can be seen from Figure 1.1, it begins with adsorption of organic compounds such as proteins, carbohydrates, lipids etc. to the surface which is also called as conditioning film formation (Abarzua & Jakubowski, 1995; Callow & Fletcher, 1994) and this reversible process is driven by physical forces such as Brownian motion, electrostatic interactions and van der Waals forces (Clare, Rittschof, Gerhart, & Maki, 1992; Yebra, Kiil, & Dam-Johansen, 2004). Conditioning film formation is followed by settlement of bacteria. Settlement starts with adsorption process that is influenced by physical forces. It proceeds with irreversible adherence process due to the covalent bond formation between adhesive extracellular binding polymers secreted from bacteria and adsorbed molecules on the surface (Abarzua & Jakubowski, 1995; Wahl, 1989).

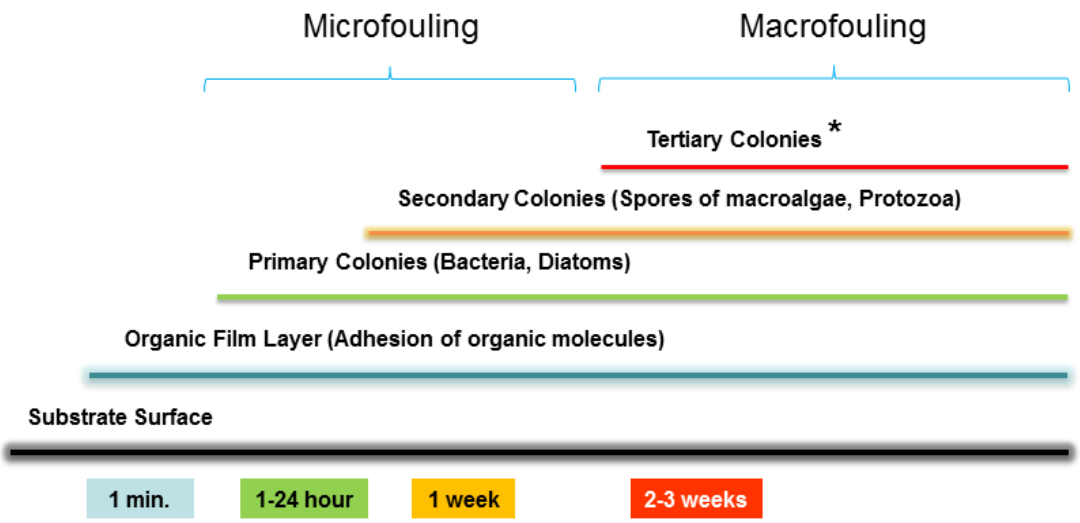

Figure 1.1 Scheme of biofouling formation on an artificial substrate surface in time course (* indicates bivalves, molluscs, tube worms and tunicates) (Modified from Abarzua & Jakubowski, 1995).

Increasing population of settled bacteria results in the formation of biofilms. This provides a good environment for the attachment of other micro and macro organisms such as diatoms, protozoa, barnacles and algal species onto artificial surface immersed in seawater (Figure 1.1) (Abarzua & Jakubowski, 1995; Almeida, Diamantino, & Sousa, 2007; Zahuranec, 1991). These organisms prefer accumulation since this behavior not only brings protection from predators and toxins but also obtaining nutrients easily by fouling onto a surface (Flemming, Griebe, & Schaule, 1996; Yebra, Kiil, & Dam-Johansen, 2004).

1.2 Effects of Biofouling on Marine Vehicles

Biofouling is a natural process and it can take place on any substrate surface. This event especially occurs on marine vehicles as well as on other artificial surfaces such as underwater pipes and docks, sonar equipment, ship bilges, oil rigs, cofferdams and aquaculture cages (Boxall, Comber, Conrad, Howcroft, & Zaman, 2000; Castrisi-Catharios, Bourdaniotis, & Persoone, 2007; Evans, Kerrigan, & Palmer, 2000; Omae 2003a, 2003b).

Figure 1.2 A ship's hull biofouled by barnacles and seaweeds (Photo: Z.A. KARABAY).

Biofouling is a major problem for the ships. As fouling organisms cover the hulls of the ships, they cause to increase of weight and reduction of speed and thus fouling leads to high fuel consumption, limitations in maneuverability and corrosion on the ship's hulls (Hall, Giddings, Soloman, & Balcomb, 1999; Hellio, De La Broise, Dufossé, Le Gal, & Bourgougnon, 2001) (Figure 1.2).

1.3 Antifouling Paint Types and Composition

In order to prevent biofouling, ship's hulls are painted with special marine paints. These paints are called as antifouling paints. They mainly consist of binders, pigments, toxicants, preservatives, fillers and thickening agents. Through their first development, different binder systems and toxicants have been used in antifouling paint compositions. One of the most used classifications in the literature for antifouling paints is related with their binder chemistry. Antifouling paints can be classified into three main types as soluble, insoluble and foul-release based on their binder chemistry (Figure 1.3). Soluble type antifouling paints can be divided again into two categories as self-polishing type and self-polishing copolymer type.

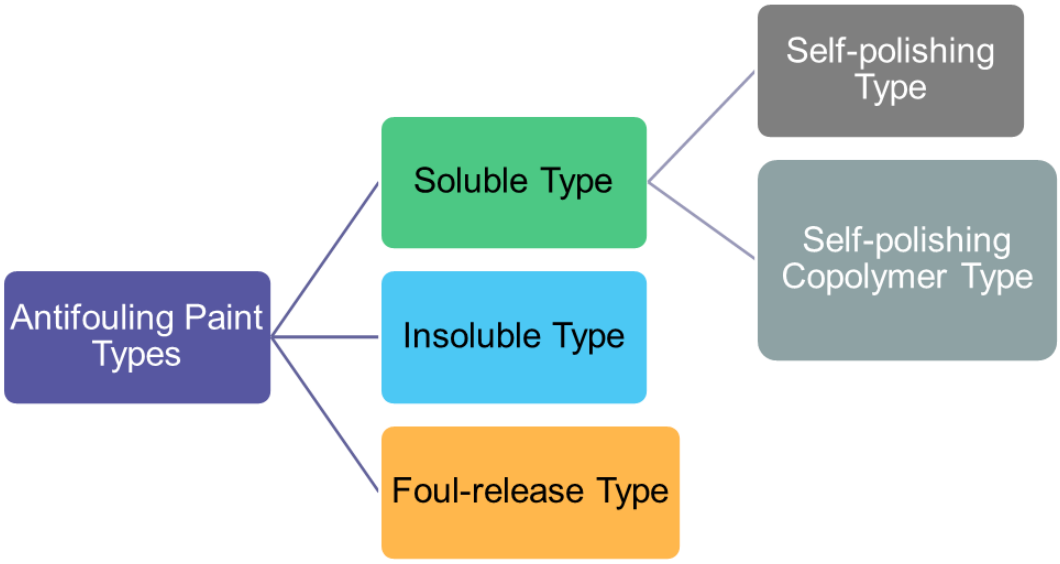

Figure 1.3 Classification of antifouling paints according to their working principles.

The self-polishing term can be defined as renewal of paint surface with the hydrolysis of binder. The working principle of these types of paints is based on unreacted and clean paint surface formation after hydrolysis of binder. The self-polishing ability of antifouling paints can be explained further with their working mechanism. Soluble resins and rosins (also known as colophony) are used as binder component in self-polishing type paints (Figure 1.4a). These paints contain high amounts of copper(I)oxide as a main biocide. Copper(I)oxide is a soluble biocide/pigment and it is highly toxic to marine organisms. As the seawater penetrates into the binder, copper(I)oxide dissolves as Cu^{+} ions and it is oxidized to more toxic Cu^{2+} ions. As the copper(I)oxide dissolves, seawater penetrates deeper parts of paint film and paint surface becomes porous. The pigment free binder layer is also called as leached layer. The porous paint surface erodes in the seawater only when ship moves at high speeds. The advantages of these paints are their low cost and fast applicability. But, the performances of these paints are low due to their limited copper(I)oxide amount and porous surface formation.

On the other hand, in self-polishing copolymer type paints, acrylic copolymers (mainly methyl methacrylate derivatives) esterified with pendant groups such as organotin, organosilyl and organotitanium moieties are used as binder component (Figure 1.4b). The working mechanism of this type of paints is based on formation of a new and smooth polymer layer after the hydrolysis of polymeric backbone. Seawater contacts with soluble pigment particles and it dissolves the pigments close to paint surface. Then, seawater hydrolyses the ester bond between pendant group and polymeric backbone. As a result of this reaction, polymeric backbone becomes more hydrophilic and new polymeric layer forms after hydrolysis of polymeric backbone. The advantages of these paints are their long service time and high performance. The major factor for their high performance is depended on their highly toxic pendant groups such as tributyltin (TBT). In these type of paints, co-biocides are also used in addition to copper(I)oxide and other pigments.

Insoluble antifouling paints are second type of antifouling paints (Figure 1.5). The binders used in these paints are insoluble in seawater. Vinyl resins, acrylic resins and

chlorinated rubbers are the most used binder types in these paints. Working mechanisms of these paints are based on dissolution of pigment and biocide particles starting from paint surface to accessible paint layer. As the soluble particles dissolves into seawater, paint surface becomes rough and amount of pigment/biocide released decreases with time. Therefore, these paints are not effective as others due to their short service time and low performance.

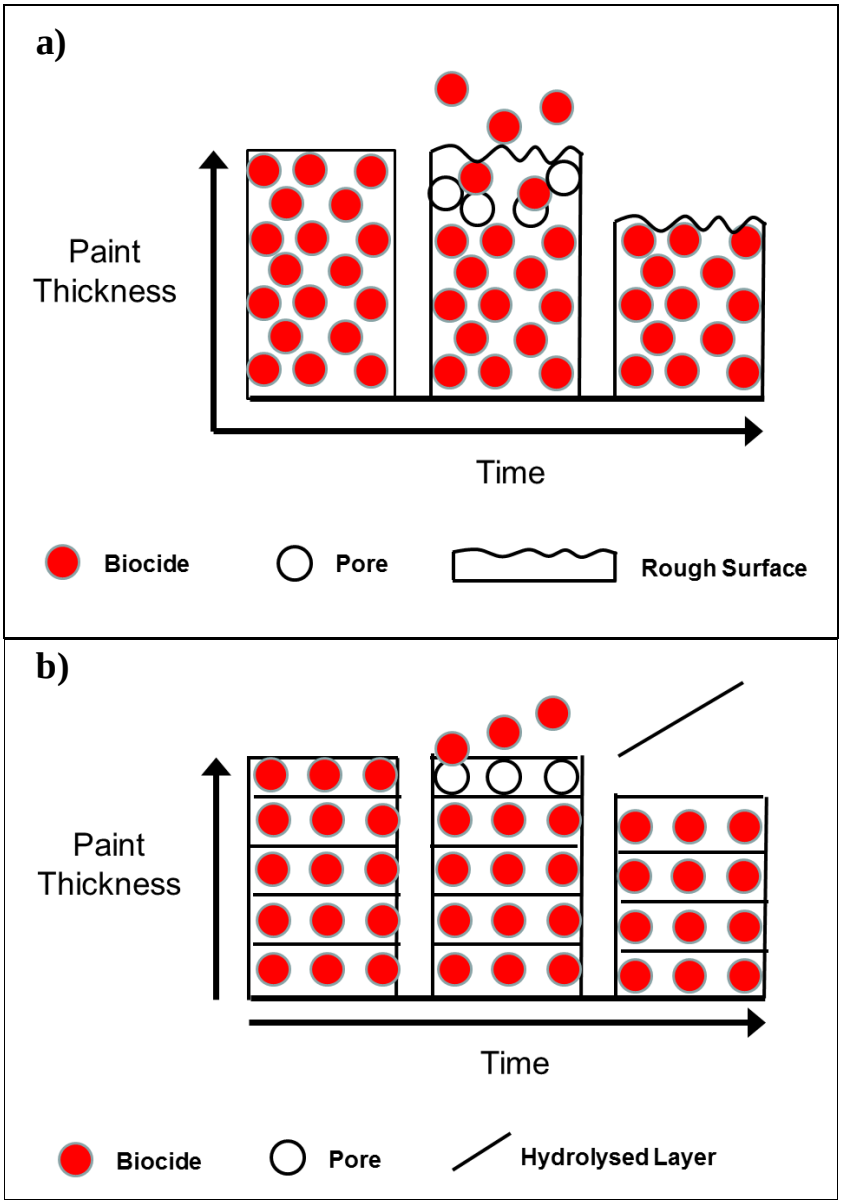

Figure 1.4 Biocide release mechanism from a) self-polishing and b) self-polishing co-polymer type antifouling paint..

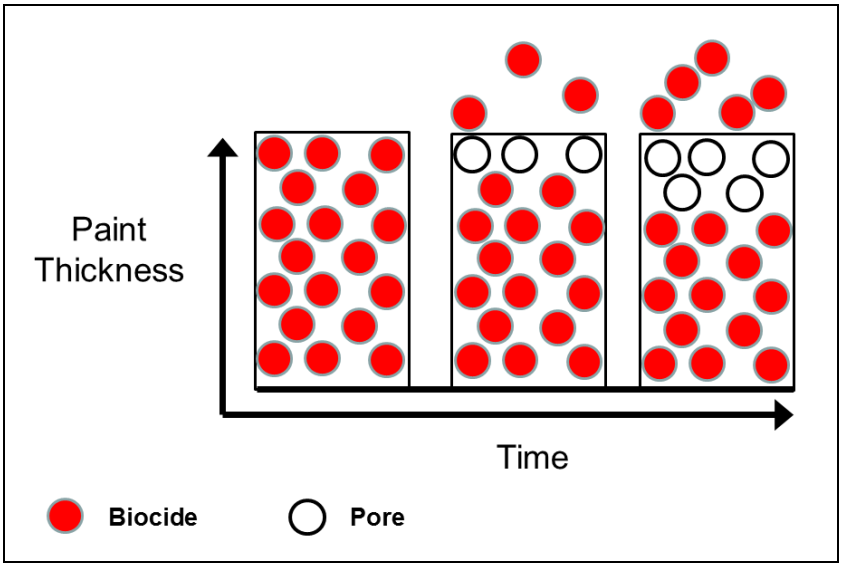

Figure 1.5 Biocide release mechanism from an insoluble type antifouling paint.

1.4 The Ban of TBT Based Self-polishing Copolymer (SPC) Antifouling Paints

The use of TBT's in antifouling coatings as its acrylate esters was first suggested by Montermoso and co-workers in 1958 (Gitlitz, 1981; Yebra, Kiil, & Dam-Johansen, 2004). Later, the use of TBT's in self-polishing copolymers was patented by Milne and Hails in 1974 (Milne & Hails, 1977; Yebra, Kiil, & Dam-Johansen, 2004). Tributyltin self-polishing antifouling paints are composed of an acrylic polymer (usually methyl methacrylate), TBT groups which are bonded to polymeric backbone as a pendant group by an ester linkage and a soluble pigment (ZnO or Cu_2O), which helps to control the polishing rate of paint (Kiil, Weinell, Pedersen, & Dam-Johansen, 2001; Olsen, 2009; Yebra, Kiil, & Dam-Johansen, 2004) (Figure 1.6).

Working mechanism of TBT-SPC paints can be summarized in 4 steps as below (Yebra, Kiil, & Dam-Johansen, 2004):

1) Soluble pigment particles dissolves when contact with seawater,
2) Seawater penetrates into pores that are formed after release of pigment particles,

3) TBT groups are released by hydrolysis of ester linkages between MMA and TBT,
4) Polymeric film becomes open to attacks of water molecules after the hydrolysis of TBT groups and polymeric film erodes as a layer by the act of moving seawater and exposes a less reacted paint surface (Figure 1.7).

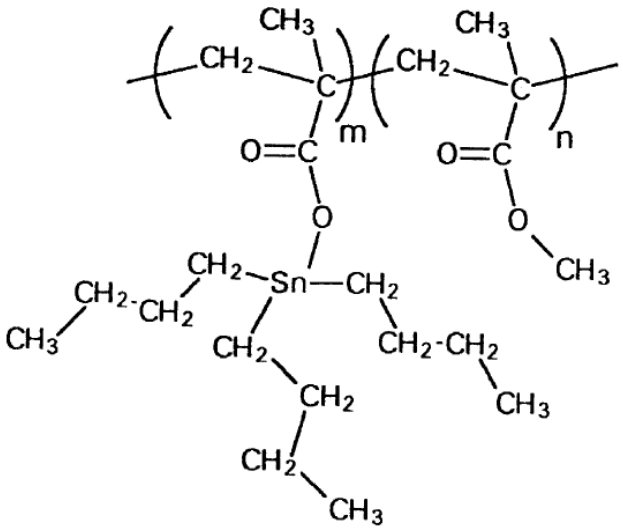

Figure 1.6 Chemical formula of a repeating unit of a copolymer of tributyltin methacrylate (TBTM) and methyl methacrylate (MMA) (Yebra, Kiil, & Dam-Johansen, 2004).

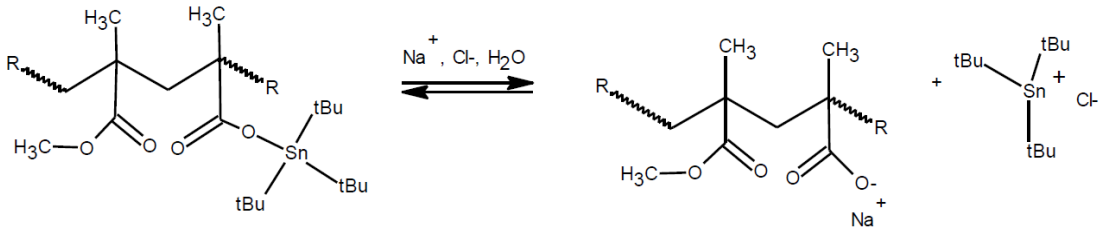

Figure 1.7 Release mechanism of TBT from an acrylic resin (here MMA) (Olsen, 2009).

TBT based SPC antifouling paints were successfully used for antifouling purposes, but application of TBT based antifouling paints were banned in 1 January 2003 and the presence of such paints on the surface of the ships were restricted after

1 January 2008 (International Maritime Organization, 2001) due to the reports on their harmful effects such as genotoxic and cytotoxic defects on non-target marine organisms (mussels, polychaetes, molluscs, fishes, etc.) (Hagger, Depledge, & Galloway, 2005; Hagger, Fisher, Hill, Depledge, & Jha, 2002 ; Jha, Hagger, & Hill, 2000; Jha, Hagger, Hill, & Depledge, 2000; Lau, Chan, Leung, Luan, Yang, & Qiu, 2007; Micael, Reis-Henriques, Carvalho, & Santos, 2007). It has been found that TBT stimulates the development imposex characteristics on *Nucella* species (Bailey & Davies, 1991; Bryan, Gibbs, Burt, & Hummerstone, 1987) and it also causes abnormal shell growth on *Crassostrea gigas* (Alzieu, 1991; Shim, Oh, Kahng, Shim, & Lee, 1998) (Figure 1.8).

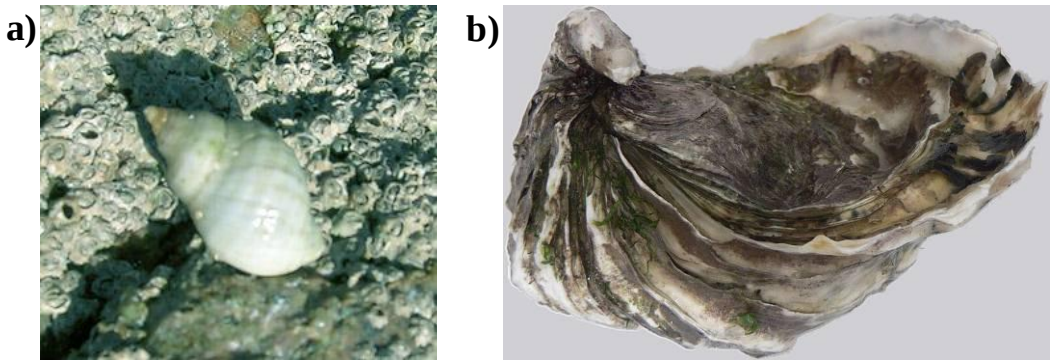

Figure 1.8 Marine organisms which were negatively affected from TBT. a) *Nucella lapillus* (Photo: http://marinebio.org/species.asp?id=536) and b) *Crassostrea gigas* (Photo: http://en.wikipedia.org/wiki/File:Crassostrea_gigas_p1040847.jpg).

1.5 Harmful Effects of Booster Biocides to Marine Ecosystem

Booster biocides are widely used as bioactive agents in antifouling paints and most common booster biocides are: chlorothalonil, dichlofluanid, diuron, irgarol 1051, zinc pyrithione, thiram, ziram, maneb, zineb, kathon 5287, TCMTB and TCMS pyridine (Konstantinou & Albanis, 2004; Voulvoulis, Scrimshaw, & Lester, 1999, Voulvoulis, Scrimshaw, & Lester, 2002; Thomas, Fileman, Readman, & Waldock, 2001; Yonehara, 2000). Two of the well-known and widely used biocides by antifouling paint producers are diuron and irgarol (Figure 1.9). Irgarol (2-methylthio-4-tert-butylamino-6-cyclopropylamino-s-triazine) is a symmetric triazine compound and its environmental hazards were widely discussed in the literature.

Irgarol is a photosynthesis inhibitor that binds to the D1 protein at photosystem II and it blocks the electron transport (Kem, 1994; Lama, Caib, Waia, Tsanga, Lama, Cheunga, Yuc, & Lama, 2005; Moreland, 1980). Half-lives of irgarol in seawater and freshwater are reported as nearly 100 and 200 days, respectively (Ciba Geigy, 1995; Konstantinou & Albanis, 2004). Its degradation rate is slow and it has a main degradation product called as M1 (2-methylthio-4-tert-butylamino-s-triazine) (Okamura, Aoyama, Liu, Maguire, Pacepavicius, & Lau, 2000). Possible degradation pathways for irgarol are biodegradation by white rot fungi (Liu, Maguire, Lau, Pacepavicius, Okamura, & Aoyama, 1997), hydrolysis catalyzed via mercuric chloride (Liu, Pacepavicius, Maguire, Lau, Okamura, & Aoyama, 1999) and sunlight photodegradation (Okamura, Aoyama, Liu, Maguire, Pacepavicius, & Lau, 1999, Okamura et al., 2000). Maximum irgarol concentrations at coastal areas were observed up to 4.2 µg/L (Basheer, Tan, & Lee, 2002), on the other hand, highest irgarol concentration in sediment samples from marinas were found to be 1 µg/g (Boxall et al., 2000).

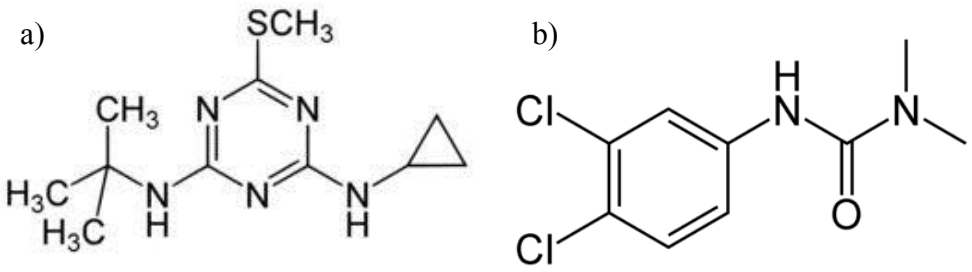

Figure 1.9 Chemical structures of a) irgarol and b) diuron.

Diuron (3-(3,4-dichlorophenyl)-1,1-dimethylurea) is a substituted urea derivative and it also inhibits electron flow in photosynthesis by reversibly binding QB binding site on the D1 protein (Jones, 2005; Tischer & Strotmann, 1977). As a result of aerobic and anaerobic degradations, diuron is degraded to following compounds: 1-(3,4-dichlorophenyl)-1,3-dimethylurea (CPDU), 1-(3,4-dichlorophenyl)-3-methylurea (DCPMU), 1-(3,4-dichlorophenyl)urea (DCPU) and demethyldiuron (Konstantinou & Albanis, 2004; Martínez and Barceló, 2001; Thomas et al., 2001; Thomas, McHugh, Hilton, & Waldock, 2002). Anaerobic half-lives of diuron and CPDU were reported as 14 and 35 days, whereas half-lives of DCPMU and DCPU

were 1 and 3 days (Konstantinou & Albanis, 2004; Thomas, McHugh, Hilton, & Waldock, 2003). Diuron concentrations increase especially in yachting season (Lamoree, Swart, van der Horst, & van Hattum, 2002) and highest diuron concentrations were found in Japan, Spain and United Kingdom up to 3054 ng/L, 2000 ng/L and 6742 ng/L, respectively (Konstantinou & Albanis, 2004).

As a result of their harmful effects on the marine ecosystem, the use of irgarol as an antifouling paint ingredient in vessels lower than 25 m and use of diuron in any type of marine paint were banned in United Kingdom in November 2002 (Advisory Committee on Pesticides, 2000; Chesworth, Donkin, & Brown, 2004). Other biocides are also used in antifouling paints solely or as a mixture of several biocides. However, negative effects of diuron and irgarol have been reported on several non-target organisms in the literature (Bellas, 2006; Faria, López, Fernández-Sanjuan, Lacorte, & Barata, 2010; Perina, Abessa, Pinho, & Fillmann, 2011; Tsunemasa & Okamura, 2011; Wang, Li, Huang, Xu, & Wang, 2011). Therefore, uses of diuron and irgarol as antifouling biocides are currently banned in some countries such as United Kingdom and Denmark and these biocides are also about to be banned in other countries in the very near future.

1.6 Eco-friendly Approaches in Antifouling Paint Production

So far, many attempts have been done to develop an eco-friendly antifouling biocide compound in the literature. Among them, Pérez, Blustein, Garcia, Amo, & Stupak (2006) have recommended cupric tannate as an alternative biocide instead of cuprous oxide based antifouling paints. In another study, Stupak, García, & Pérez (2003) have demonstrated that tannins have narcotic effects on nauplii of *Balanus amphitrite*. Bellotti, del Amo, & Romagnoli (2012) have investigated the antifouling performance of coatings containing zinc complex of tara tannins at Mar del Plata harbor. Bellotti, del Amo, & Romagnoli (2012) have found that one of the coating containing zinc tannate was able to keep its efficiency for eight months. Tannins, especially found in higher plants and brown algae, are phenolic compounds and they are able to form complexes with metals and precipitate proteins (Figure 1.10). Due to

their phenolic structure tannic acid derivatives show anti-corrosive, anti-bacterial and antifouling properties (Pérez et al., 2006; Pérez, Garcia, Blustein, & Stupak, 2007). Potassium sorbate which is presently being used as food preservative is another potential eco-friendly biocide. According to Blustein, Pérez, García, Stupak, & Cerruti (2009), potassium sorbate have reversible inhibitory effect on the settlement of nauplii and cyprids of *Balanus amphitrite* for a wide range of concentrations.

a)

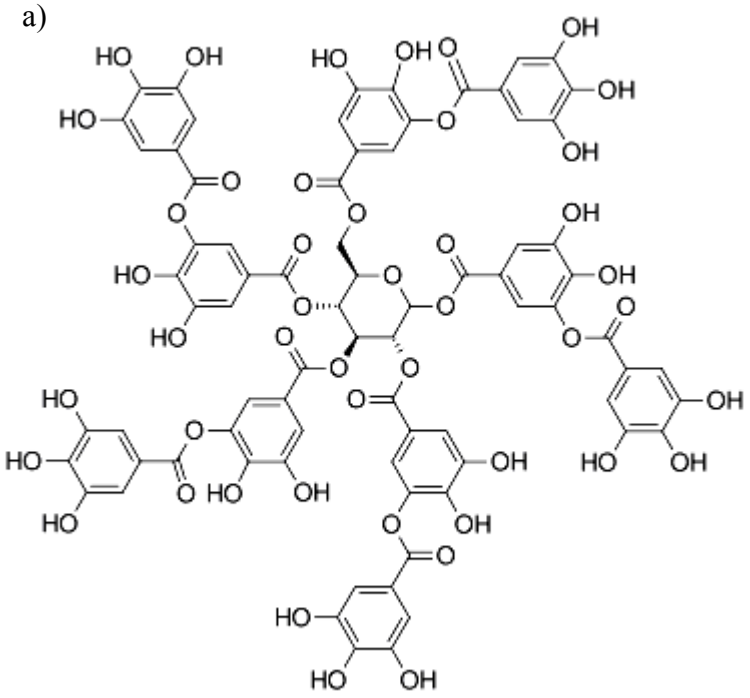

b)

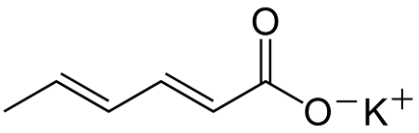

Figure 1.10 Chemical structures of a) tannic acid ($C_{76}H_{52}O_{46}$) and b) potassium sorbate.

Alyuruk, Doner, Karabay, & Cavas (2010) have studied the antifouling performances of five eco-friendly biocides, zinc oxide (ZnO), copper(I)oxide (Cu_2O), potassium sorbate (KS), tannic acid (TA), cupric tannate (CT), and *Caulerpa prolifera* extract (CPE), embedded in phytagels and tested for one month immersed

in inner bay of İzmir, Turkey. Alyuruk et al. (2010) have found that the best antifouling performance was achieved with Cu_2O and the antifouling performances of other eco-friendly biocides were decreased in the order of CT, ZnO, KS, TA, and CPE.

1.7 Marine Plants and Their Secondary Metabolite Chemistry

There are many algae species in sea ecosystems and they are exposed to marine fouling. They have developed their antifouling properties against fouling organisms during their evolutions. Most of algae species have many different types of secondary metabolites to get rid of the fouling organisms. Among marine algae, *Caulerpa* genus is famous because of its two exotic-alien members, *Caulerpa racemosa* var.*cylindracea* (hereafter *C. racemosa*) and *Caulerpa taxifolia* (Figure 1.11). Although *C. taxifolia* is more famous compared to *C. racemosa*, the latter one has invaded 13 Mediterranean countries (Albania, Algeria, Croatia, Cyprus, France, Greece, Italy, Libya, Malta, Monaco (M.Verlaque, pers. commun.), Spain, Tunisia and Turkey (Klein, & Verlaque, 2008). *C. taxifolia* has been reported from 7 Mediterranean countries.

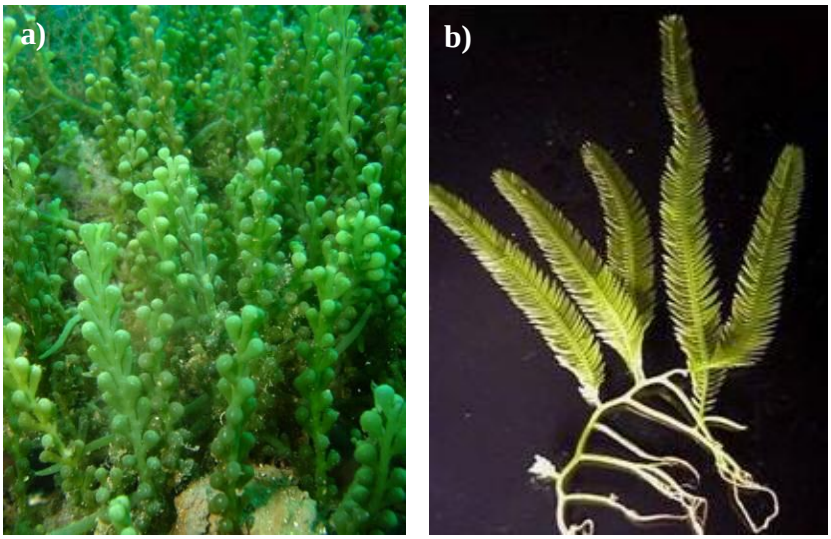

Figure 1.11 a) *Caulerpa racemosa* var. *cylindracea* (Photo: Levent CAVAS), b) *Caulerpa taxifolia* (Photo: http://www.uni-jena.de/prof_pohnert.html).

Two species are well known and well studied invasive species in the Mediterranean Sea. Their successes are associated with their joint secondary metabolite called caulerpenyne (CYN) (Figure 1.12) (Boudouresque, Lemée, Mari, & Meinesz, 1996; Cavas, Baskin, Yurdakoc, & Olgun, 2006; Jung, Thibaut, Meinesz, & Pohnert, 2002; McConnell, Hughes, Targett, & Daley, 1982). CYN has sesquiterpene structure and shows antiproliferative and antiviral as well as antimicrobial properties (Barbier, Guise, Huitorel, Amade, Pesando, Briand, & Peyrot, 2001; Cavas et al., 2006; Nicoletti, Pieta, Calderone, Bandecchi, Pistello, Morelli, & Cinelli, 1999; Smyrniotopoulos, Abatis, Tziveleka, Tsitsimpikou, Roussis, Loukis, & Vagias, 2003). Therefore, CPE can be an ideal antifouling booster biocide.

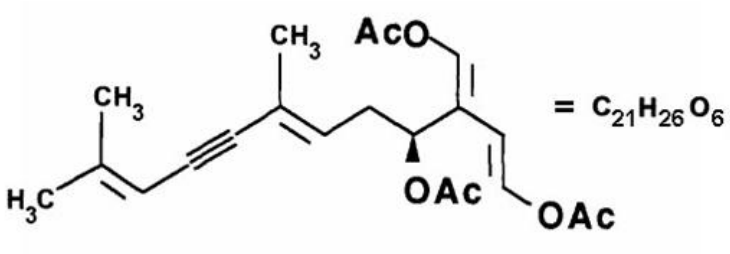

Figure 1.12 Chemical structure of caulerpenyne.

Seagrasses are aquatic angiosperms that are found in marine environment. The seagrass term is often used for grass-like structure of its members. They form an ecological group rather than taxonomic group. There are four members of seagrass families as follows: Zosteraceae, Cymodoceaceae, Posidoniaceae, and Hydrocharitaceae (dan Hartog & Kuo, 2006). Among other seagrasses, *Zostera* genus is a widespread and also one of the well-studied groups of seagrasses (Moore & Short, 2006). *Zostera* genus is generally found in shores affected from tide events. They form a critical habitat for other organisms by providing feeding ground, enhancing the local productivity, filtering the water and functioning in nutrient cycle (Fredette, Diaz, van Montfrans, & Orth, 1990; Rasmussen, 1977; Fonseca, Zieman, Thayer, & Fisher, 1983; Fonseca & Fisher, 1986; Fonseca, 1992; Hansen, Udy, Perry, Dennison, & Lomstein, 2000; Heiss, Smith, & Keith, 2000; Short, 1987; Moore & Short, 2006).

Seagrasses are continuously under biofouling threat by marine micro-organisms. In order to protect themselves from harmful micro-organisms, some seagrasses like *Zostera* sp. are known to secrete their secondary metabolites for defensive purposes. The natural antifouling agent produced by *Zostera* sp. is called Zosteric Acid (ZA). ZA is a sulfated form of p-coumaric acid and it is soluble in water. According to scientific studies, ZA is not harmful to marine organisms but it prevents settlement of biofouling organisms by inhibiting their adhesion (Callow & Callow, 1998; Geiger et al., 2004; Ram, Purohit, Newby, & Cutright, 2012; Stanley, Callow, Perry, Alberte, Smith, & Callow, 2002; Shin, Smith, & Haslbeck, 2001; Todd, Zimmerman, Crews, & Alberte, 1993). ZA was investigated in this thesis, because of its non-toxic antifouling effects. ZA was also synthesized in order to compare its efficiency and effectiveness against natural ZA.

Zostera noltii and *Cymodocea nodosa* are two of the widespreaded seagrasses after *Posidonia oceanica* in the Aegean coastlines of Turkey (Figure 1.13). *Z. noltii* is especially populated at lagoons where tide event can be observed. On the other hand, *C. nodosa* can be found at shallow areas or can form mixed populations with other seagrasses like *Zostera* sp. Whereas *Z. noltii* contain ZA as main antifouling agent like other *Zostera* sp., *C. nodosa* has two cytotoxic agents called cymodiene and cymodienol (Figure 1.14) (Kontiza et al., 2005).

Because of their high abundance along Aegean coastlines and they were not scientifically investigated from Turkish coastlines before, we have decided to use *Z. noltii* in this thesis in comparison with *C. nodosa* as eco-friendly and natural antifouling agent source. Sampling areas for both seagrasses were located in Dikili and Gülbahçe, İzmir. The sampling areas were tracked for monthly periods and tide event was observed in winter season at both locations. An example to tide event observed in Gülbahçe was given in Figure 1.15.

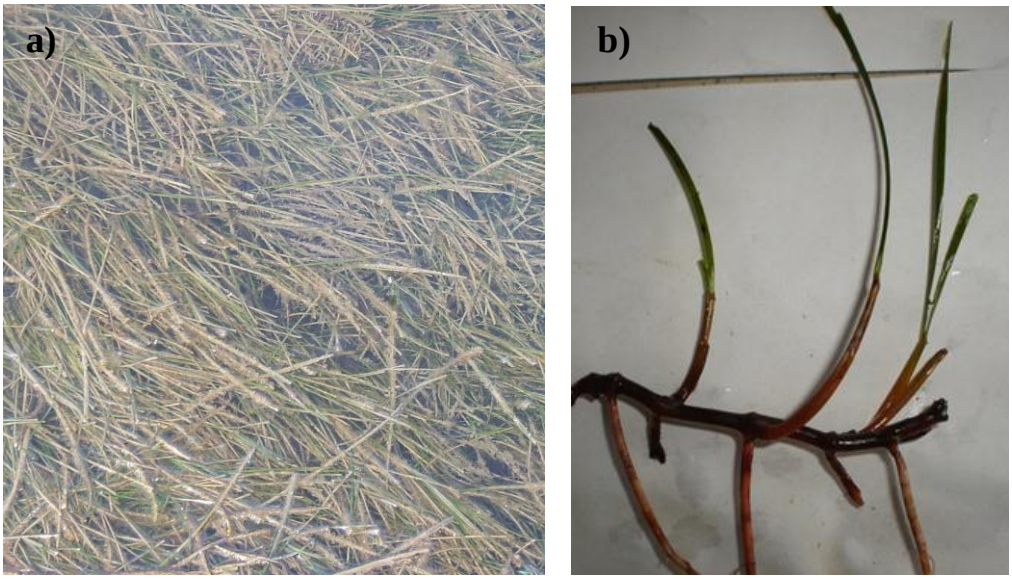

Figure 1.13 a) *Zostera noltii*, b) *Cymodocea nodosa*.

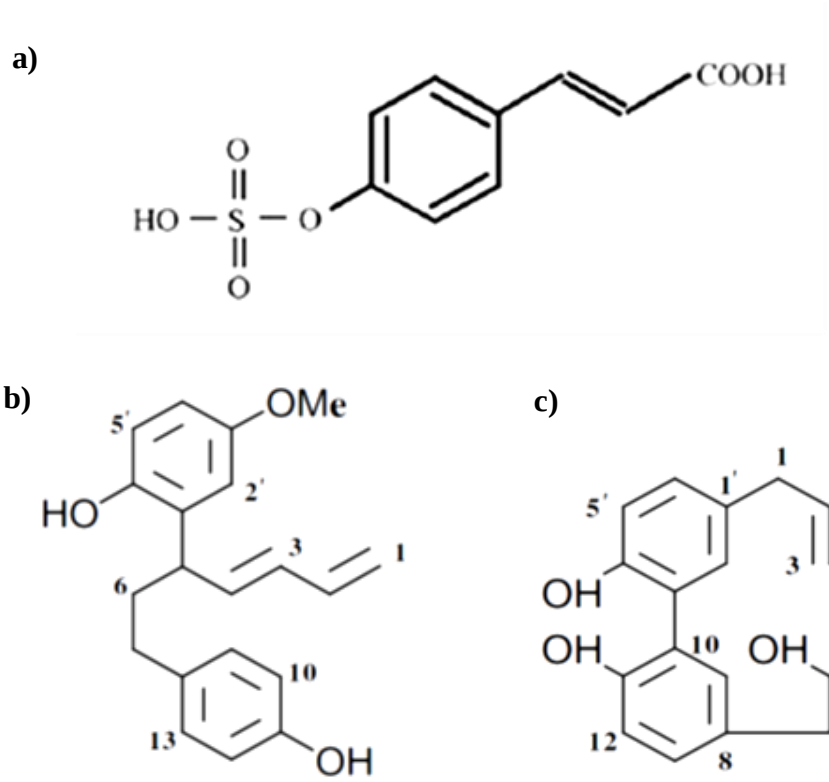

Figure 1.14 a) Zosteric acid, b) Cymodiene, and c) Cymodienol.

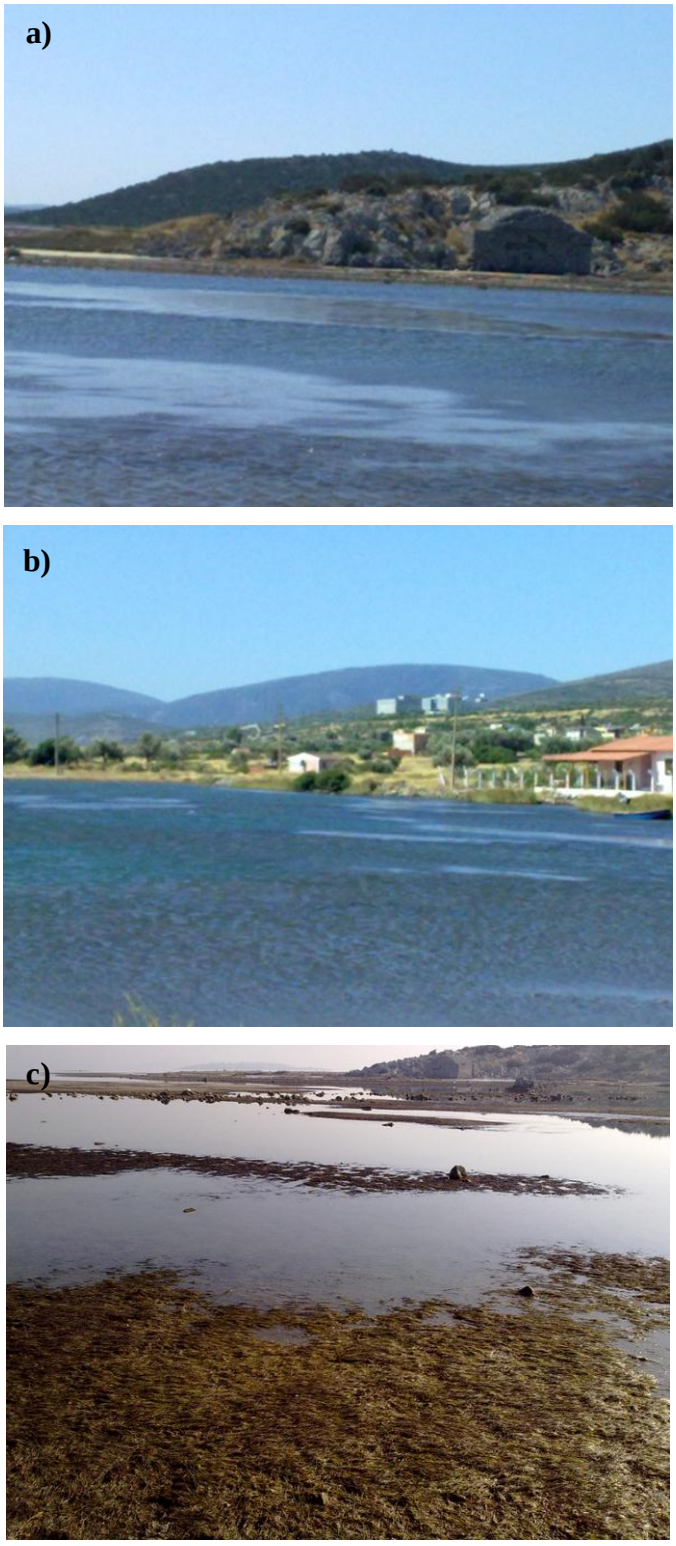

Figure 1.15. *Zostera noltii* beds located in Gülbahçe-İzmir, Turkey. a) summer (July 2011), b) summer (July 2011) and c) winter (December 2011).

1.8 Importance of Toxicity Tests in Development of Biocides

Artemia salina (brine shrimp) is an invertebrate found in salt lakes and marine environments (Figure 1.16). It has an important role in the energy flow of the food chain (Kanwar, 2007; Lewan, Anderson, & Morales, 1992). Besides of its role in food chain, *A. salina* is characterized with several important abilities like its adaptability to wide ranges of salinity (5-250 g/L) and temperature (6-35 °C), ease of culture, low cost, commercial availability of dry cysts, short life cycle, high hatching ability, high adaptability to adverse environmental conditions and resistance to wide ranges of toxic substances (Barahona & Sánchez-Fortún, 1999; Koutsaftis & Aoyama, 2008; Nunes, Carvalho, Guilhermino, & Van Stappen, 2006).

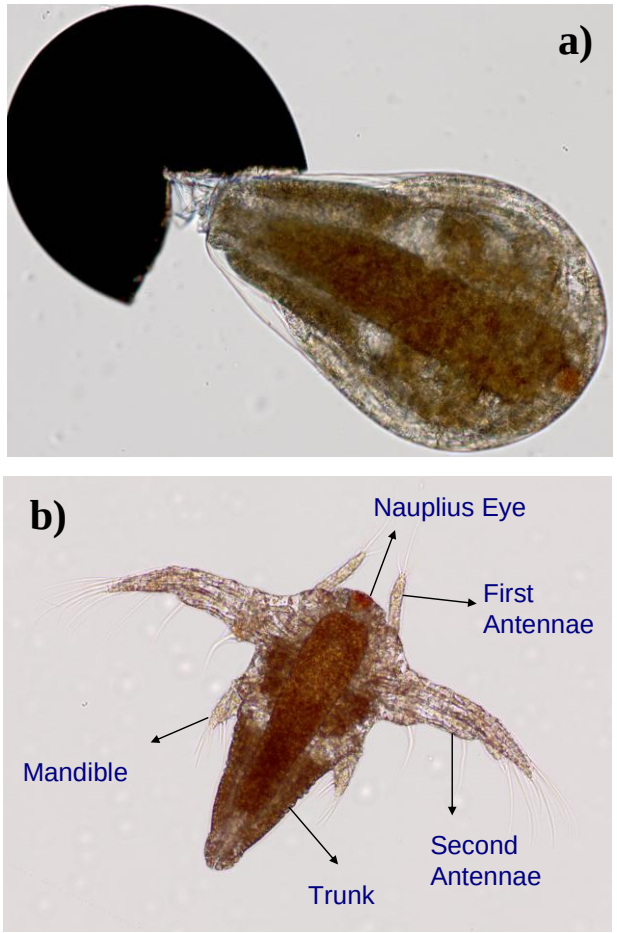

Figure 1.16. Developmental stages of *Artemia salina*. a) Pre-hatch stage, b) nauplius at post-hatch stage and its body parts.

Because of these characteristics, *A. salina* and other *Artemia* species were used in the literature for the screening of acute toxicities of booster biocides (Bartolomé & Sánchez-Fortún, 2005; Katranitsas, Castritsi-Catharios, & Persoone, 2003; Koutsaftis & Aoyama, 2007, 2008; Löschau & Krätke, 2005; Panagoula, Panayiota, & Iliopoulou-Georgudaki, 2002). Toxicities of booster biocides were also reported on the embryos of some marine organisms such as freshwater mussels, zebra mussels, blue mussels, sea urchins, oysters and sea squirts (Bellas, 2006; Faria, López, Fernández-Sanjuan, Lacorte, & Barata, 2010; Perina, Abessa, Pinho, & Fillmann, 2011; Tsunemasa & Okamura, 2011; Wang, Li, Huang, Xu, & Wang, 2011).

The toxic effects of booster biocides in comparison with eco-friendly and reference biocides were investigated on *A. salina* through acute toxicity, hatching percentage and larval morphology tests. The eco-toxicities of eco-friendly biocides (diuron, irgarol, zinc pyrithione, copper pyrithione, *Zostera noltii* extract, *Cymodocea nodosa* extract, potassium dichromate, p-coumaric acid, sodium sulphate and zosteric acid) were determined with acute toxicity tests on *A. salina*. Since the motion of some nauplii exposed to booster biocides were slower than the control in acute toxicity tests, AChE in crude extract of *A. salina* were characterized and inhibitory effects of booster biocides (diuron, irgarol) were investigated on AChE from *Electrophorus electricus*. In order to analyze slow or fast moving nauplii without personal errors, a video processing algorithm was also developed and used for the determination of acute toxicities of potassium dichromate and p-coumaric acid.

CHAPTER TWO
MATERIALS AND METHODS

2.1 Preparation of Marine Plant Extracts

The detritus of *Zostera noltii* and *Cymodocea nodosa* were collected in July 2011 from Gülbahçe, Urla, Turkey. The sampling area was located at the entrance of a lagoon. The samples were collected from shore and allowed to dry in a dark and cool place. Then, the samples were powdered with a grinder and kept in glass bottle until use. The powdered samples (15 g) were exhaustively extracted with 200 mL of methanol for 8 h. After the extraction, the extracts were concentrated with rotary evaporator. In order to determine the number of fractions, the extracts were subjected to TLC plates with 1:1 ethyl acetate:petroleum ether and 1:1 methanol:petroleum ether as mobile phases.

2.2 Synthesis of Sodium Zosterate

There are two synthesis methods for sodium zosterate in the literature (Alexandratos, 1999; Villa, Albanese, Giussani, Stewart, Daffonchio, & Cappitelli, 2010). In this study, the method proposed by Villa et al. (2010) was applied because product yield was higher than the first method (Figure 2.1).

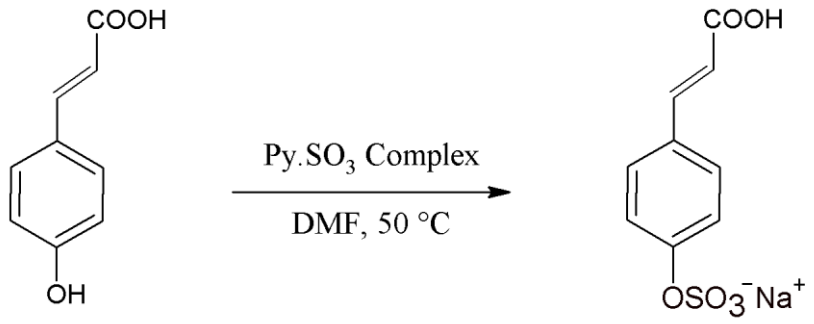

Figure 2.1 Synthesis of sodium zosterate by sulfonation of p-coumaric acid with Py·SO_3 complex in DMF.

Briefly, 16.46 g of trans-4-hydroxycinnamic acid was dissolved in 30 mL of anhydrous *N,N*-dimethylformamide, DMF. Then, 25.68 g of sulfur trioxide pyridine complex ($Py \cdot SO_3$) was added to reaction vessel and stirred at 50 °C for 2 h in water bath. In order to maintain a better agitation, reaction media was diluted with some water. After the reaction, reaction mixture was allowed to cool to room temperature and 30% NaOH was added dropwise to reaction media until the pH 7. The precipitated white solid was filtered and remaining solution was extracted three times with 20 mL of dichloromethane (CH_2Cl_2). Methanol was added to clear solution by dropwise causing the precipitation of a white solid that was removed with first filtration. The white precipitate was removed again by filtration and filtrate was evaporated to dryness. Finally, 27 of sodium zosterate were obtained after evaporation. The synthesized sodium zosterate was characterized by ^{1}H-NMR, FT-IR, and TLC methods. FT-IR spectroscopy was performed according to KBr disc method with Perkin Elmer (Spectrum BX) to analyze functional group changes between synthesis steps. Thin layer chromatography was applied on silica (F60) coated aluminum plates with 1:1 ethyl acetate:petroleum ether and 1:1 methanol:petroleum ether as mobile phases. The TLC spots belong to fractions were analyzed under visible, 254 nm and 366 nm UV-lights. ^{1}H-NMR measurements were performed at 400 MHz in DMSO as solvent.

2.3 Acute Toxicity Tests on Model Organism *Artemia salina*

Dry cysts of *A. salina* were hatched in saline water (35‰ NaCl) at constant aeration, illumination (2300 lux) and temperature (28°C). After 24h of hatching period, *A. salina* nauplii (10 individual) were transferred to 250 µL test medium, 96 well plates, by pipetting at 20 µL volume. Test medium was prepared at 270 µL total volume to contain test chemicals, irgarol, diuron, zinc pyrithione (ZnP), copper pyrithione (CuP), *Zostera noltii* extract, *Cymodocea nodosa* extract, potassium dichromate (PDC), p-coumaric acid (p-CA), zosteric acid and sodium sulphate at different concentrations. Potassium dichromate was used as a reference substance in acute toxicity tests on *A. salina*. Stock solutions of all test chemicals were prepared at 1 mg/mL concentration and they were initially dissolved in DMSO except for

PDC, zosteric acid and sodium sulphate. Acute toxicity tests were conducted for 6 h and test plates were kept in a dark place. After the toxicity tests, survival percentages were calculated by counting the nauplii that moves more than 30 s. The experiments were replicated four times.

2.4 Acute Toxicity and Sublethal Behavior Determination with Video Processing

A. salina nauplii were reared under same conditions as stated in Section 2.3. After 24h of hatching period, *A. salina* nauplii (5-8 individuals) were transferred to 130 µL test medium, 96 well plates, by pipetting at 20 µL volume. Test medium was prepared at 150 µL volume to contain test chemicals, PDC and p-CA, from 7 to 100 mg/L concentration range. Stock solutions of PDC and p-CA were prepared at 1000 mg/L concentration and p-CA was initially dissolved in DMSO. Acute toxicity tests were conducted for 24 h and kept in a dark place. During the acute toxicity tests, videos of each test well were recorded in AVI format with digital microscope controlled through Image Acquisition Toolbox of MATLAB at 640 x 480 resolution and 30 fps frame rate at predefined time intervals, 0 h, 3 h, 6 h, 8 h, 21 h and 24 h . Then, recorded video for each well were analyzed with a video processing algorithm under MATLAB. The experiments were replicated three times.

In this thesis, an approach that is computationally efficient yet accurate algorithm to detect moving *A. salina* was used. It was aimed to reach high level of accurate results by fusing the results of two simple techniques with this approach. We choose to use adaptive median filtering and neural network based color segmentation as the two parallel blocks whose outputs are fused. Since it was able to compensate the deficiencies of each block by using parallel classification structure, the detection performance was increased without sacrificing computational time. After detecting moving *A. salina*, blob analysis was applied to compute statistics (area, centroid, orientation and bounding box) of connected regions in the binary image. Obtained centroid coordinates in consecutive frames are used to identify the trajectories of moving objects. The maximum value of the histogram that shows the distribution of

the number of detected blobs in a period of 30 sec are taken as the number of living *A. salina*.

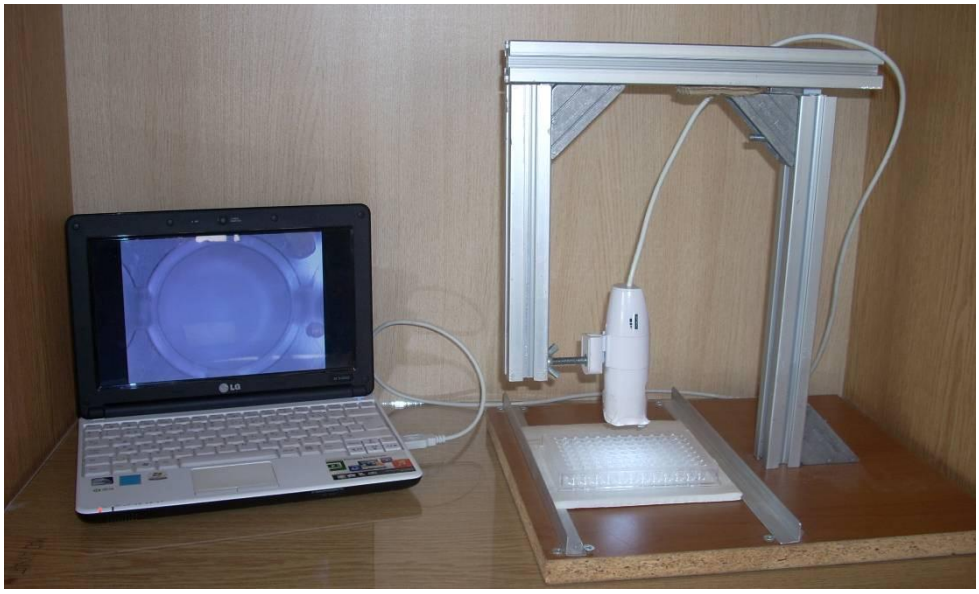

Figure 2.2 Experimental setup for sublethal behavior determination on *Artemia* nauplii by video processing.

2.5 Hatching Success and Larval Morphology of *A. salina* Exposed to Booster Biocides

The chemicals used in the toxicity tests, diuron and irgarol, were provided by Moravia Marine and Industrial Coatings Company, İstanbul, Turkey. Stock solutions of diuron and irgarol were prepared first by dissolving in DMSO and then by diluting with artificial seawater at 35‰ salinity. Maximum DMSO ratio in test solutions was not exceeded 3%. While the concentrations of irgarol were 1 and 5 mg/L, the concentrations of diuron were 1 mg/L, 5 mg/L and 25 mg/L. The experiments were performed with 20 mL glass test tubes placed in tube racks that were submerged into water until the water covers the midpoint of the tubes (Figure 2.2). Constant aeration, illumination (2300 lux) and temperature (28°C) were maintained and the replicate number was 18 in the experiments. In the hatching experiments, about 50 mg of *A. salina* cysts were hydrated in 50 mL of distilled water for 5h at room temperature. For each test group, 10 mL of test solution was transferred to 20 mL test tubes. Exactly, 10 hydrated cysts were added to test tubes at 20 µL volumes and then 24 h

hatching period was initiated. After the hatching period, hatching percentages (HPs) of cysts were determined by counting completely hatched nauplii number. In order to estimate the 50% effective concentration (EC_{50}), hatching failure (found by subtracting hatched nauplii number from total group size) data was used. EC_{50} values were determined with probit analysis (Finney, 1971) by using normal distribution in Minitab 16.1.1. The experiments were replicated eighteen times.

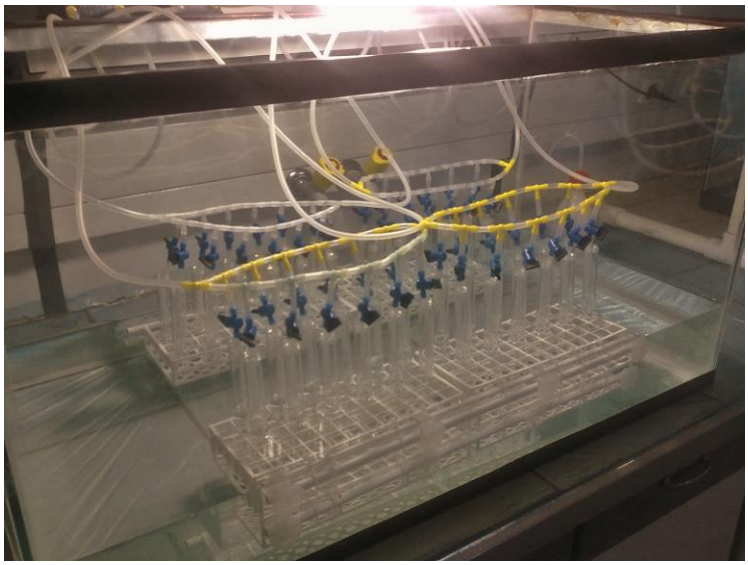

Figure 2.3 Experimental setup for toxicity tests.

After 24 h of hatching period, morphological disorders on nauplii and unhatched cysts were investigated under optical microscope (Olympus BX51TF, 10x objective lens, zoom 1.00). Snapshots of nauplii and unhatched cysts from each concentration range were recorded with microscope camera (Olympus DP25). Total body length for *A. salina* nauplii was also measured under optical microscope and its software (DP2-BSW 1.4).

2.6 Investigation of Acetylcholine Esterase Inhibitory Activities of Booster and Eco-friendly Biocides

S-Acetylthiocholine iodide (hereafter ATC) and 5,5'-Dithiobis(2-nitrobenzoic acid) (hereafter DTNB) were purchased from Alfa Aesar. Acetylcholine esterase from *Electrophorus electricus* (Type VI-S, lyophilized powder - C3389) was

obtained from Sigma. Booster co-biocide, irgarol, was kindly provided by Moravia Marine and Industrial Coatings, İstanbul – Turkey.

AChE activity assays were performed on a microplate reader (ELx800, Biotek Instruments, USA). AChE activity was determined according to the method of Ellman, Courtney, Andres, & Featherstone (1961) with modifications for microplate reader (Galgani & Bocquene, 1991; Holth & Tollefsen, 2012). Briefly, 25 µL of buffer, DMSO or irgarol in DMSO were added to 2.5 mL of 1 µg mL^{-1} AChE in 0.1 M Tris buffer (pH 8.0) and equilibrated in an orbital shaking water bath (GFL 1092) at 20°C. Then, 100 µL enzyme solution, 155 µL 0.6 mM DTNB solution in 1.1 mM $NaHCO_3$ and 85 µL ATC solution were added to microplate wells to start the reaction. Substrate concentrations were studied between 0.2 – 1.0 mM range. Enzyme activity of AChE was expressed as nmol acetylthiocholine converted to thiocholine by per mg AChE per minute. The molar extinction coefficient (ε) for TNB was used as 1.36 x 104 mL $mmol^{-1}$ cm^{-1} (Holth & Tollefsen, 2012). Enzyme activity was presented with Michaelis-Menten and Lineweaver-Burk plots. K_m, V_{max} and K_i values were also calculated from Lineweaver-Burk plot. The experiments were replicated three times.

The preparation crude extract from *A. salina* nauplii was carried by following freze-thaw method. Briefly, 70 mg of *Artemia* cysts were hatched in 30 mL saline water (35‰ NaCl) for 24 h. Hatched nauplii was washed with 0.1 M PB (pH 7.5) on 0.1 µm nylon filter to remove salt. Washed nauplii were transferred to 2 mL eppendorf tubes and 1 mL PB (pH 7.5) was added. The eppendorfs were stored in refrigerator for overnight. After thawing, nauplii was homogenised with IKA homogenizator for 3 min with 30 s intervals. The homogenate was sonicated in ultrasonic bath for 1 min. The resulting crude extract was centrifuged at 5000 rpm for 15 min and the supernatant was re-centrifuged for 15 min at 12000 rpm. The latter supernatant was transferred to eppendorf tubes at 250 µL aliquots and stored in refrigerator at -20 °C until use. The AChE activity in crude extracts of *A. salina* was determined by the method of Ellman, Courtney, Andres, & Featherstone (1961) as explained in previous paragraph.

2.7 Field Tests: Incorporation of Secondary Metabolite Cocktails of Marine Plants into Rosin Based Self-polishing Antifouling Paints

The antifouling performances of eco-friendly secondary metabolite cocktails of *Z. noltii* and *C. nodosa*, a commercial antifouling paint, commercial biocides (diuron and irgarol), sodium zosterate, powdered *Z. noltii*, powdered *C. nodosa*, biocide free paints were investigated in field tests. The compositions of prepared antifouling paints are listed in Table 2.1. Antifouling paints were prepared by changing only the biocide type.

The antifouling paints were applied by a brush on two sides of the planar steels. Before the application of antifouling paints, steel surfaces were initially treated with sandpaper and then, primer coating was applied in order to prevent corrosion. Painted steels were allowed to dry for one week. Field tests of prepared antifouling paints were performed at 50 cm depth from sea surface by hanging on a wooden timber. The test samples were photographed per 15 days until the 90 days of immersion. Tests were performed at Levent Marina, İzmir, Turkey (Figure 2.3).

Table 2.1 Antifouling paint compositions prepared for field test.

Paint Component	**Percent by weight (w/w%)**
Rosin	23
Lutanol M40	8
Oil	8
ZnO	12
Cu_2O	5
Biocide	6
$CaCO_3$	2
Xylene	36

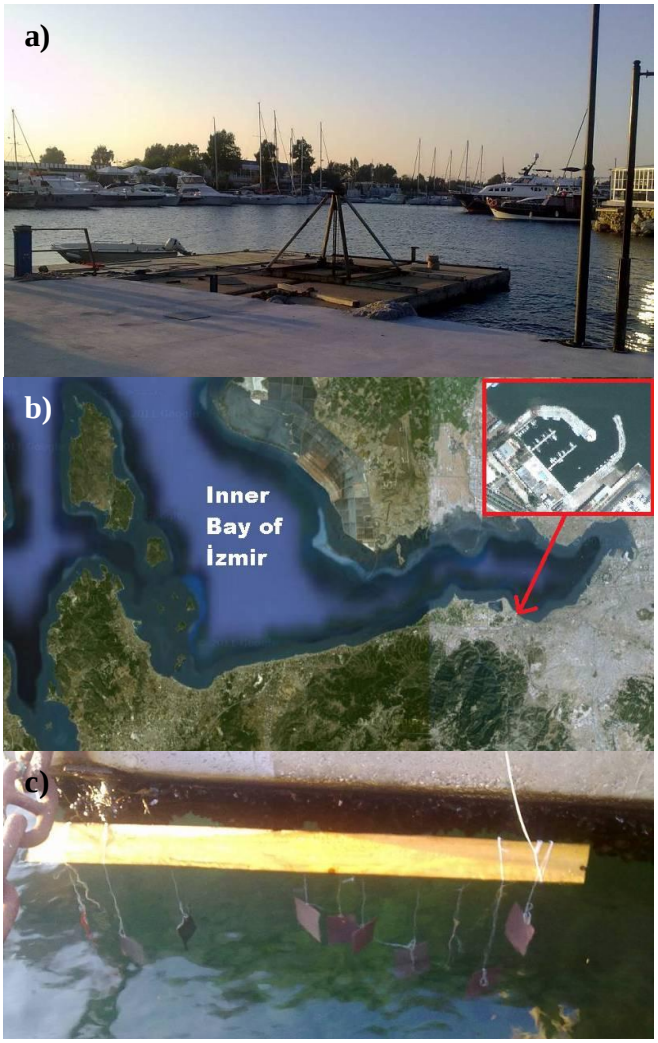

Figure 2.4 a) Levent Marina, İzmir, b) Satellite view of test area (38.406371 N, 27.068832 E), and c) Experimental setup for test panels.

2.8 Fouling Criteria

In the literature, fouling criteria have been used to classify the surfaces of antifouling paint test panels according to abundance of settled micro and macro fouling organisms. For this purpose several fouling criteria have been proposed (Arimura, Hiyoshi, Nakamura & Tsuboi, 2004; Karabay, 2011). According to these papers, the fouling criteria constitutes five fouling levels as follows,

Level 1. There are no fouling organisms on the surface.

Level 2. Microfilm layer formation is present on the surface.

Level 3. Microfilm layer is present and macrofouling is at the beginning state.

Level 4. Micro- and macrofouling organisms (macroalgae and crustaceans) are present on the surface.

Level 5. The surface is heavily fouled (>50%) by micro- and macrofouling organisms (macroalgae and crustaceans).

2.9 Statistical Test

MINITAB 16.1.1 statistical software was used for evaluation of the data. One-way ANOVA followed by Tukey's test was used to compare the experimental data. Statistical significance was set at 0.05 for one-way ANOVA tests.

CHAPTER THREE
RESULTS AND DISCUSSION

3.1 TLC Results for *Z. noltii* and *C. nodosa* extracts

Extracts of *Z. noltii* and *C. nodosa* in four different solvents (acetone, ethanol, methanol and water) were subjected to TLC plates for determination of the number of possible bioactive fractions. The results of TLC analysis showed that both *Z. noltii* and *C. nodosa* extracts were composed of many fractions. There were more than five well-separated fractions when acetone extract of *Z. noltii* was developed with 1:1 ethyl acetate:petroleum ether (Figure 3.1).

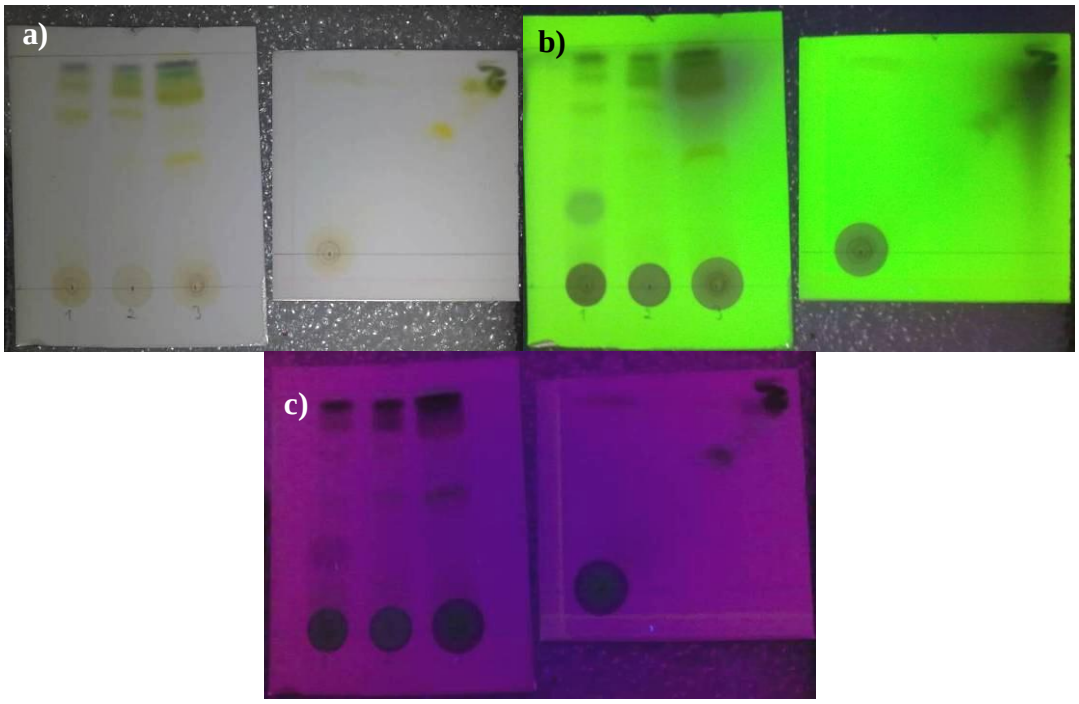

Figure 3.1 1-D (left) and 2-D (right) TLC fractions of *Zostera noltii* extracts developed in 1:1 ethyl acetate: petroleum ether mobile phase: a) visible region, b) 254 nm and c) 366 nm (Spot 1:methanol, 2:ethanol, and 3:acetone extract, respectively).

However, there were incompletely separated and fewer amount of fractions in methanol and ethanol extracts of *Z. noltii*. On the other hand, acetone extracts of both marine plants were much denser than other solvent extracts. There were three

distinguishable fractions when acetone extract of *Z. noltii* was developed with 1:1 methanol:petroleum ether mobile phase (Figure 3.2). In addition, fractions obtained for *Z. noltii* extracts with 1:1 methanol:petroleum ether mobile phase were not separated well from each other. However, 1:1 methanol:petroleum ether mobile phase was resulted a better separation for *C. nodosa* extracts (Figure 3.3). There were two well separated fractions in acetone extracts of *C. nodosa* developed in 1:1 methanol:petroleum ether.

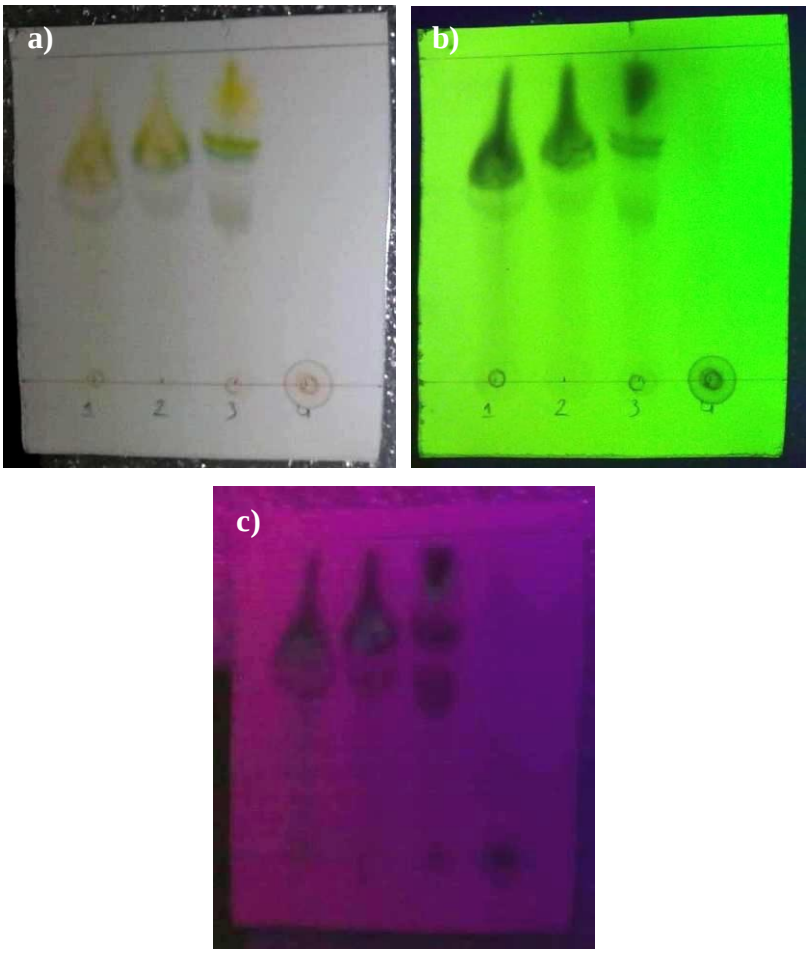

Figure 3.2 1-D TLC fractions of *Zostera noltii* extracts developed in 1:1 methanol: petroleum ether mobile phase: a) visible region, b) 254 nm and c) 366 nm (Spot 1:methanol, 2:ethanol, 3:acetone and 4:water extract, respectively).

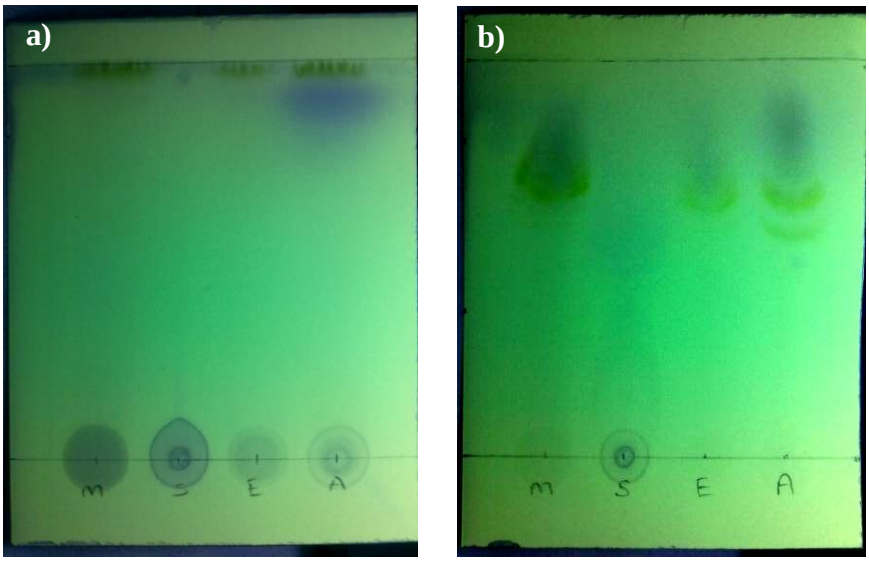

Figure 3.3 1-D TLC fractions of *Cymodocea nodosa* extracts monitored at 254 nm in: a) 1:1 ethyl acetate: petroleum ether and b) 1:1 methanol: petroleum ether mobile phase (Spot M:methanol, E:ethanol, A:acetone and S:water).

3.2 Synthesis of Sodium Zosterate

After the synthesis of sodium zosterate, it was characterized by TLC, FT-IR and ^{1}H-NMR spectroscopy. In TLC analysis, development of p-coumaric acid and sodium zosterate in 1:1 ethyl acetate:methanol mobile phase were compared based on their R_f values (Figure 3.4). When distances covered by two compounds compared, p-coumaric acid (R_f =0.81 ± 0.04) was developed faster than sodium zosterate (R_f=0.76 ± 0.04). The results of TLC analysis showed that p-coumaric acid was more likely to dissolve in mobile phase than sodium zosterate. This result also confirmed the reaction between p-coumaric acid and Py·SO_3 complex.

According to ^{1}H-NMR spectra of sodium zosterate, there were four doublets of doublet peaks in the aromatic region (Figure 3.5 and Table 3.1). Since the aromatic ring was substituted at para direction in sodium zosterate and aromatic hydrogens were symmetric, two of the doublet peaks were signs of aromatic hydrogens located at orto and meta positions. Other doublet peaks were resulted from double bond in the structure of sodium zosterate. Since the double bond was bonded to aromatic ring a shift to higher chemical shift values were observed and it was located between

peaks of aromatic ring. The intensities of aromatic hydrogen peaks were two times higher than that of double bond because each aromatic ring peak reflects two aromatic hydrogens whereas each double bond peaks were consist of single hydrogen. Since all hydrogens are symmetrically positioned in sodium zosterate, coupling constants of each peak are equal.

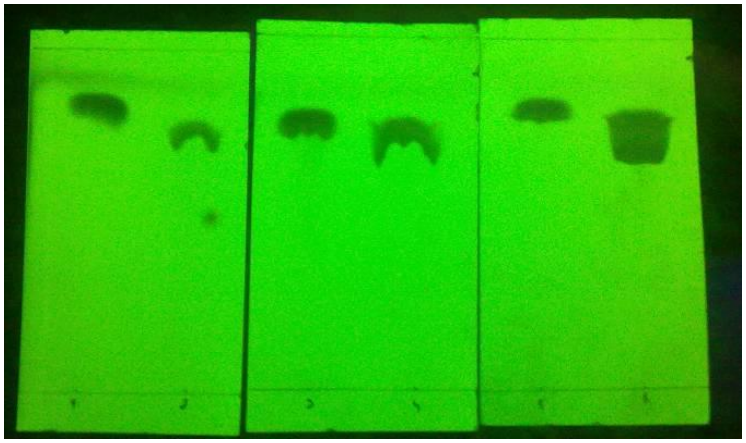

Figure 3.4. TLC of synthesized sodium zosterate (2, 4, 6) compared with p-coumaric acid (1, 3, 5) as three replicate.

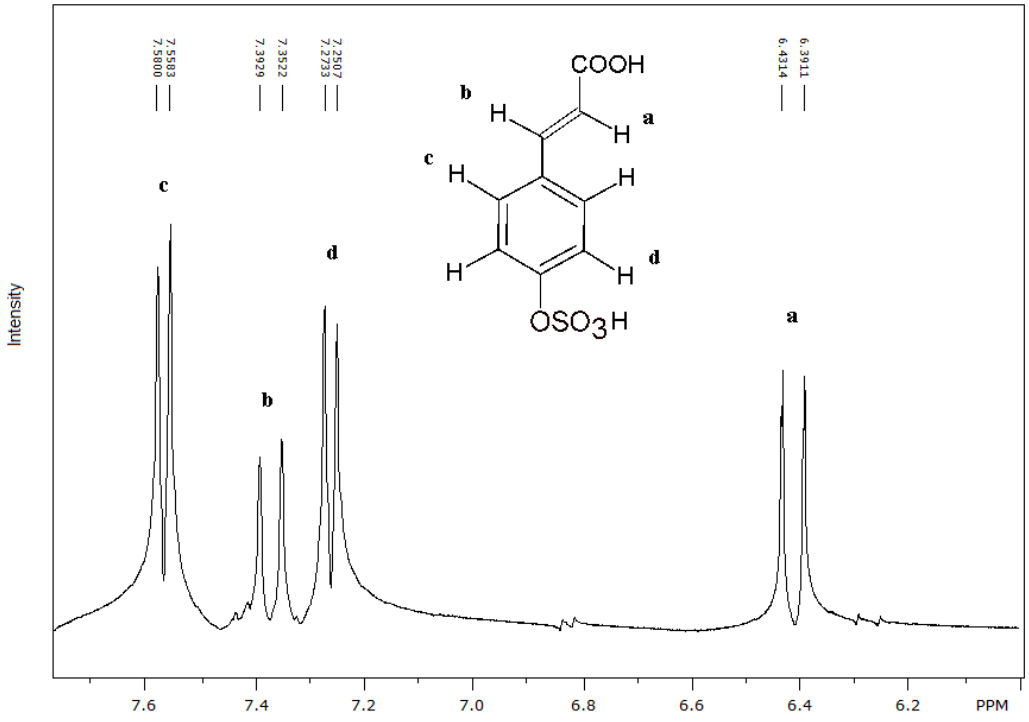

Figure 3.5. ^{1}H-NMR spectra of synthesized sodium zosterate.

Table 3.1 NMR data representing chemical shift (δ), splitting, number of protons and coupling constant (J) for zosteric acid.

δ (ppm)	Splitting	# H	J (Hz)
7.57	d	2	8.8
7.37	d	1	16.7
7.26	d	2	8.8
6.41	d	1	16.7

In order to determine functional group change during synthesis of sodium zosterate, FT-IR spectra of precipitates obtained in each step were recorded. Characteristic peaks found in FT-IR spectra of p-coumaric acid are as follows (Figure 3.6): O-H stretch of carboxyl group (3376 cm^{-1}), C=O stretch of carboxyl group (1672 cm^{-1}), olefinic C=C (1600 cm^{-1}), out-of-plane C-H bending (980 cm^{-1}), and p-substituted aromatic out of plane C-H bending (832 cm^{-1}). P-coumaric acid was used as starting material for sodium zosterate and its purity was over 95%. Characteristic peaks found in FT-IR spectra of the white precipitate after addition of NaOH are as follows (Figure 3.7): O-H stretch of sulphoxy group (3632 cm^{-1}), O-H stretch of carboxyl group (3412 cm^{-1}), olefinic C-H (3152 cm^{-1}), aromatic C-H (3052 cm^{-1}), C=O stretch of carboxyl group (1648 cm^{-1}), olefinic C=C (1568 cm^{-1}) and p-substituted aromatic out of plane C-H bending (848 cm^{-1}). Since the white precipitate after addition of NaOH contains solvents, unreacted starting materials and high amount of sodium sulphate, the intensities of peaks were not high as pure compounds; but, functional group changes were clearly identified. Characteristic peaks found in FT-IR spectra of the white precipitate after addition of methanol are as follows (Figure 3.8): O-H stretch of sulphoxy group (3632 cm^{-1}), O-H stretch of carboxyl group (3488 cm^{-1}), aromatic C-H (3036 cm^{-1}), C=O stretch of carboxyl group (1640 cm^{-1}), olefinic C=C (1556 cm^{-1}) and p-substituted aromatic out of plane C-H bending (852 cm^{-1}). The IR spectra of white precipitate after addition of methanol depicted characteristic peaks of sodium zosterate and theoretical estimations were well in line with experimental results. However, the amount of sodium zosterate was very low in precipitate after methanol addition, the higher amounts of sodium zosterate was obtained by evaporating the solvent until dryness.

The photographs of reaction media after each synthesis step were given in Figure 3.9. After evaporation step, 27.25 g of sodium zosterate was obtained with 94% efficiency.

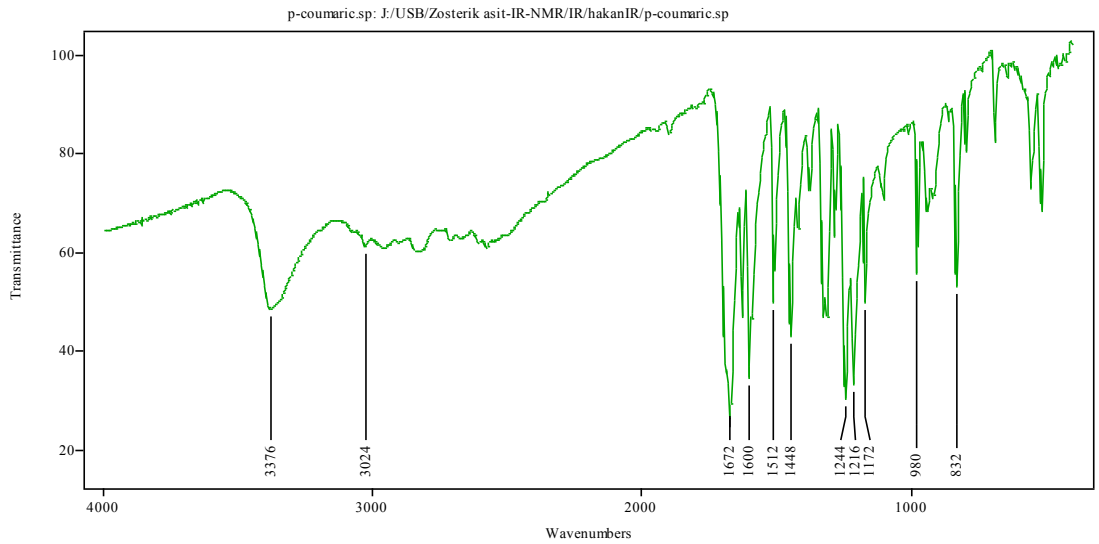

Figure 3.6 IR spectra of p-coumaric acid.

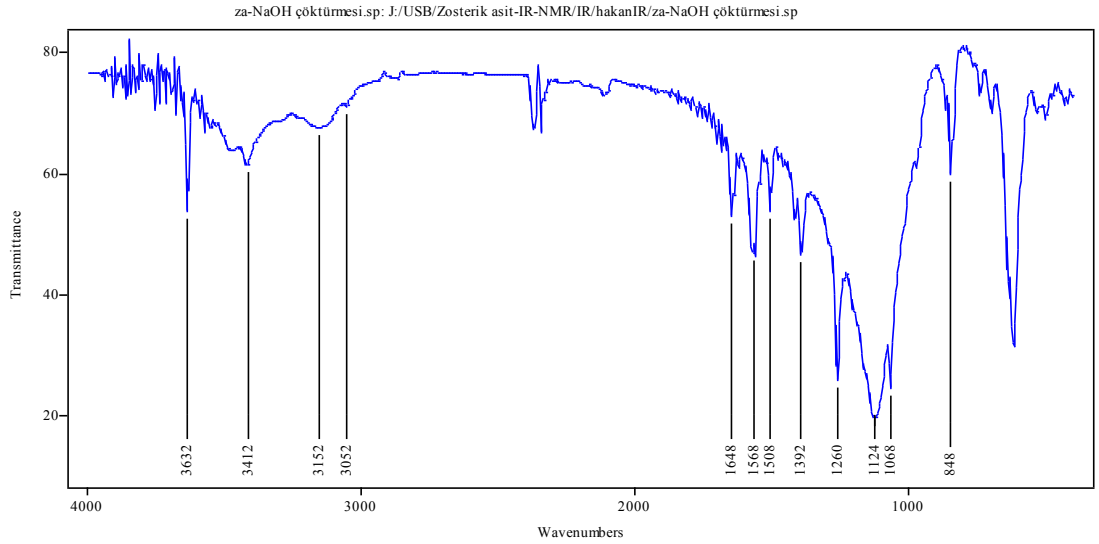

Figure 3.7 IR spectra of white precipitate obtained after addition of NaOH.

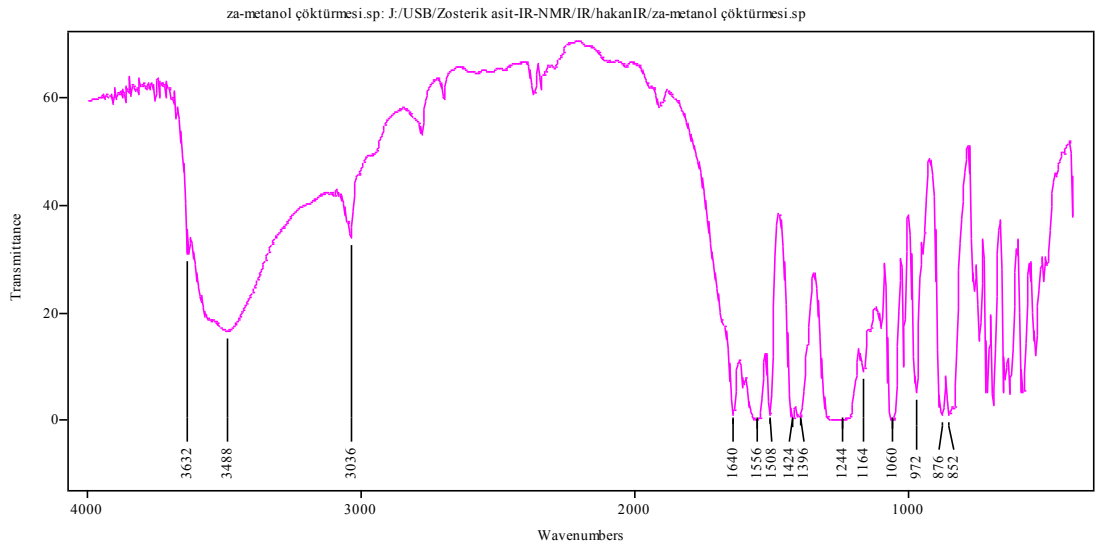

Figure 3.8 IR spectra of white precipitate obtained after addition of methanol.

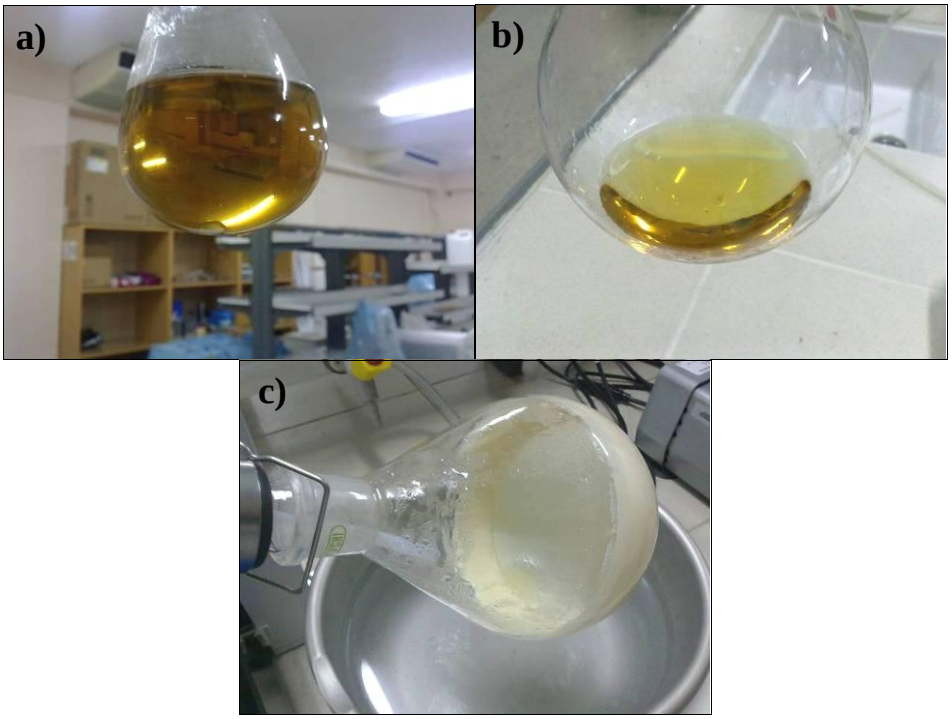

Figure 3.9 Photographs of reaction media and precipitated sodium zosterate in different synthesis steps: a) Just after reaction, b) after extraction and precipitation with methanol, c) zosteric acid after evaporation of DMF.

3.3 Results of Acute Toxicity Tests on *A. salina*

According to results of toxicity tests, toxicities of tested compounds were increased in the order of zosteric acid, sodium sulphate, *C. nodosa* extract, *Z. noltii*

extract, diuron, potassium dichromate, p-coumaric acid, CuP, ZnP and irgarol. The acute toxicity results of irgarol were given in Figure 3.10. More than 80% of the test organisms were dead just after 2 h of exposure to 185 µg/mL of irgarol. After the test, all test organisms were dead at 185 and 93 µg/mL of irgarol. Also, more than 50% of test organisms were dead in 37 µg/mL irgarol and 50 µL DMSO containing control. The acute toxicity results of diuron were given in Figure 3.11. Diuron showed its toxicity after 5 h of exposure. The survival percentages of living test organisms for all concentrations of diuron were above 50% at the end of the test. The acute toxicity results of ZnP were given in Figure 3.12. The effect of ZnP was observed after 2nd hour of the test. The survival percentage of test organisms at 2nd hour of the test was more than 80% at 185 µg/mL ZnP. At the end of the test, there were more than 50% deaths at 185 and 93 µg/mL ZnP containing wells. The acute toxicity results of CuP were given in Figure 3.13. CuP showed its toxicity after 3 h of exposure. There were any living organisms in 185 µg/mL CuP wells at the end of the test. However, the mortality percentage was below 30% at lower concentrations of CuP except 50 µL DMSO containing control. The acute toxicity results of *Z. noltii* extracts were given in Figure 3.14. *Z. noltii* extracts were not toxic as booster biocides. Maximum mortality was below 30% at all *Z. noltii* extract concentrations. The acute toxicity results of *C. nodosa* extracts were given in Figure 3.15. *C. nodosa* extracts were more toxic than *Z. noltii* extracts but its toxicity was weaker than booster biocides. The maximum mortality percentage was lower than 50% at 20 µL *C. nodosa* extract. The acute toxicity results of potassium dichromate were given in Figure 3.16. Potassium dichromate is used as reference chemical in acute toxicity tests when *A. salina* selected as test organism. Toxicity of potassium dichromate was over 50% on *A. salina* at highest concentration. Potassium dichromate showed its toxic effects just after first hour of toxicity test. The acute toxicity results of p-coumaric acid were given in Figure 3.17. P-coumaric acid showed its toxic effects after 2nd hour of the test. P-coumaric acid decreased the survival percentage of *A. salina* more than 80% at 5th hour of the toxicity test. The acute toxicity test results of sodium sulphate were given in Figure 3.18. Sodium sulphate was one of the compounds with low toxicity. Its toxic effect on *A. salina* was below 30% exposed to

185 µg/mL at the end of the test. The toxicity test results of zosteric acid were given in Figure 3.19. Zosteric acid was not toxic to *A. salina* at all studied concentrations.

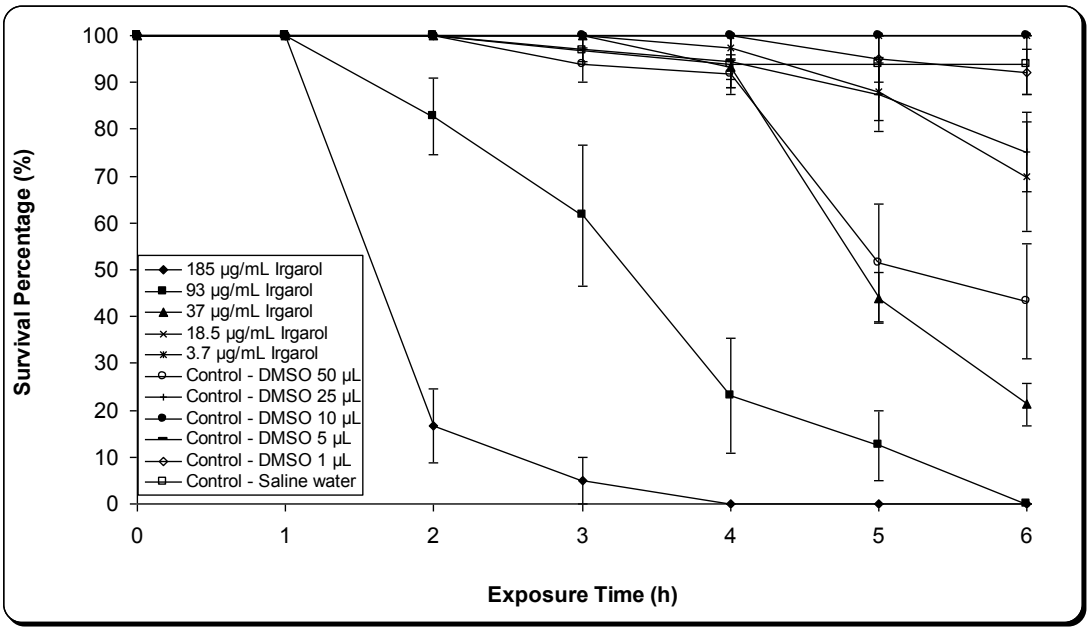

Figure 3.10 Acute toxicity of irgarol on *A. salina* nauplii. Data are given as Mean±SEM (with four replicates at each point).

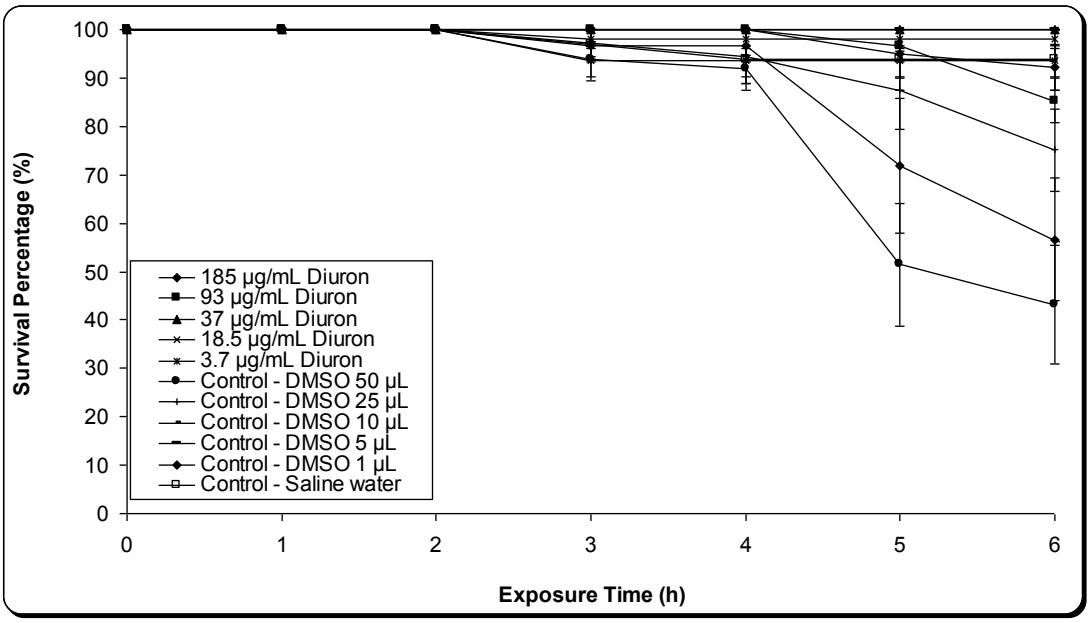

Figure 3.11 Acute toxicity of diuron on *A. salina* nauplii. Data are given as Mean±SEM (with four replicates at each point).

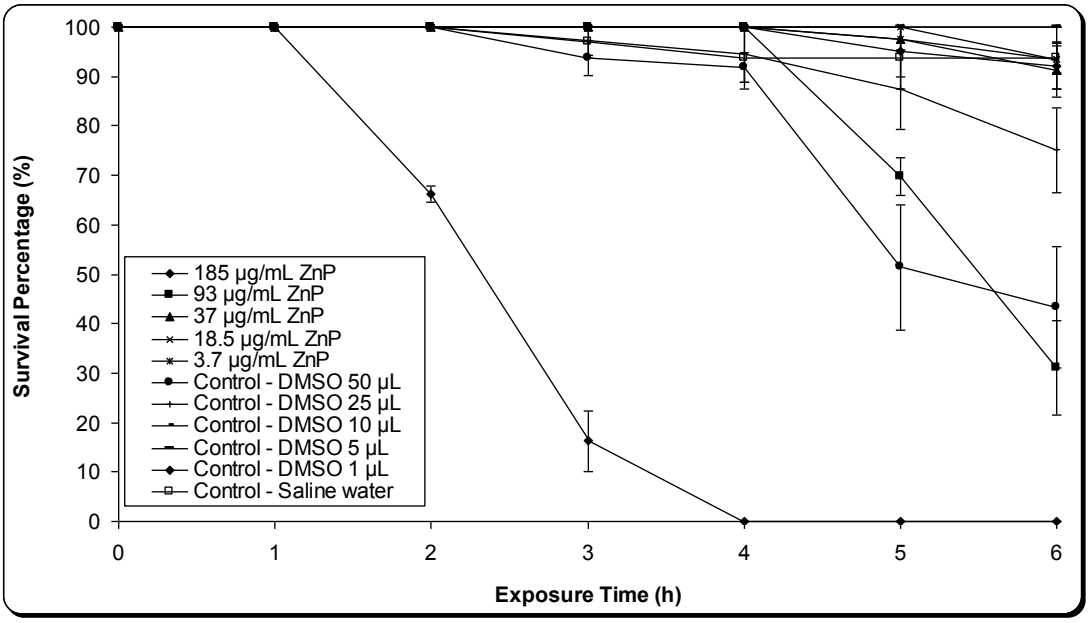

Figure 3.12 Acute toxicity of zinc pyrithione (ZnP) on *A. salina* nauplii. Data are given as Mean±SEM (with four replicates at each point).

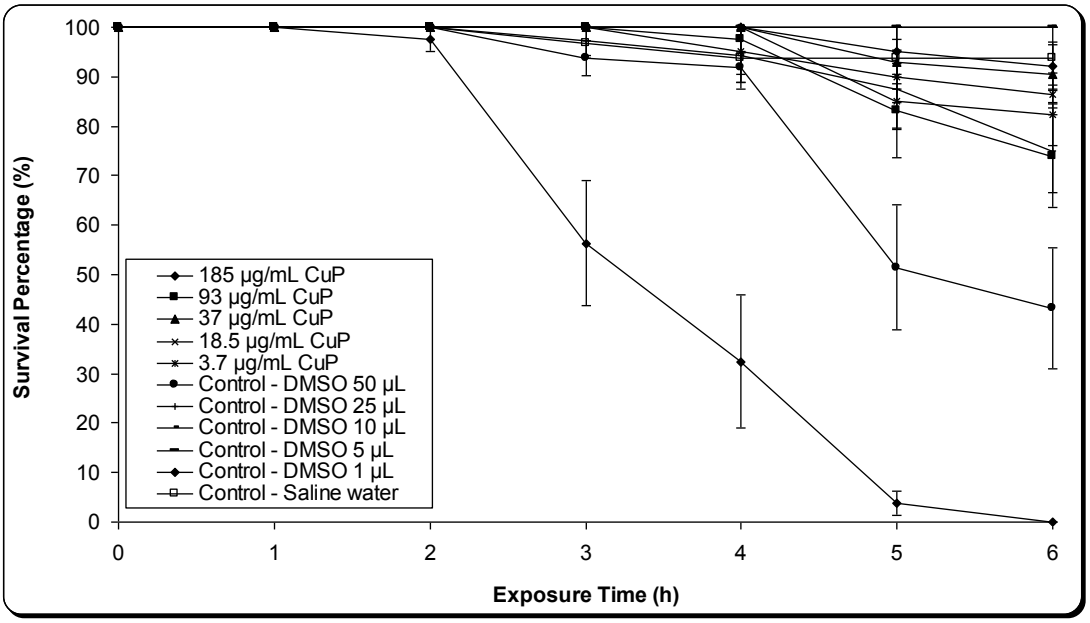

Figure 3.13 Acute toxicity of copper pyrithione (CuP) on *A. salina* nauplii. Data are given as Mean±SEM (with four replicates at each point).

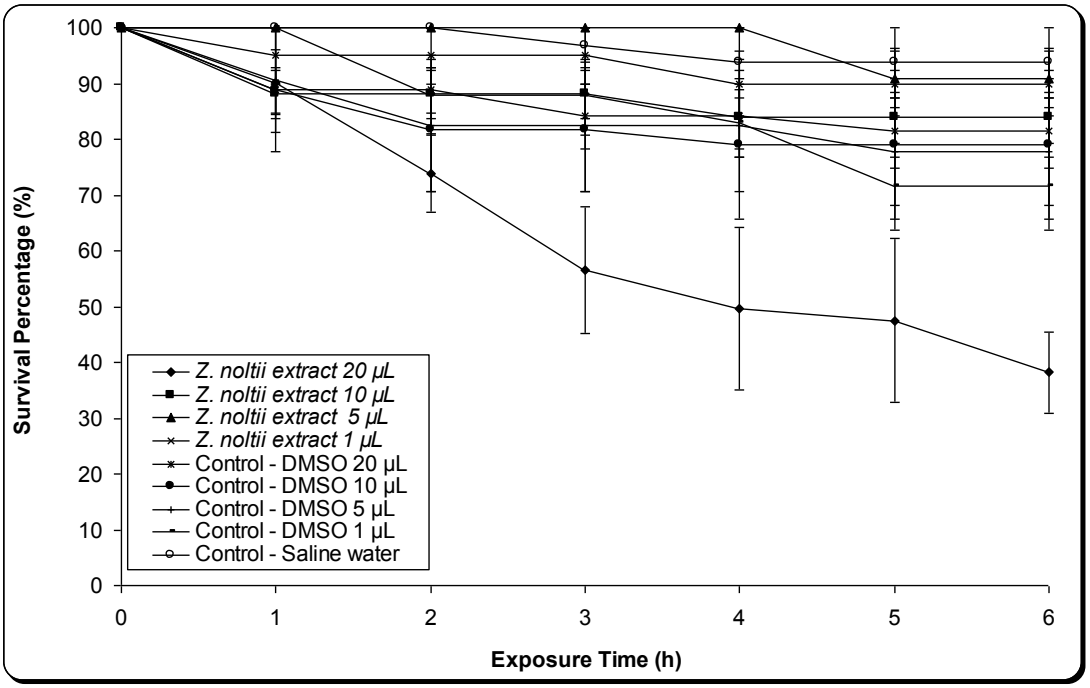

Figure 3.14 Acute toxicity of *Z. noltii* extract on *A. salina* nauplii. Data are given as Mean±SEM (with four replicates at each point).

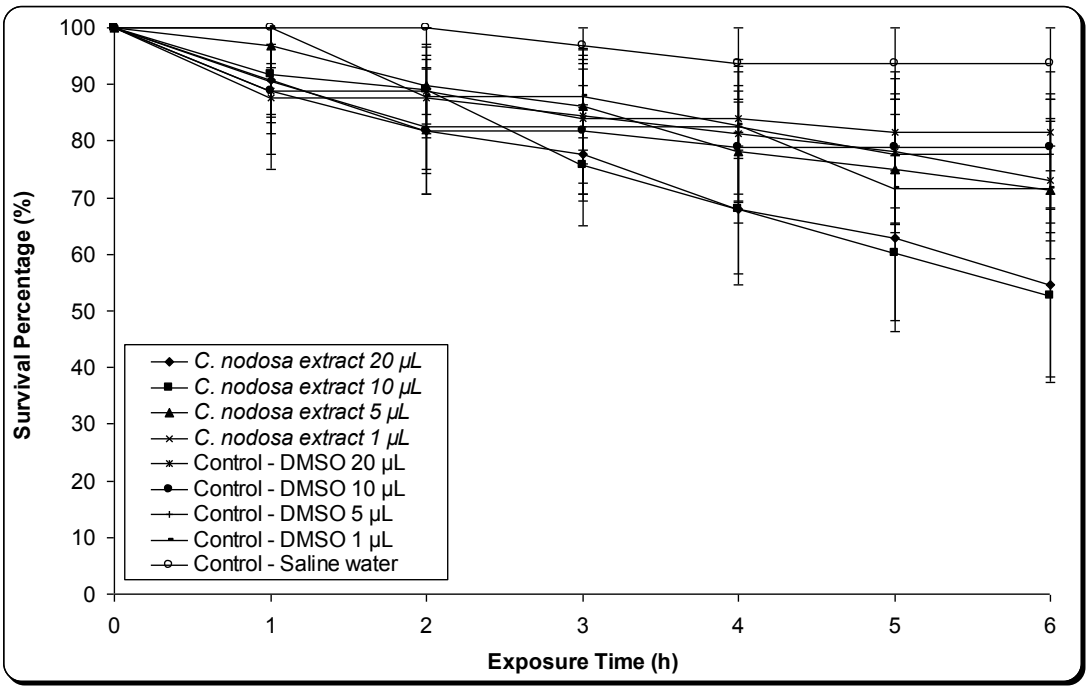

Figure 3.15 Acute toxicity of *C. nodosa* extract on *A. salina* nauplii. Data are given as Mean±SEM (with four replicates at each point).

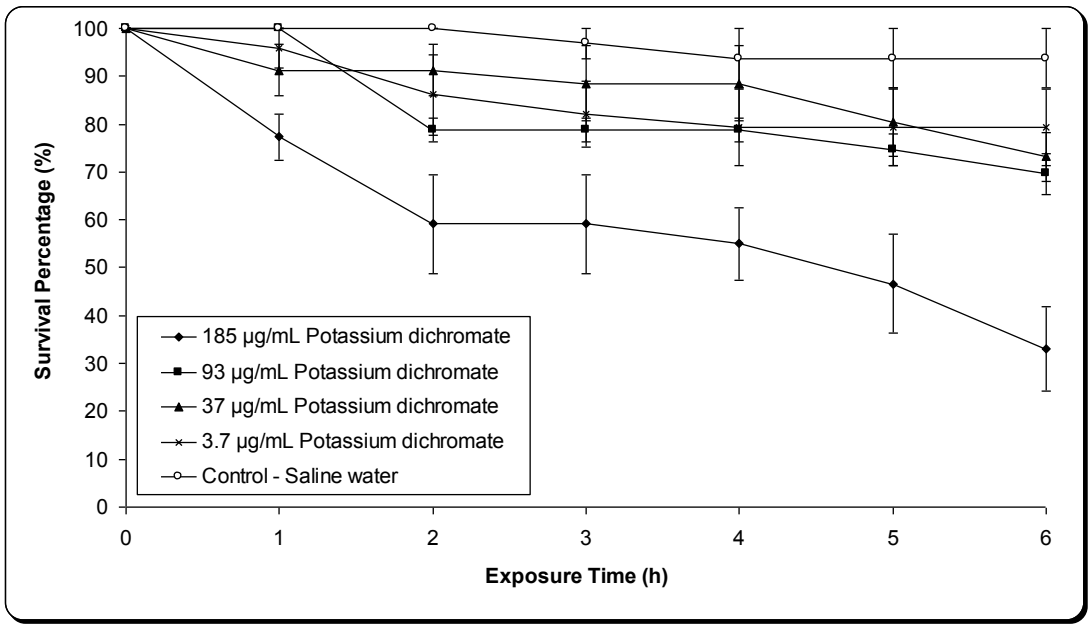

Figure 3.16 Acute toxicity of potassium dichromate on *A. salina* nauplii. Data are given as Mean±SEM (with four replicates at each point).

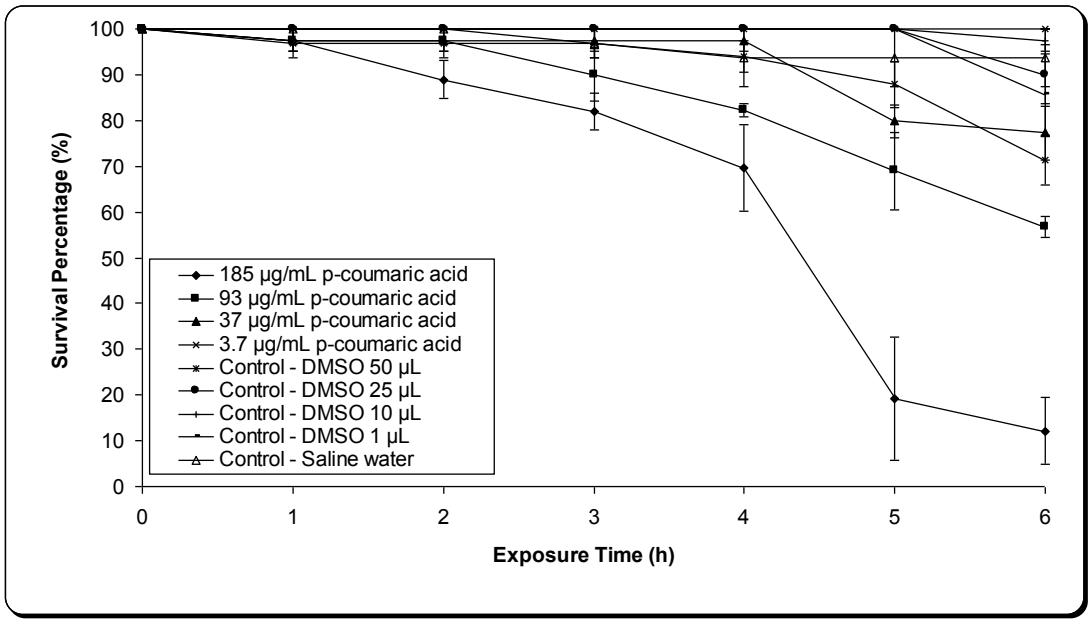

Figure 3.17 Acute toxicity of p-coumaric acid on *A. salina* nauplii. Data are given as Mean±SEM (with four replicates at each point).

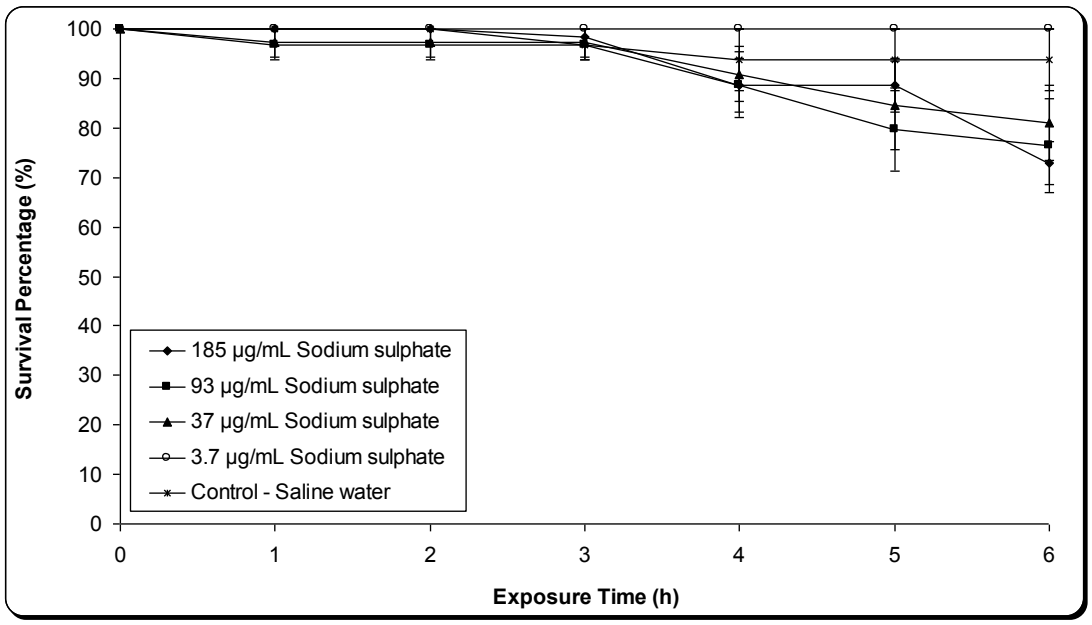

Figure 3.18 Acute toxicity of sodium sulphate on *A. salina* nauplii. Data are given as Mean±SEM (with four replicates at each point).

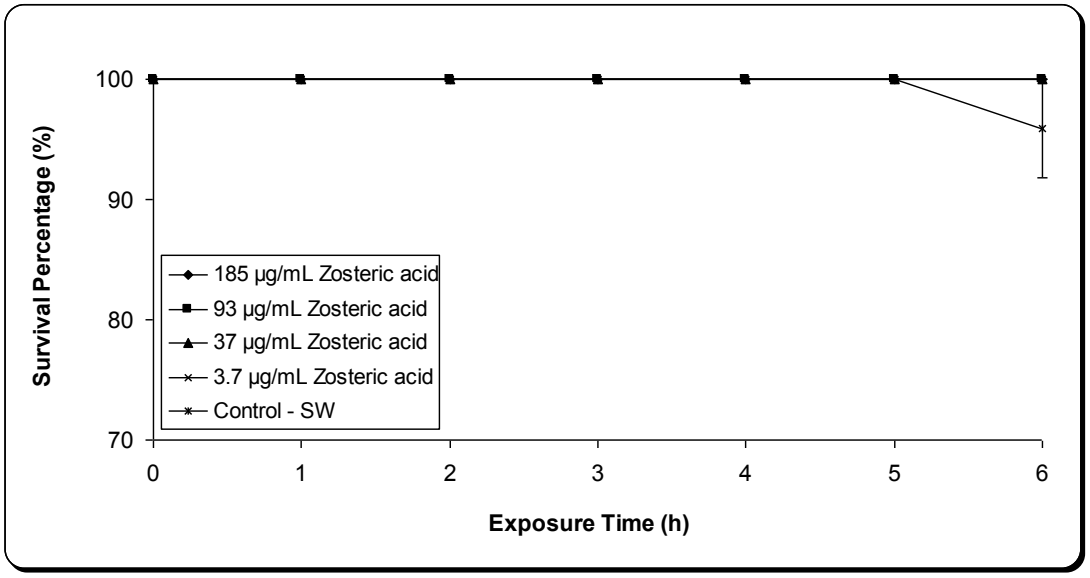

Figure 3.19 Acute toxicity of zosteric acid on *A. salina* nauplii. Data are given as Mean±SEM (with four replicates at each point).

3.4 Results of Hatching Success and Larval Morphology Tests on *A. salina*

According to the HP results, irgarol was not effective on the hatching of *A. salina* cysts even at the highest concentration available in saline water (Figure 3.20). In

addition, statistically significant differences were not observed between test groups and control ($p<0.05$). HPs for control, 1 and 5 mg/L Irgarol groups were 68.3±3.3%, 63.9±3.1% and 54.4±5.8%, respectively. On the other hand, diuron significantly decreased the HPs of *A. salina* cysts at studied concentrations (Figure 3.21). While HPs of control and 1 mg/L diuron treated groups were not remarkably different from each other, statistically significant decrease was observed in HP of 25 mg/L diuron treated group and hatching percentage of this group was found as 33.9±2.8% ($p<0.05$). Diuron was effective than irgarol on the HP of *A. salina* cysts. Embryonic toxicity of CuP was higher than irgarol and diuron (Figure 3.22). CuP was decreased hatching percentage of nauplii more than 50% compared to control group. As the concentration of CuP increased, hatching percentage did not change proportionally. There were not any significant differences between hatching percentages at different concentrations.

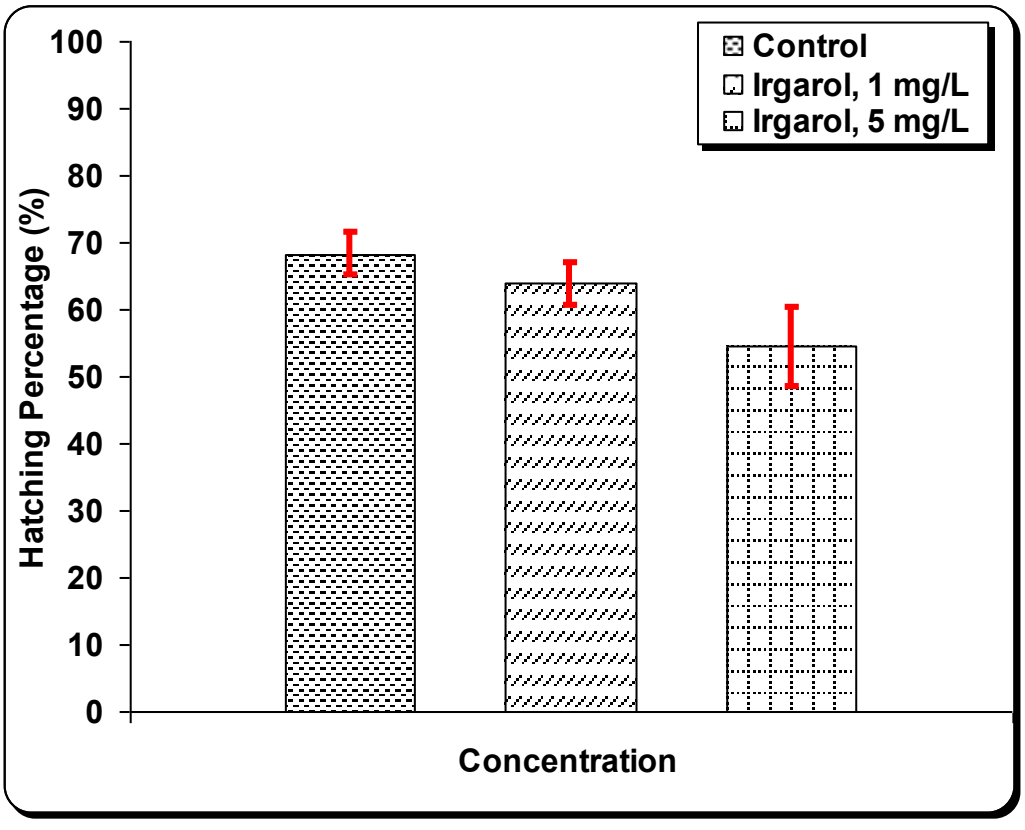

Figure 3.20 Hatching percentages of *A. salina* cysts exposed to different irgarol concentrations. According to One-Way ANOVA results, there was no statistical difference between data groups ($p<0.05$). Data are given as Mean±SEM (with four replicates at each point).

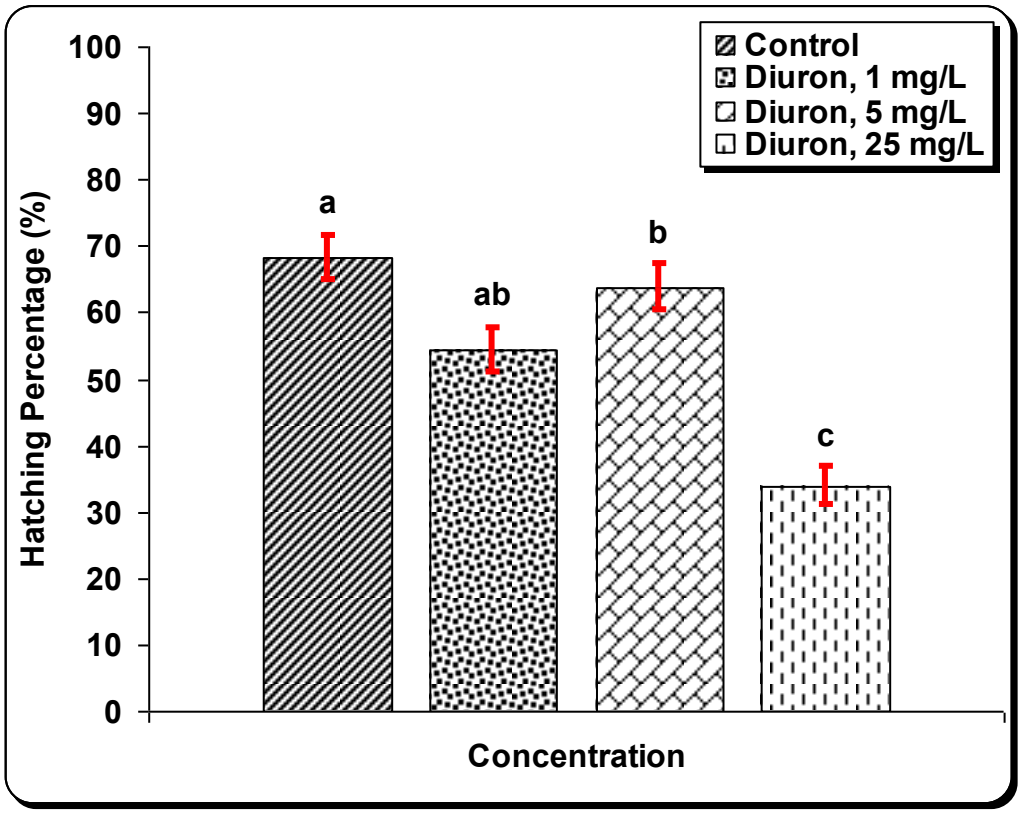

Figure 3.21 Hatching percentages of *A. salina* cysts exposed to different diuron concentrations. According to One-Way ANOVA results, there were statistically significant differences between data groups ($p<0.05$). Data are given as Mean±SEM (with four replicates at each point).

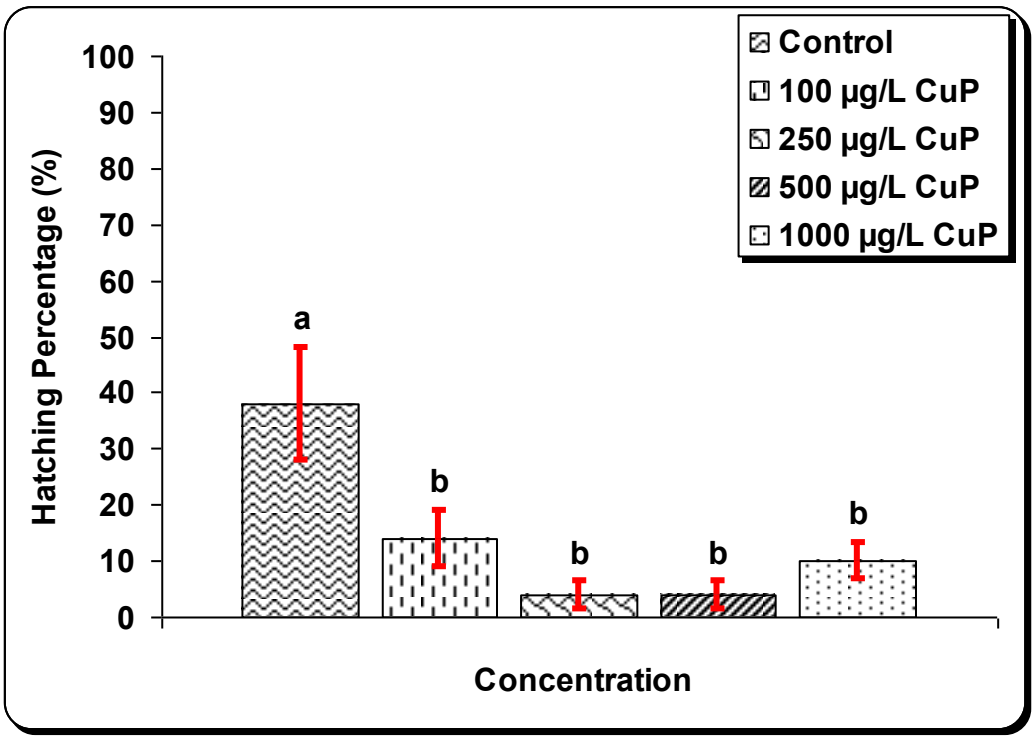

Figure 3.22 Hatching percentages of *A. salina* cysts exposed to different CuP concentrations. According to One-Way ANOVA results, there were statistically significant differences between data groups ($p<0.05$). Data are given as Mean±SEM (with four replicates at each point).

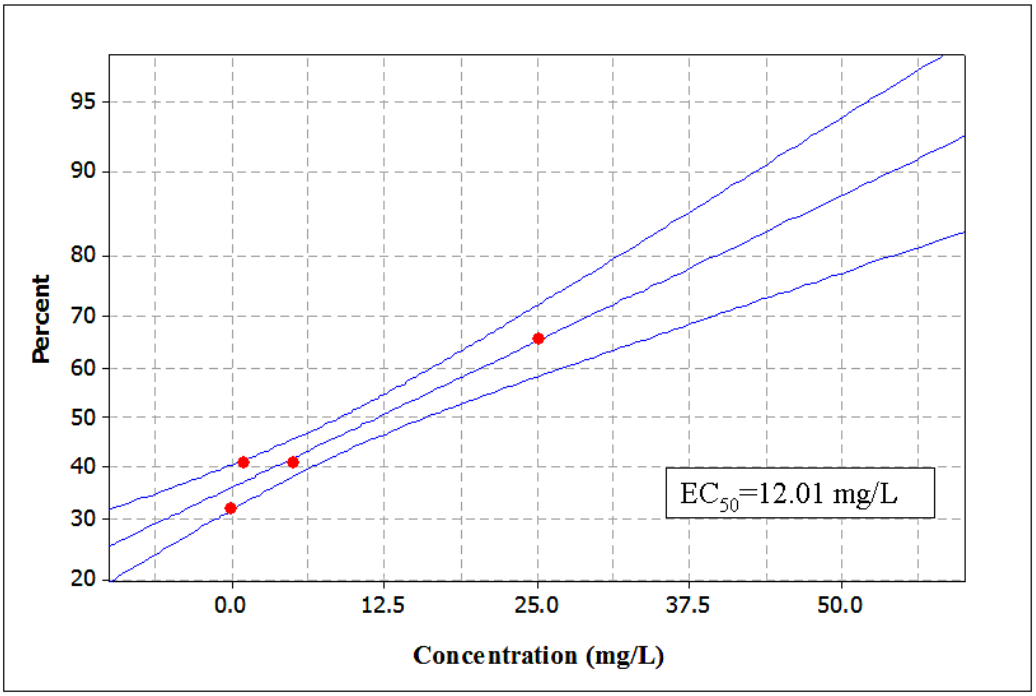

Figure 3.23 Probability plot used in estimation of EC_{50} for diuron (CI 95%).

According to the results of probit analysis, EC_{50} value for diuron was found as 12.01 mg/L (Figure 3.23). However, it was not possible to calculate EC_{50} value for irgarol, because irgarol did not show remarkable toxicity even at a concentration very close to its solubility limit. Since there are few studies on the inhibition of hatching percentage of *A. salina*, it was not possible to compare the EC_{50} value of diuron with other biocides. In the scientific literature, the inhibitory effects of different toxicants have been reported on the hatching percentage of *A. salina* and the effect of diuron was compared with current literature in Table 3.2 (Brix, Gerdes, Adams, & Grosell, 2006; Caldwell, Bentley, & Olive, 2003).

According to the results of morphological analysis, morphologies of test group treated with irgarol were not different compared to control group (Figures 3.24 and 3.25). This result also confirms the HP result of irgarol treated test groups. On the other hand, diuron did not alter the morphology of cysts or nauplii but affected the hatching ability of cysts. As can be seen from Figure 3.26, some nauplii exposed to 25 mg/L diuron concentration were unsuccessful to break cyst wall completely. The retardations and arrestments were observed on developing *Artemia* embryos at pre-nauplius E-1 and E-2 stages in groups treated with diuron. On the other hand, there were no morphological changes in embryo exposed to CuP (Figure 3.27). Total length of newly hatched nauplii was not affected from irgarol and diuron (Table 3.3). Mean total length for control group was 0.54±0.03 mm. However, mean total lengths for 5 mg/L irgarol and 25 mg/L diuron treated groups were 0.54±0.02 and 0.56±0.06 mm, respectively. These results indicated that diuron and irgarol were not effective on the body length of *A. salina* nauplii.

Table 3.2. EC_{50} values of different chemicals in comparison with diuron for embryo of *Artemia* sp.

Tested Chemicals	Test Method/Period	Concentration	Reference
Cadmium	EC_{50}/48 h	11.9 mg/L	Brix et al., 2006
Copper	EC_{50}/48 h	11.8 µg/L	Brix et al., 2006
Zinc	EC_{50}/48 h	289.0 µg/L	Brix et al., 2006
2E,4E-decadienal	EC_{50}/72 h	3.9 µg/mL	Caldwell, Bentley, & Olive, 2003
Diuron	EC_{50}/24 h	12.0 mg/L	This thesis

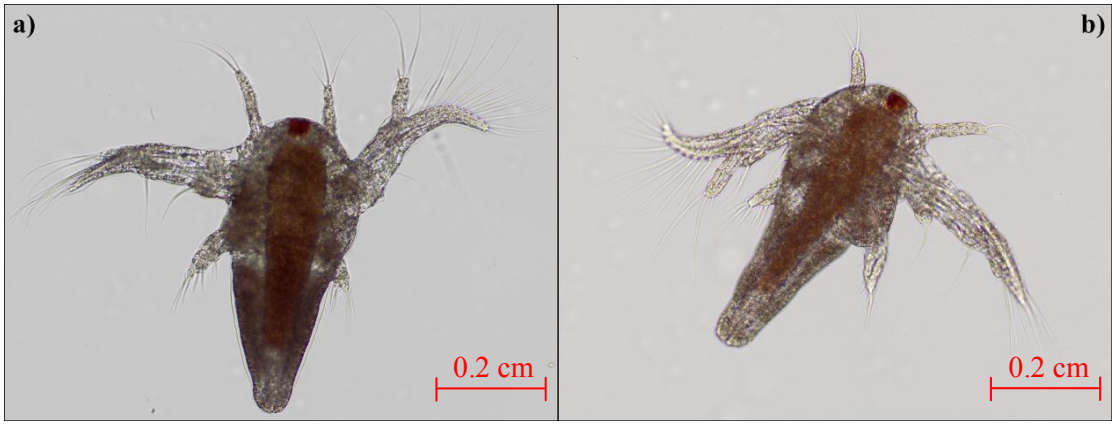

Figure 3.24 Morphological characteristics of *A. salina* nauplii after 24 h exposure to a) Control, and b) 0.5 mL DMSO containing control.

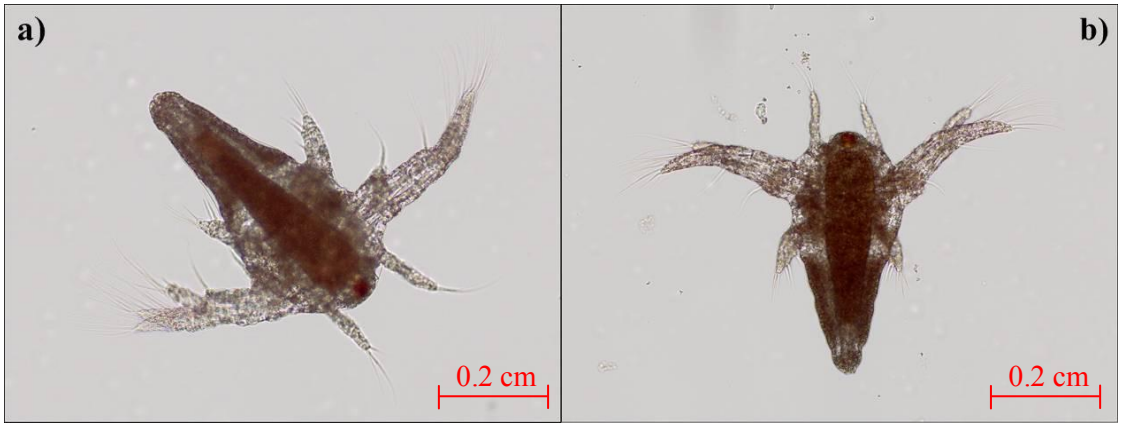

Figure 3.25 Morphological characteristics of *A. salina* nauplii after 24 h exposure to a) 1 mg/L Irgarol, and b) 5 mg/L Irgarol.

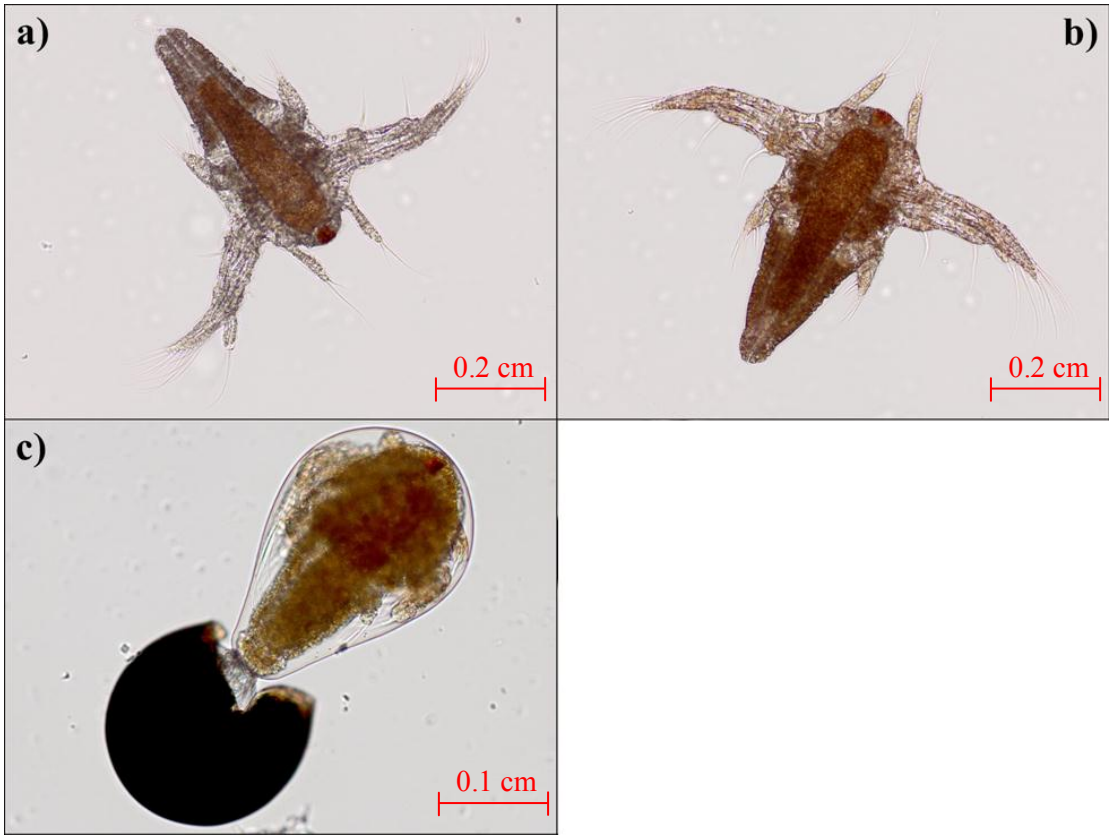

Figure 3.26 Morphological characteristics of *A. salina* nauplii after 24 h exposure to a) 5 mg/L Diuron, b) 25 mg/L Diuron, and c) 25 mg/L Diuron.

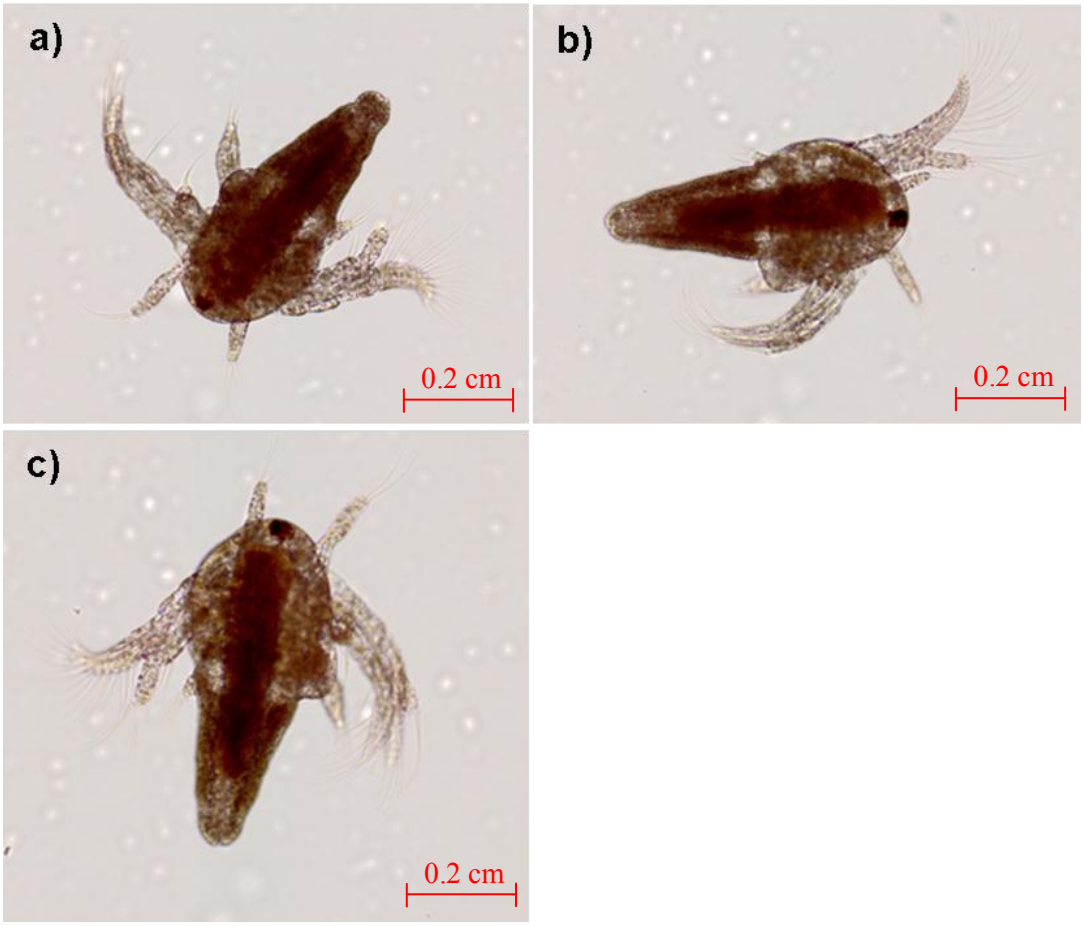

Figure 3.27 Morphological characteristics of *A. salina* nauplii after 24 h exposure to a) Control, b) 100 µg/L CuPT, and c) 1000 µg/L CuPT.

Table 3.3 Total length of newly hatched nauplii after 24 h hatching period in different irgarol and diuron concentrations (N: population number, SD: Standart deviation).

Concentration	N	Mean±SD (mm)	Minimum (mm)	Maximum (mm)
Control	12	0.54±0.03	0.51	0.59
1 mg/L Irgarol	12	0.53±0.03	0.51	0.60
5 mg/L Irgarol	12	0.54±0.02	0.51	0.59
5 mg/L Diuron	12	0.53±0.02	0.49	0.57
25 mg/L Diuron	12	0.56±0.06	0.52	0.73

3.5 Results of Acetylcholine Esterase Activity Screening Experiments

Before the kinetic analysis, acetylcholine esterase from *A. salina* was characterized based on homogenization type, stability and effects of storing conditions, temperature, pH and substrate concentration. Higher enzyme activity was obtained with freeze-thaw method compared to direct homogenization (Figure 3.28). This could be a result of better disruption of tissues with freeze-thaw method. Stability of the enzyme was not dramatically changed depended on storage time and conditions (Figure 3.29). The effect of temperature on the enzyme activity was given in Figure 3.30. The activity of the enzyme was decreased as the temperature increased. Optimum temperature for AChE was found as 25 °C. The activity of the enzyme was nearly zero above temperatures higher than 65 °C. The effect of the pH on enzyme activity was depicted in Figure 3.31. Optimum pH was found as 8.5. The enzyme activity was followed the Michaelis-Menten behavior (Figure 3.32). Between 0.05-0.5 mM substrate concentrations, enzyme activity was reached to steady state at 0.43 U/mL. Michaelis-Menten constants were found from the Lineweaver-Burk plot (Figure 3.33). K_m and V_{max} for AChE from *A. salina* were found as 0.004 mM and 1.448 μmol min^{-1} mg $enzyme^{-1}$, respectively.

The inhibitory effect of irgarol, diuron and zosteric acid on AChE was studied with kinetic experiments. According to Michaelis-Menten plots, irgarol has shown inhibitory effect on AChE in the range of studied concentrations (Figure 3.34). However, diuron and zosteric acid did not inhibited AChE. As can be seen from Figure 3.34, irgarol decreased the maximum enzyme activity about two folds. According to results, AChE from *E. electricus* was inhibited by irgarol reversibly. The inhibition type of the enzyme was determined from the Lineweaver-Burk plots as competitive type inhibition for irgarol when compared to free enzyme (Figure 3.35). The Michaelis-Menten constants and maximum velocities for free enzyme and irgarol were given in Table 3.4. The V_{max} and K_m values for free enzyme were found as 153.8 nmol mg $enzyme^{-1}$ min^{-1} and 1.17 mM, respectively.

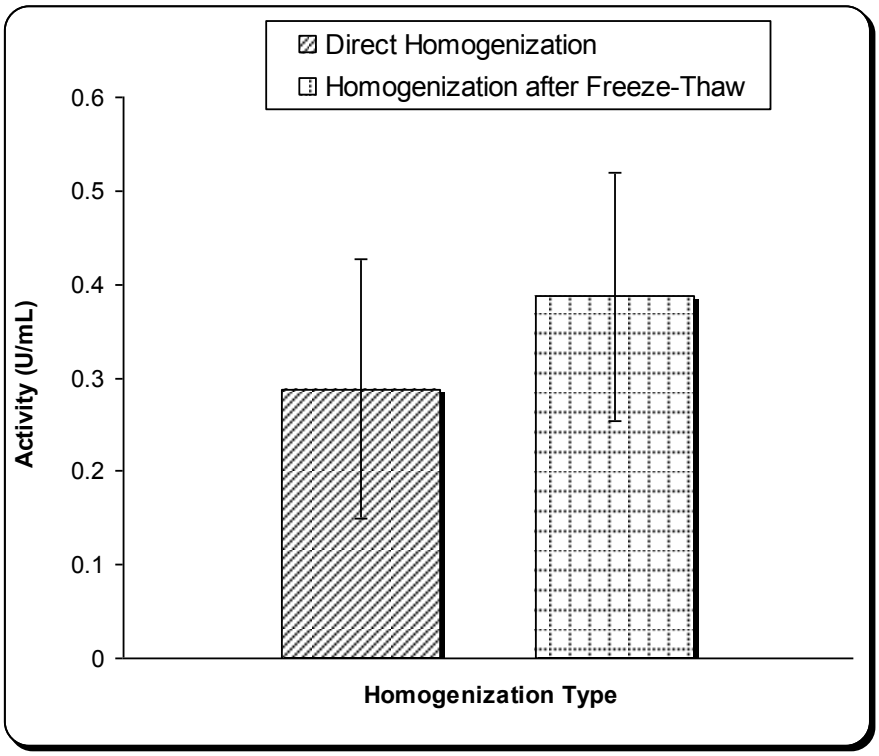

Figure 3.28 Effect of homogenization type on the activity of acetylcholine esterase from *A. salina*. Data are given as Mean±SD (with three replicates at each point).

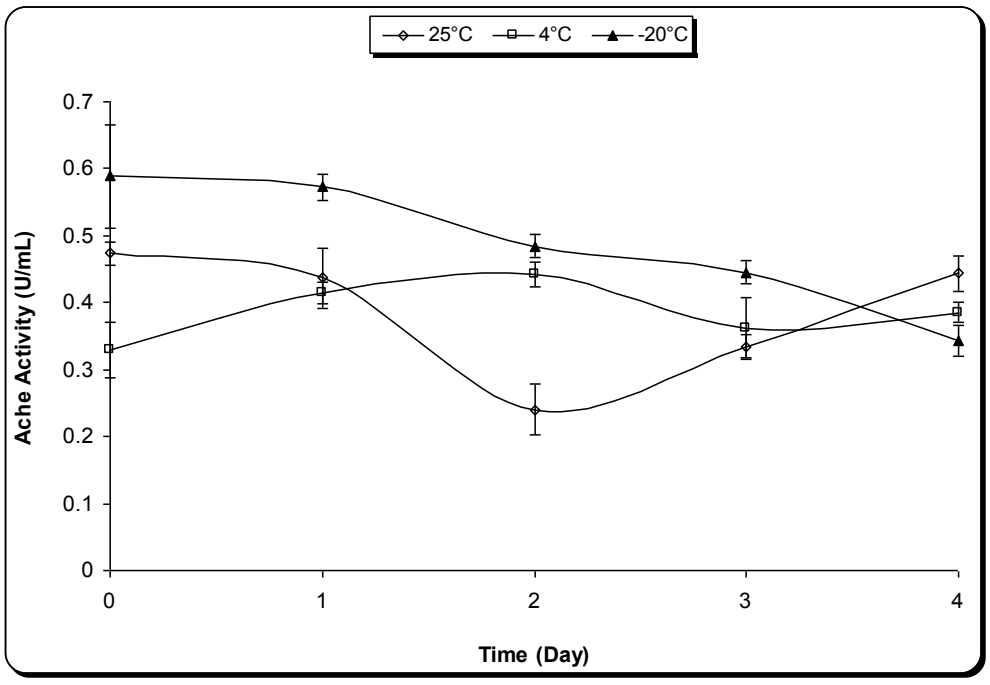

Figure 3.29 The effect of time and storage conditions on the activity of acetylcholine esterase from *A. salina* (-20 °C, 4 °C and 25 °C). Data are given as Mean±SD (with three replicates at each point).

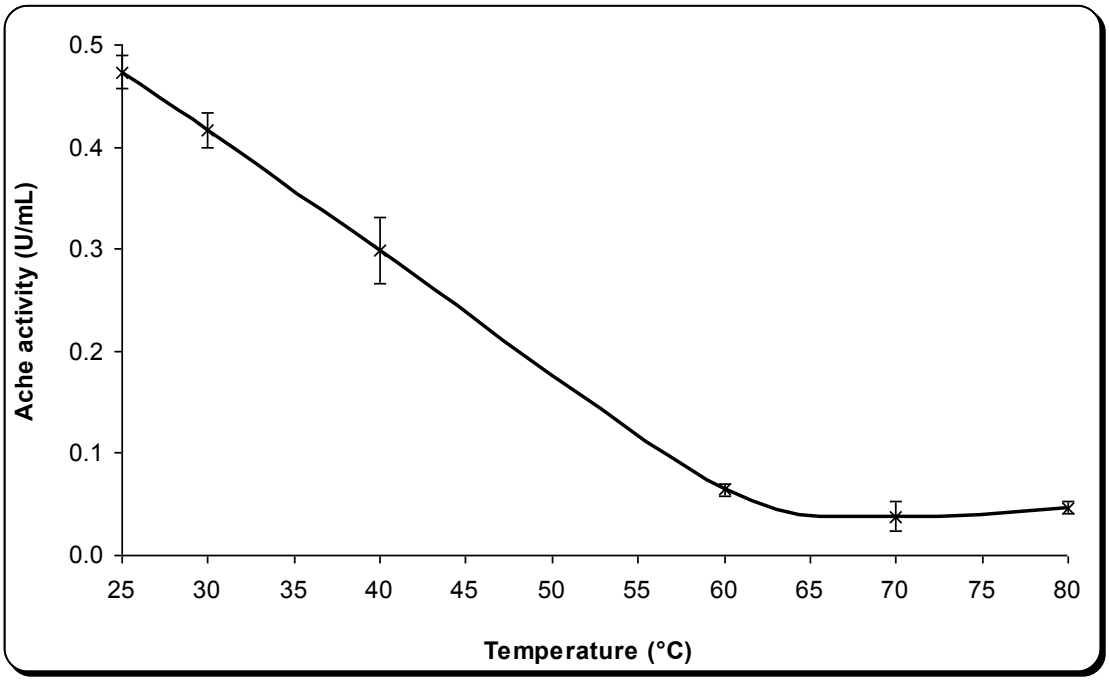

Figure 3.30 The effect of temperature on the activity of acetylcholine esterase from *A. salina*. Data are given as Mean±SD (with three replicates at each point).

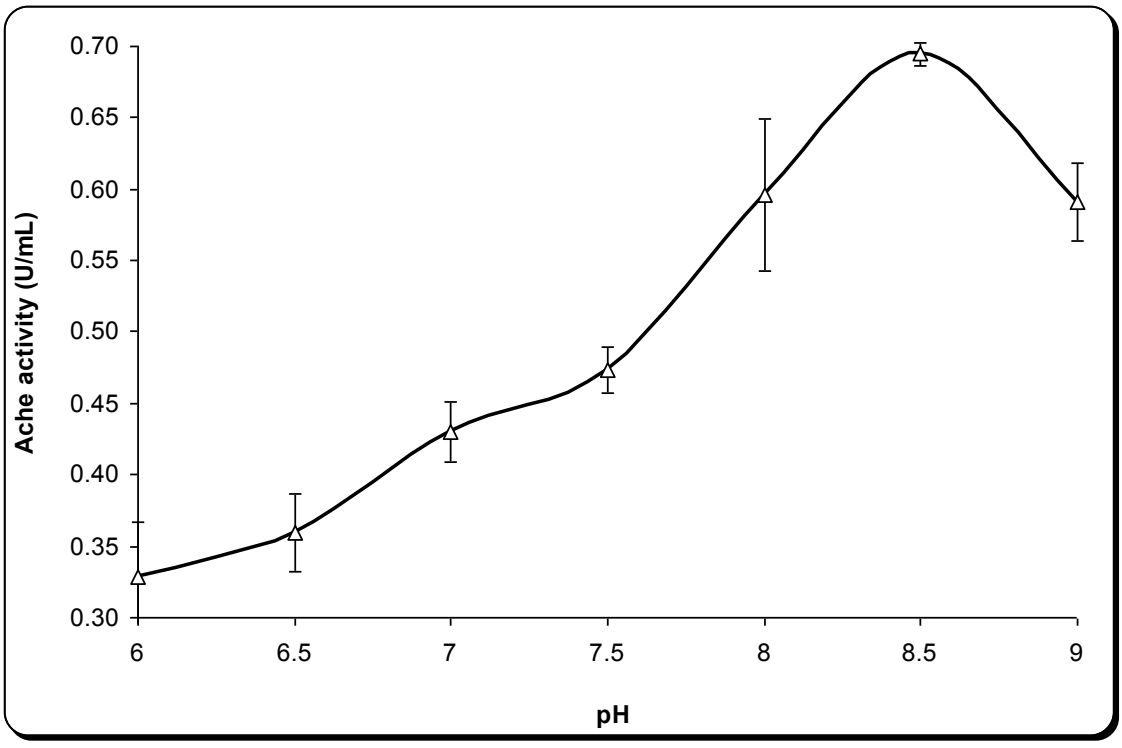

Figure 3.31 The effect of pH on the activity of acetylcholine esterase from *A. salina.* Data are given as Mean±SD (with three replicates at each point).

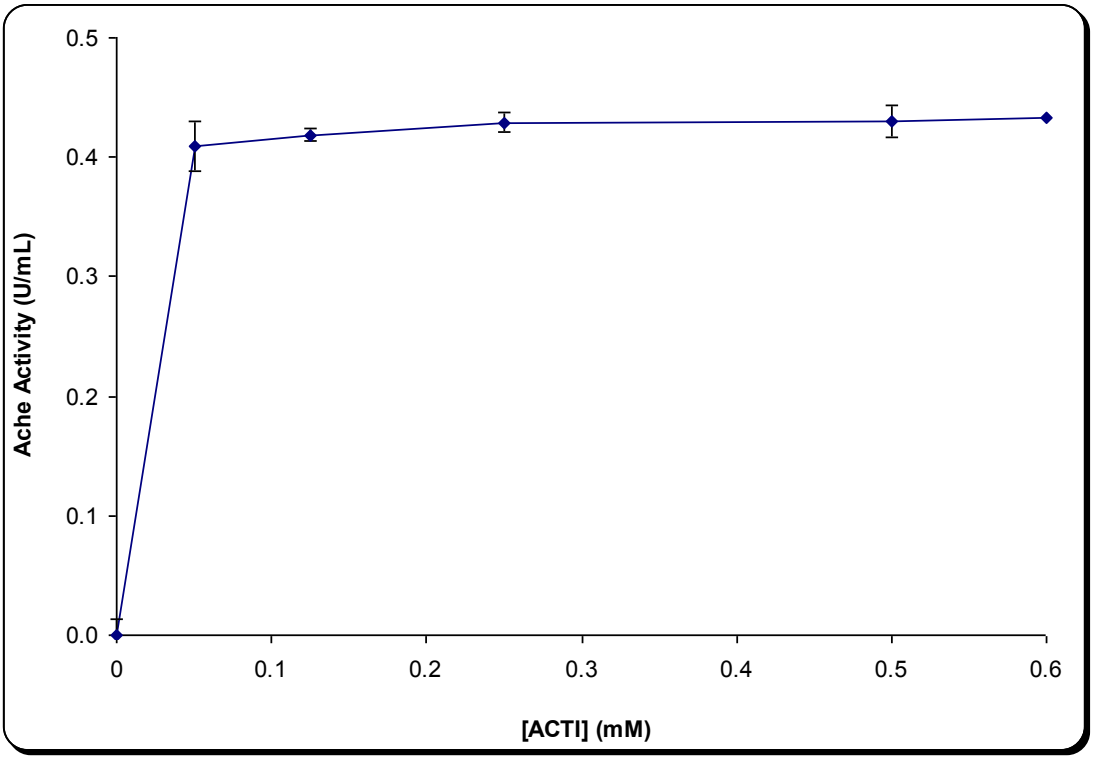

Figure 3.32 The effect of substrate concentration (acetylcholine iodide) on the activity of acetylcholine esterase from *A. salina*. Data are given as Mean±SD (with three replicates at each point).

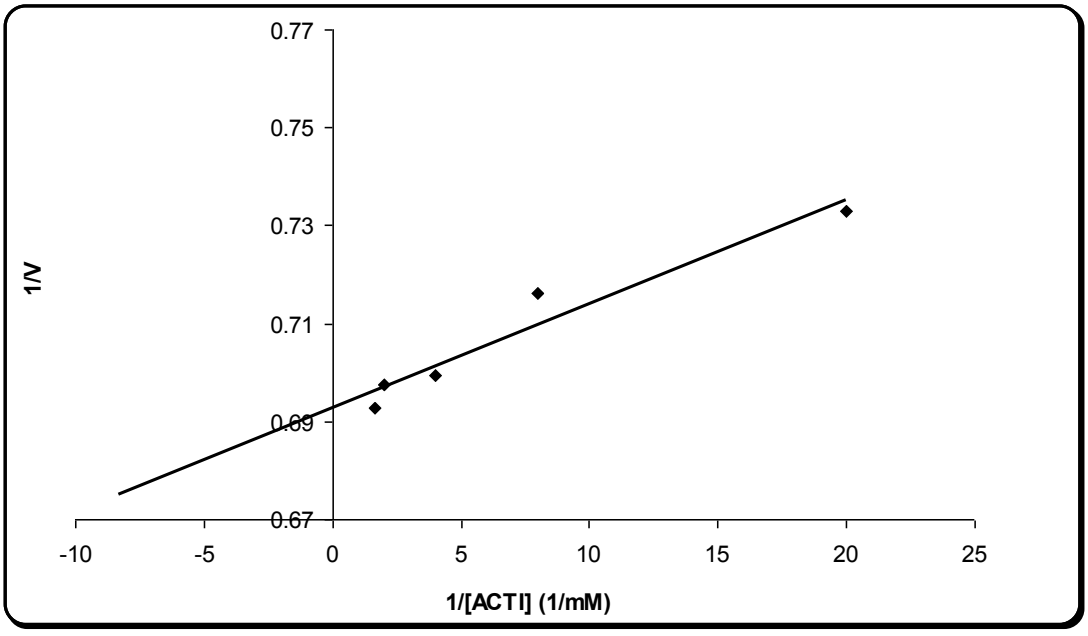

Figure 3.33 Lineweaver-Burk plot for acetylcholine esterase from *A. salina*. Data are given as Mean±SE (with three replicates at each point).

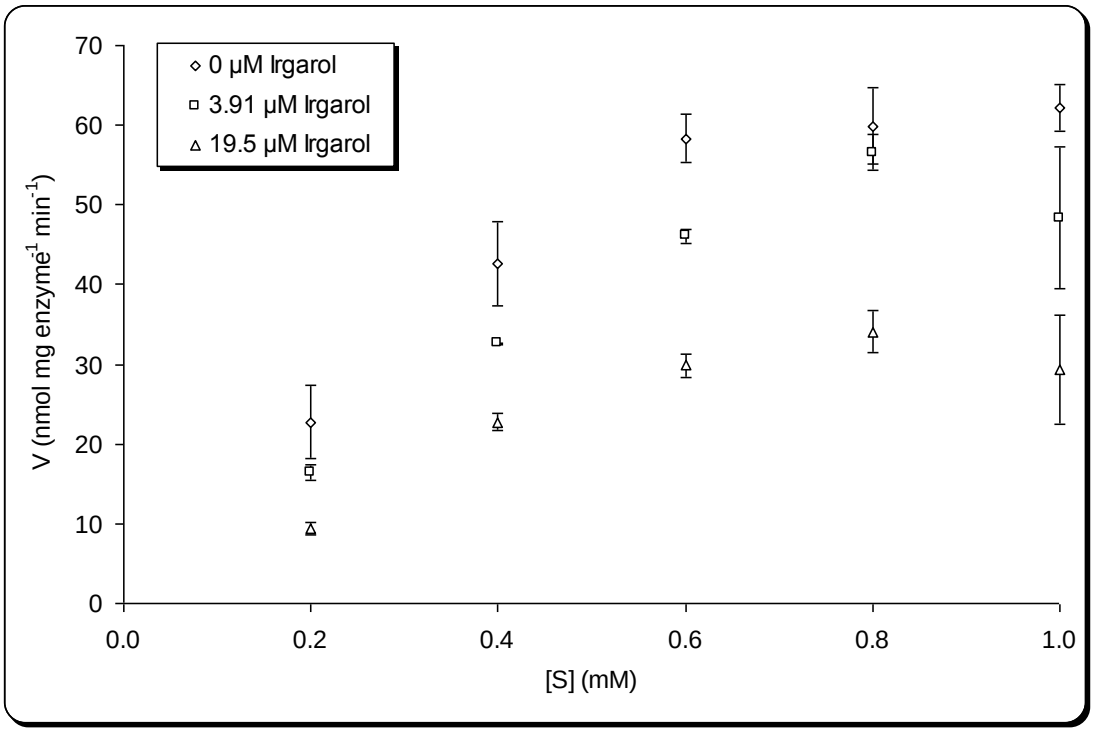

Figure 3.34 Michaelis-Menten plot for the inhibition of AChE by irgarol. Data are given as Mean±SD (with three replicates at each point).

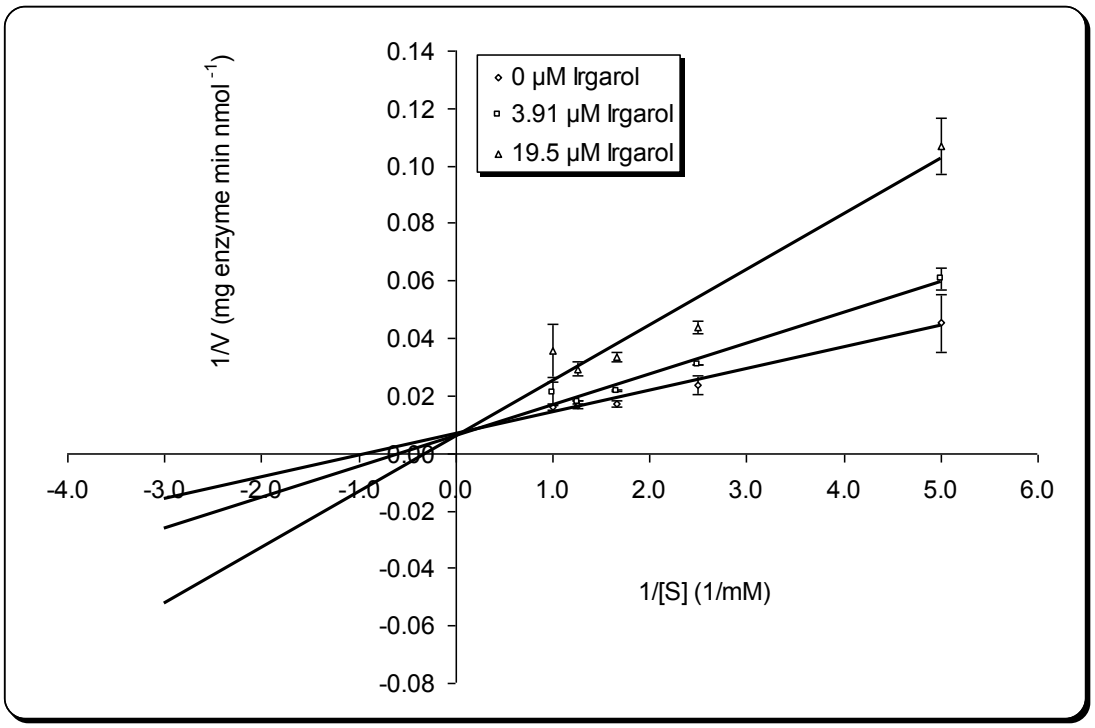

Figure 3.35 Lineweaver-Burk plot for the inhibition of AChE by irgarol. Data are given as Mean±SD (with three replicates at each point).

The inhibition constant (K_i) for the inhibition of AChE by irgarol was calculated from Lineweaver-Burk equation (2), the linear form of Michaelis-Menten equation (1), for competitive type inhibition as below:

$$V_0 = \frac{V_{\max} \cdot [S]}{\alpha K_m + [S]} \quad (1)$$

$$\frac{1}{V_0} = \frac{\alpha K_m}{V_{\max}} \frac{1}{[S]} + \frac{1}{V_{\max}} \quad (2)$$

$$\alpha = 1 + \frac{[I]}{K_i} \quad (3)$$

where V_{max} is the maximum velocity of the reaction, K_m is the Michaelis-Menten constant, [I] is the inhibitor concentration, K_i is the equilibrium constant for inhibitor binding to enzyme, $\alpha.K_m$ is equal to appearent K_m ($K_{m.app}$) in competitive inhibition (Nelson & Cox, 2008).

Inhibition constant for a competitive inhibitor can be found by plotting slope of Lineweaver-Burk plot against inhibitor concentration. Then, K_i can be calculated from the slope of the line by solving the combination of Eq. 2 and Eq. 3.

Let the slope of Lineweaver-Burk equation equal to "m":

$$m = \frac{\alpha K_m}{V_{\max}} \quad (4)$$

If we replace α with Eq. 2, we get:

$$m = 1 + \frac{[I]}{K_i}\left(\frac{K_m}{V_{\max}}\right) \quad (5)$$

Linear form of Eq. 5 is:

$$m = \frac{K_m}{V_{\max} K_i} \cdot [I] + \frac{K_m}{V_{\max}} \quad (6)$$

Inhibition constant (K_i) for irgarol was calculated as 13.3 µM from Eq. 6 (Figure 3.36 and Table 3.4). A comparison table that lists K_i values of reversible inhibitors of AChE from *E. electricus* was given in Table 3.5 (Chiou, Lai, Tsai, Lee, Lin, & Lin, 2005; Gadepalli et al., 2007; Pietsch & Gutschow, 2005).

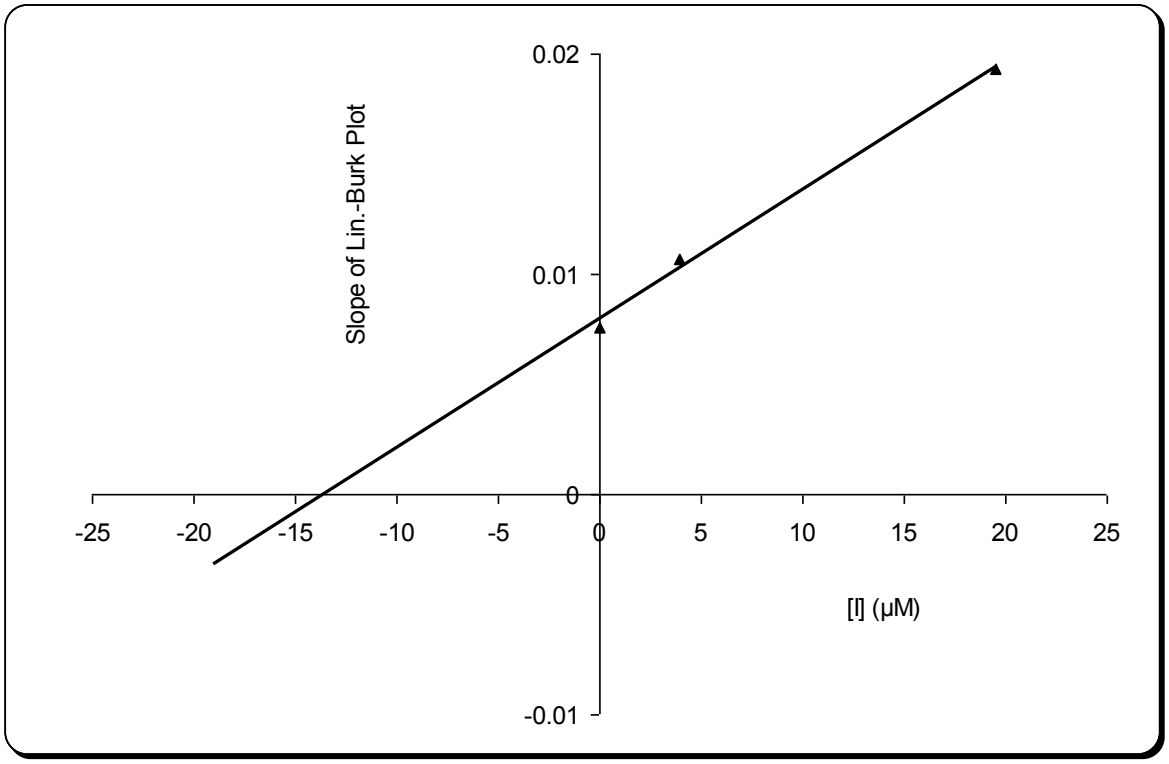

Figure 3.36 Plot of Lineweaver-Burk plot slopes versus inhibitor concentration.

Table 3.4 Michaelis-Menten constant (K_m), maximum velocity (V_{max}) and inhibition constant (K_i) of irgarol for the inhibition of AChE from *E. electricus* (For free enzyme, [I]=0, $K_{m.app}$ is equal to K_m).

Inhibitor	[I] (µM)	$K_{m.app}$ (mM)	V_{max} (nmol mg enzyme^{-1} min^{-1})	K_i (µM)
Irgarol	0.0	1.17	153.8	13.3
	3.9	1.81	169.5	
	19.5	2.85	172.4	

Table 3.5 Comparison table for K_i values of reversible inhibitors of AChE from *E. electricus*.

Inhibitor	K_i (μM)	Reaction conditions	Reference
Hydralazine HCl	7.00 ± 2.00		Chiou et al., 2005
Chlordiazepoxide HCl	50.0 ± 7.0		Chiou et al., 2005
(S)-(-)-fenoxon sulfoxide	21.0 ± 3.0	pH 8.0, 25°C	Gadepalli et al., 2007
Galanthamine	1.56 ± 0.07	pH 7.0, 30°C	Pietsch & Gutschow, 2005
Tacrine	0.027 ± 0.001	pH 7.0, 30°C	Pietsch & Gutschow, 2005
Irgarol	13.3	pH 8.0, 25°C	This thesis

3.6 Results of Computer Based Toxicity Screening Program

Acute toxicity tests showed that p-CA was more toxic than PDC and both chemicals were significantly reduced the survival percentage of nauplii at high concentrations (Figures 3.37 and 3.38). As the survival of nauplii is considered on the time scale, toxicity of PDC was not changed proportional to its concentration at studied time intervals except for 21h. Toxicity of PDC on survival percentage of *A. salina* nauplii was observed at 100 mg/L as 24.8±14.3%. On the other hand, 7 mg/L PDC was the least toxic concentration as expected. Mean velocities of *A. salina* nauplii at the beginning of the toxicity test were between 0.9-1.0 mm/s ranges (Figures 3.39 and 3.40). However, mean velocities of alive nauplii were decreased as the test proceeded. While minimum mean velocity for nauplii exposed to 100 mg/L PDC was 0.534±0.088 mm/s, maximum mean velocity was observed as 0.907±0.014 mm/s for control nauplii at 24 h of toxicity test. On the other hand, minimum velocity of nauplii exposed to 100 mg/L p-CA was found as 0.241±0.121 mm/s. The paths traveled by nauplii during 24 h of toxicity test were decreased as the test proceeded (Figures 3.41 and 3.42). While the toxic effect of PDC was detectable after 21 h of test, the toxicity of p-CA was become obvious after 8 h of test. After 24

h of toxicity test, movement of nauplii exposed to both test chemicals was only slightly detectable.

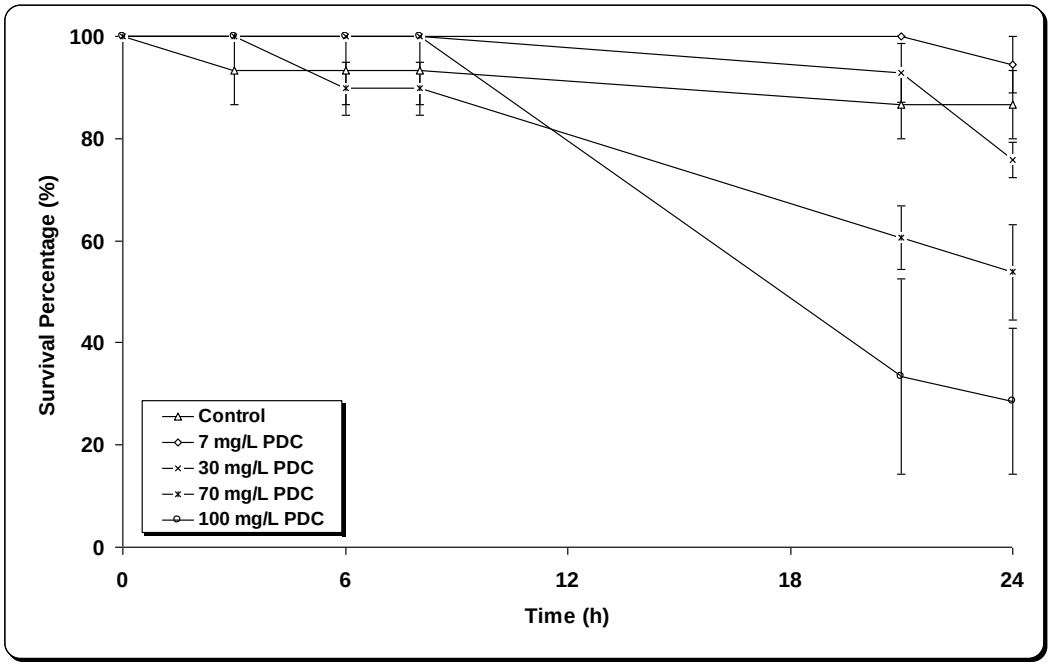

Figure 3.37 Survival percentages of *A. salina* nauplii exposed to different PDC concentrations during acute toxicity test. Data are given as Mean±SEM (with three replicates at each point).

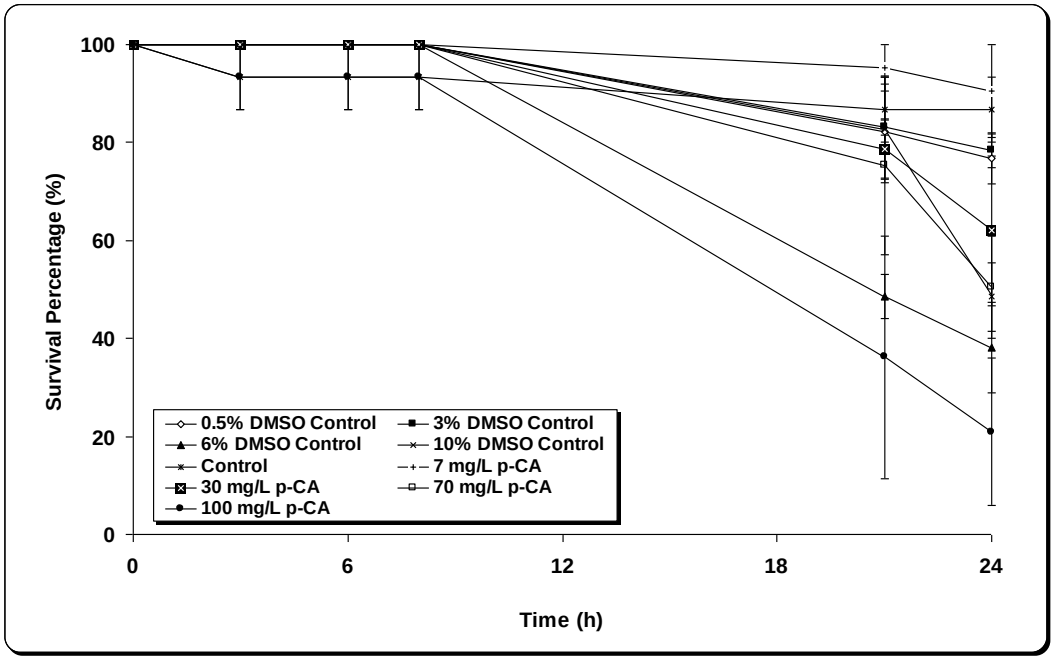

Figure 3.38 Survival percentages of *A. salina* nauplii exposed to different p-CA concentrations during acute toxicity test. Data are given as Mean±SEM (with three replicates at each point).

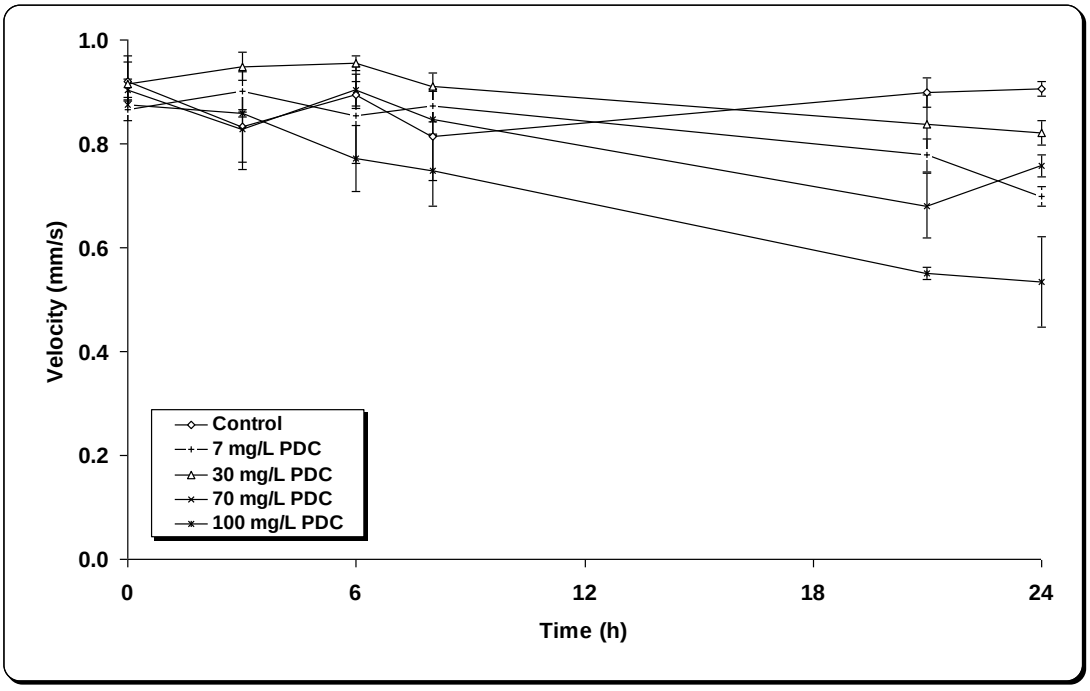

Figure 3.39 Mean velocities of *A. salina* nauplii exposed to different PDC concentrations during acute toxicity test. Data are given as Mean±SEM (with three replicates at each point).

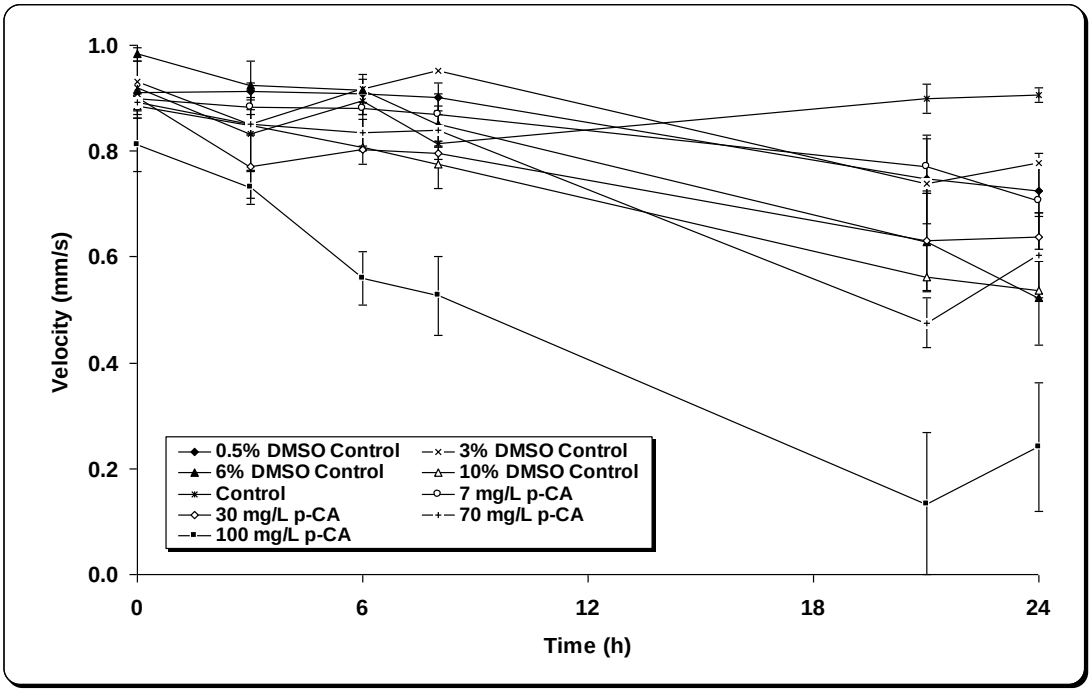

Figure 3.40 Mean velocities of *A. salina* nauplii exposed to different p-CA concentrations during acute toxicity test. Data are given as Mean±SEM (with three replicates at each point).

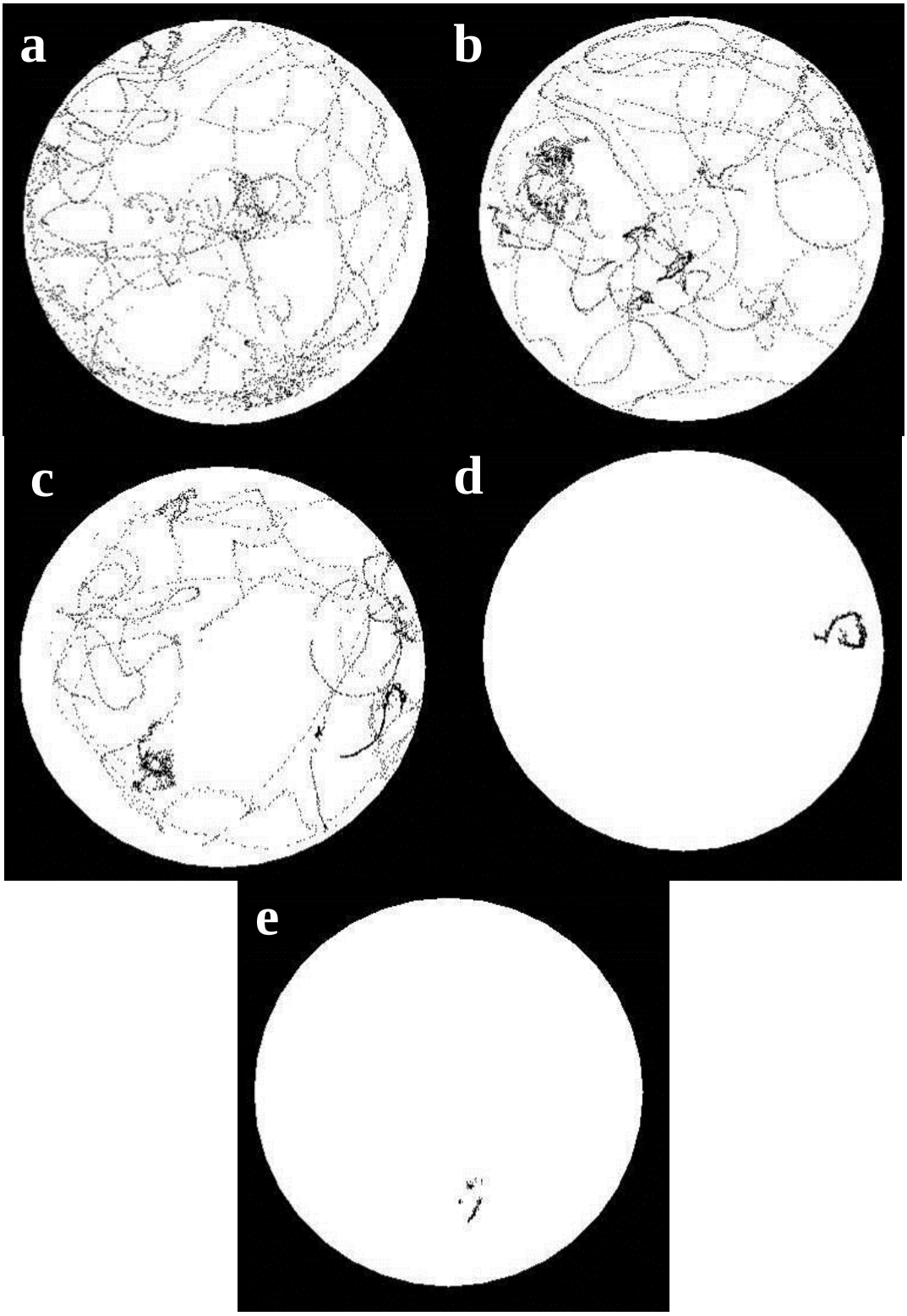

Figure 3.41 The paths traveled by alive *A. salina* nauplii exposed to 100 mg/L PDC during acute toxicity test.

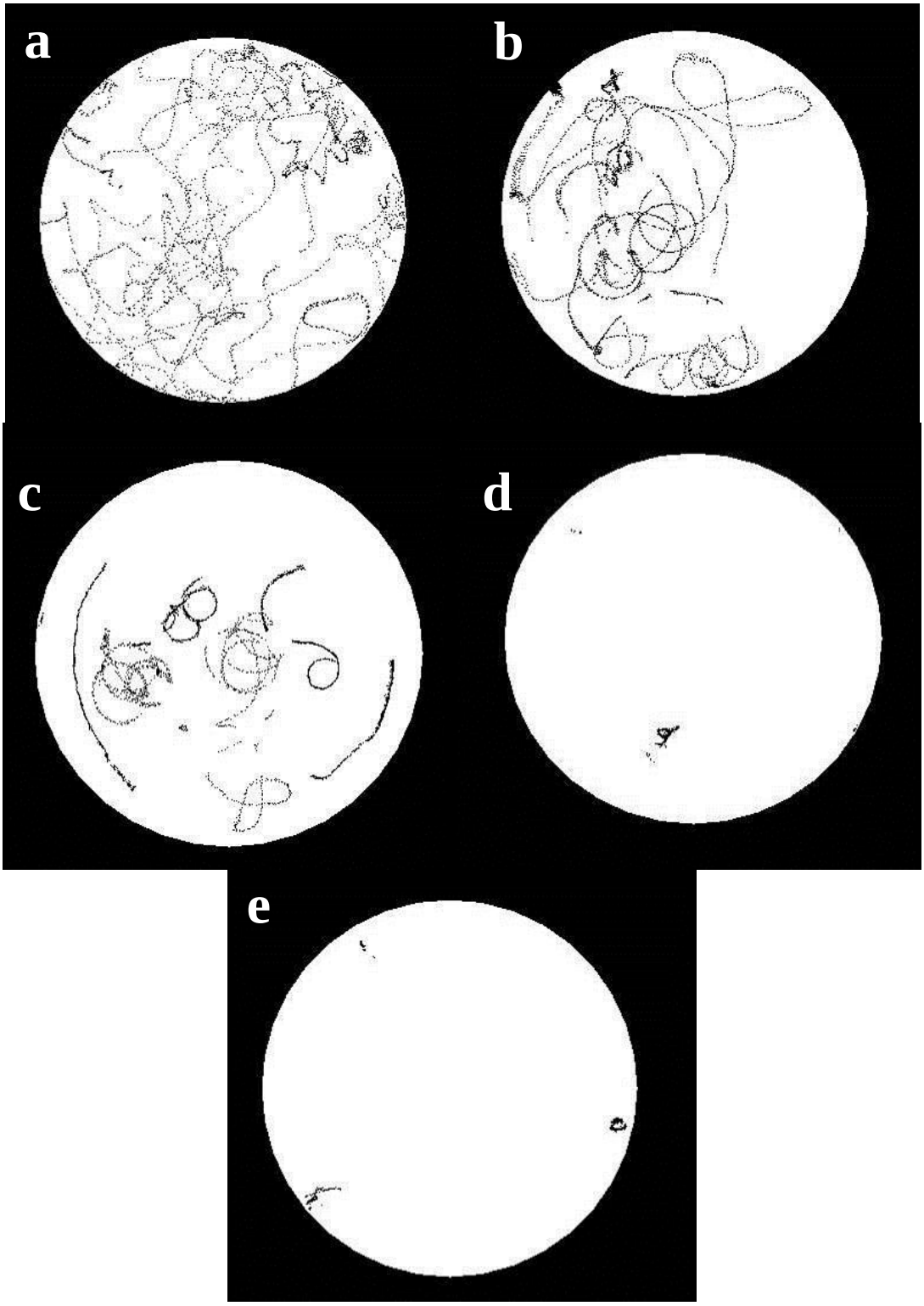

Figure 3.42 The paths traveled by alive *A. salina* nauplii exposed to 100 mg/L p-CA during acute toxicity test.

3.7 Results of Field Tests

Field tests were performed in two periods: December 2011-March 2012 and March 2012-May 2012. According to results of first test season, extract or powder containing paints were not effective as commercial AF paint, irgarol and diuron containing AF paints and their surfaces were covered with micro-slime layer. The surface of commercial AF paint was cleaner than other paints in the first season. When the micro-slime layers on test panels were investigated, different types of fouling organisms (mostly diatoms) were identified. The list of marine organisms attached to the surfaces of test panels was as follows: *Achnanthes brevipes*, *Plagiotropis* sp., *Licmophora abbreviate*, *Navicula* sp., *Gyrosigma* sp., *Thalassionema nitzschioides*, *Synedra duhemi*, *Ardissonia fulgens*, *Licmophora flabellate*, Shell of a tintinniade, *Navicula* sp., *Achnanthes longipes*, *Melosira moniliformis*, and *Cylindrotheca closterium*. In the second field test, the test panels other than commercial AF paint were covered by micro-slime layer non-homogenously. In addition, the surfaces of paint free and primer coated panels were covered by some macro-fouling organisms like serpulidae (*Hydroides elegans*), bryozoans (*Bugula neritina*) and barnacles (*Balanus amphitrite*) (Figure 3.43). The best antifouling performance was observed for commercial AF paint. On the other hand, zosteric acid containing paint was successfully prevented macrofouling during 90 days of test period. The surfaces of diuron and irgarol containing paints were only slightly covered by micro-slime layer. After 90 days of immersion (Figure 3.63), the surface of unpainted panel was fully covered by macro-fouling organisms. However, the surface of the commercial antifouling paint coated panel was cleaner than other panels. The performance of zosteric acid containing paint was effective against many fouling organisms with an exception of algae species. The photographs belong to coated panels at December 2011 – March 2012 and March 2012 – May 2012 seasons were given in Figures 3.44 to 3.51 and 3.52 to 3.62, respectively. Also, the surfaces of test panels were evaluated based on the antifouling performances of tested paints. The fouling criteria consist of five grades which are based on the quantity of organisms and species type. The fouling grades of test panels were given in Table 3.6.

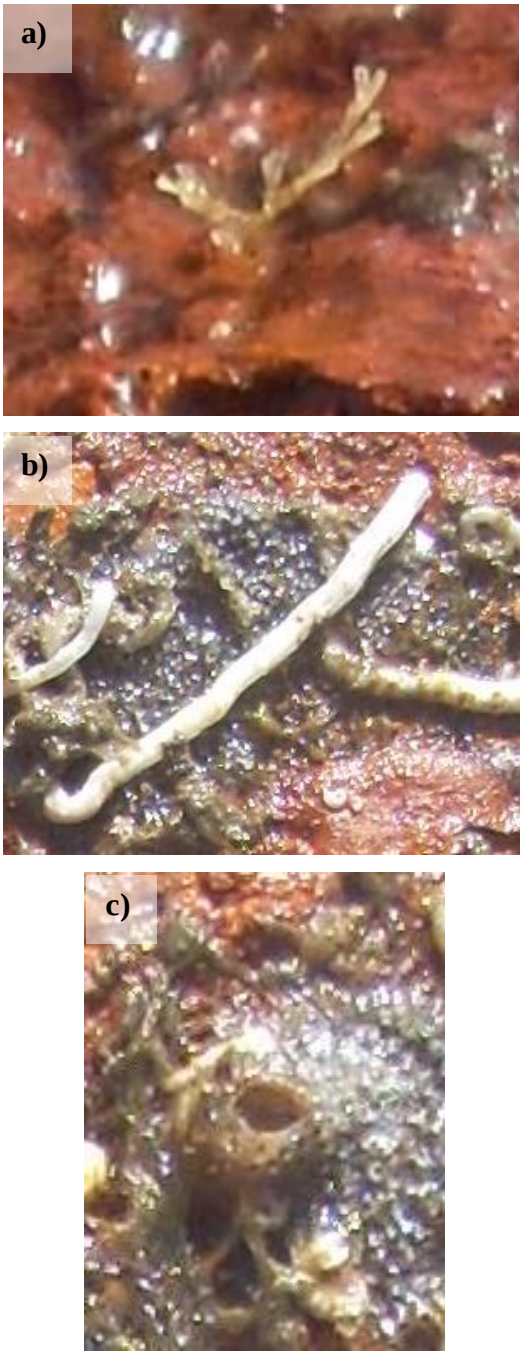

Figure 3.43 Macrofouling organisms on the test panels: a) Bryozoa, *Bugula neritina*, on paint free test panel, b) Serpulidae, *Hydroides elegans*, on primer coated test panel, and c) Barnacle, *Balanus amphitrite,* on paint free test panel.

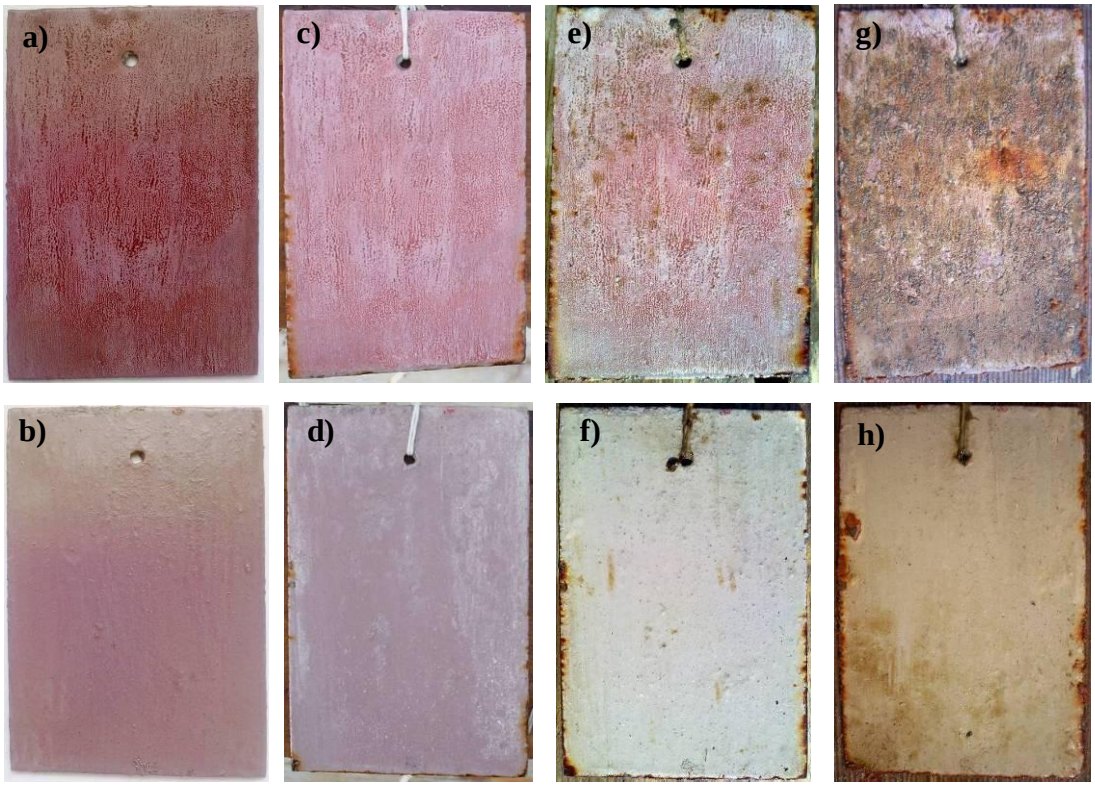

Figure 3.44 Photographs belong to two sides of test plates painted with biocide free paint before and after immersion for 2 months: a-b) Before immersion, c-d) after 16 days, e-f) after 45 days and g-h) after 60 days (Above: side 1, below: side 2).

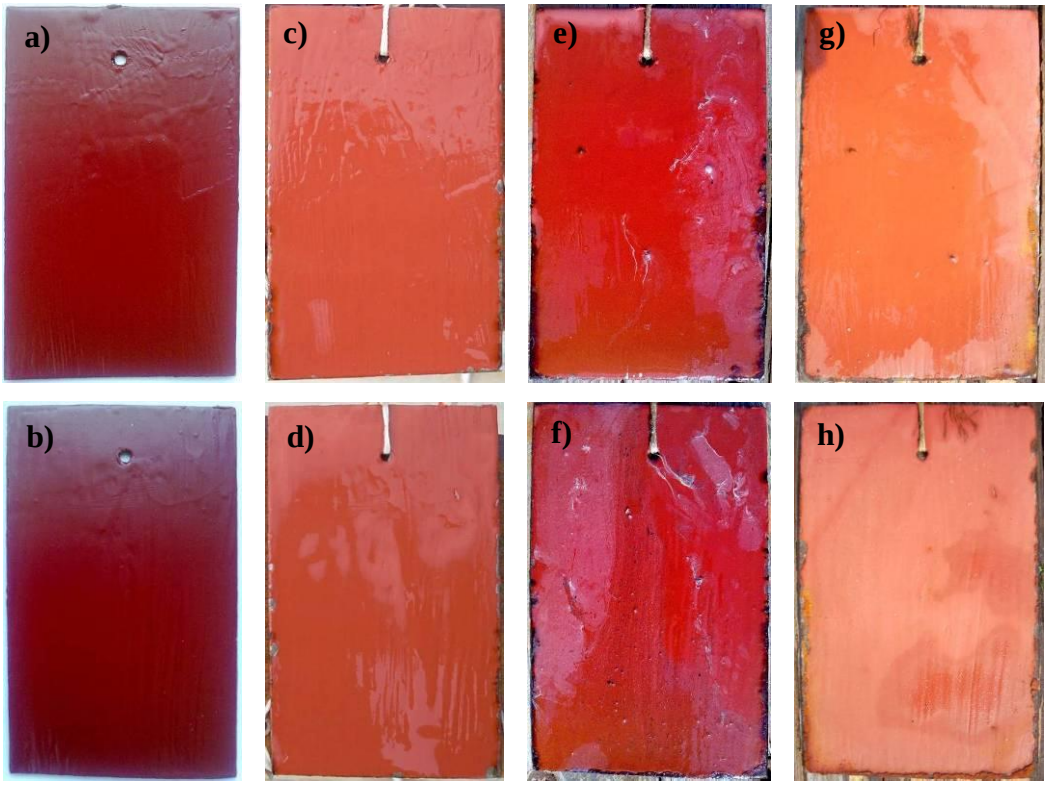

Figure 3.45 Photographs belong to two sides of test plates painted with commercial antifouling paint before and after immersion for 2 months: a-b) Before immersion, c-d) 16 days, e-f) 45 days and g-h) 60 days after (Above: side 1, below: side 2).

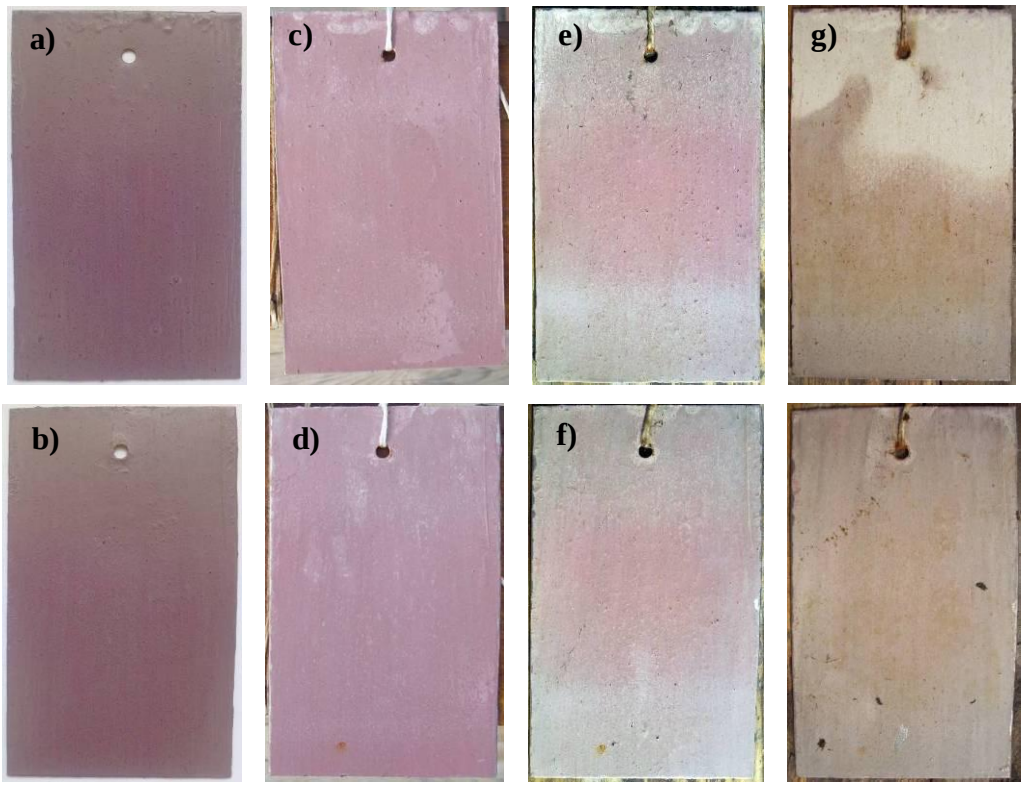

Figure 3.46 Photographs belong to two sides of test plates painted with diuron containing antifouling paint before and after immersion for 2 months: a-b) Before immersion, c-d) 16 days, e-f) 45 days and g-h) 60 days after (Above: side 1, below: side 2).

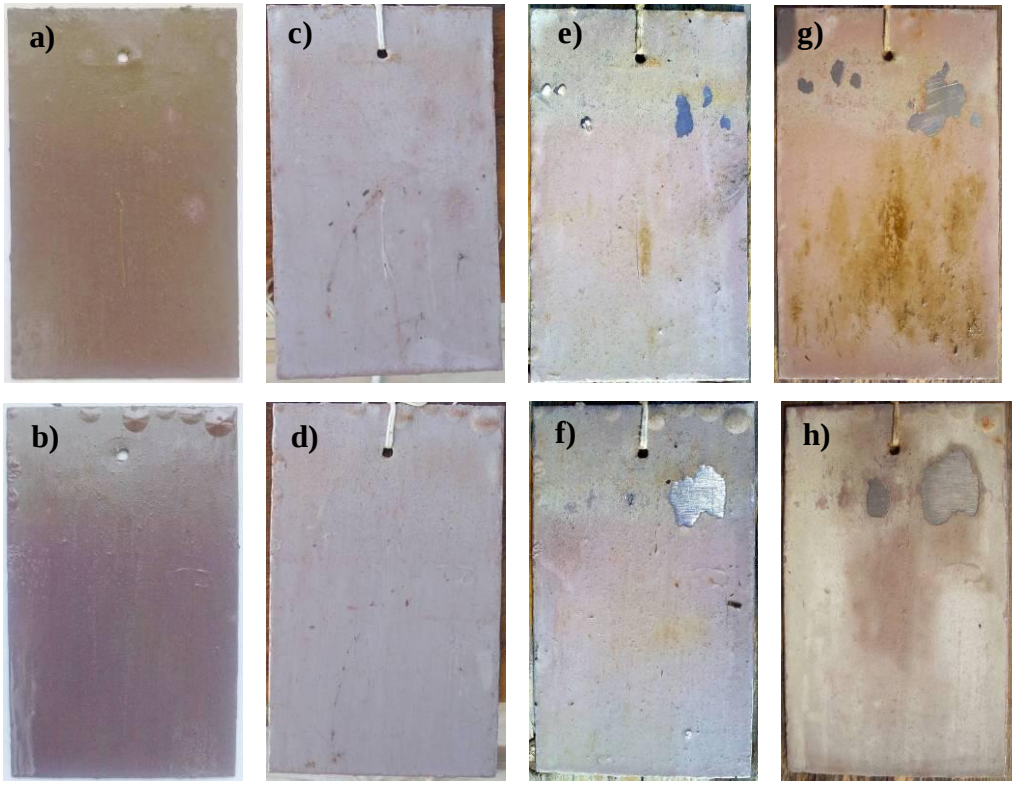

Figure 3.47 Photographs belong to two sides of test plates painted with irgarol containing antifouling paint before and after immersion for 2 months: a-b) Before immersion, c-d) 16 days, e-f) 45 days and g-h) 60 days after (Above: side 1, below: side 2).

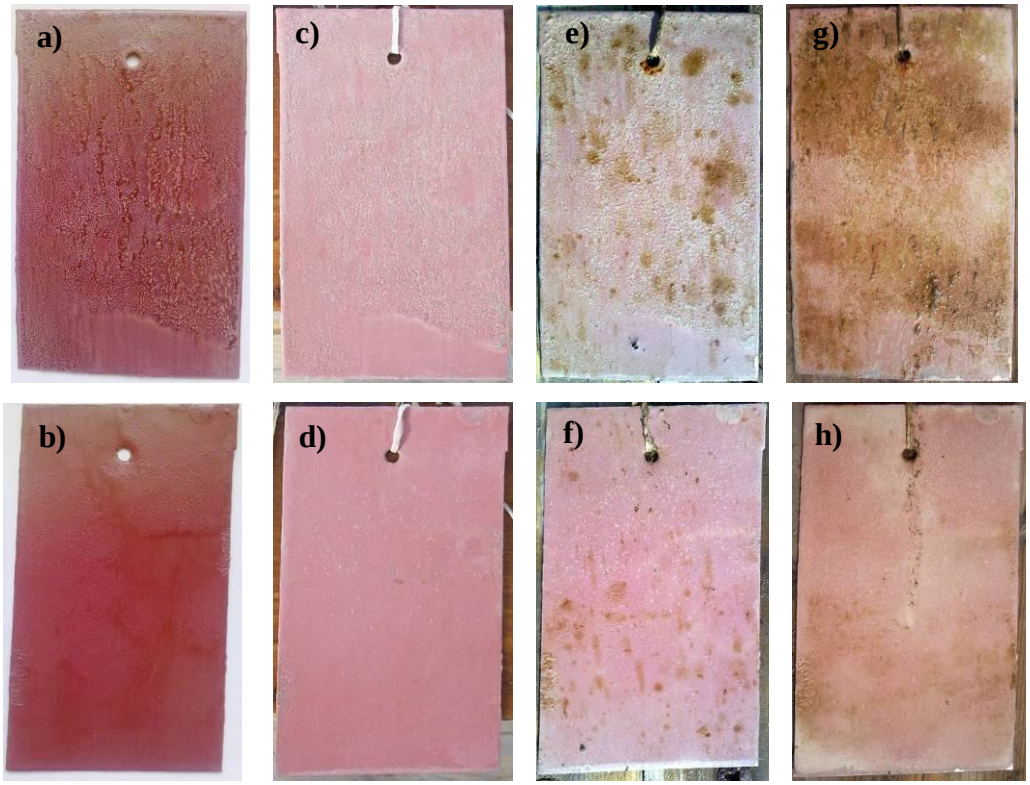

Figure 3.48 Photographs belong to two sides of test plates painted with *Cymodocea nodosa* extract containing antifouling paint before and after immersion for 2 months: a-b) Before immersion, c-d) 16 days, e-f) 45 days and g-h) 60 days after (Above: side 1, below: side 2).

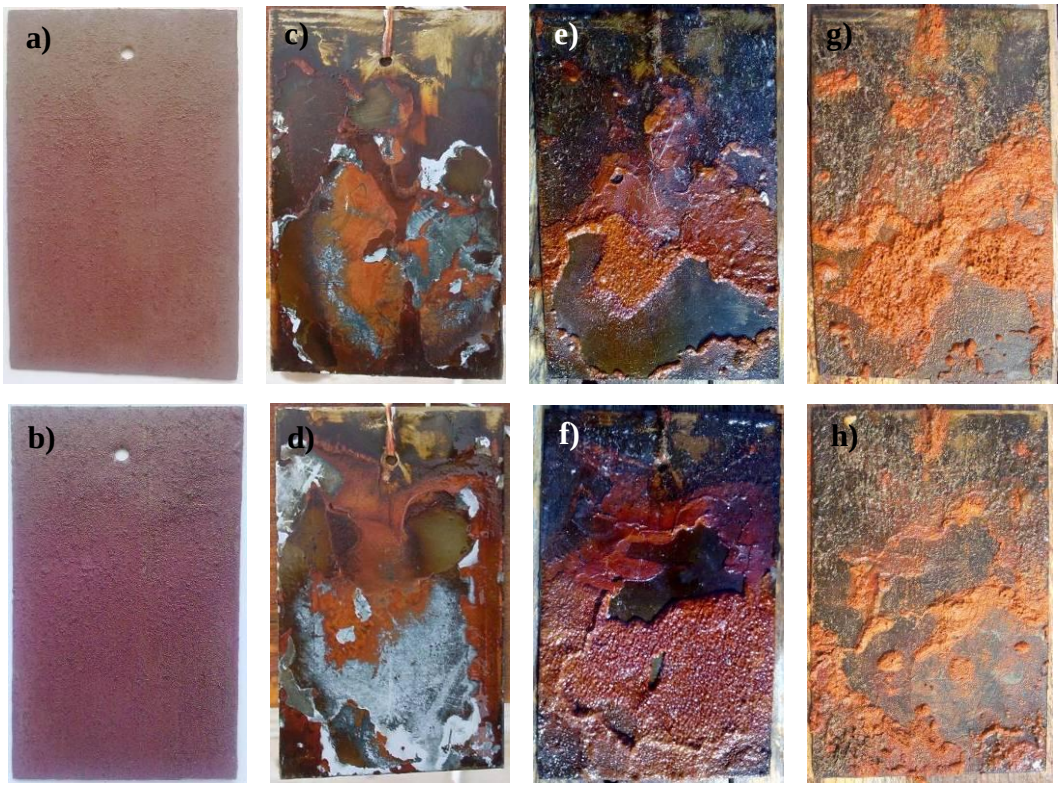

Figure 3.49 Photographs belong to two sides of test plates painted with *Cymodocea nodosa* powder containing antifouling paint before and after immersion for 2 months: a-b) Before immersion, c-d) after 16 days, e-f) after 45 days and g-h) after 60 days (Above: side 1, below: side 2).

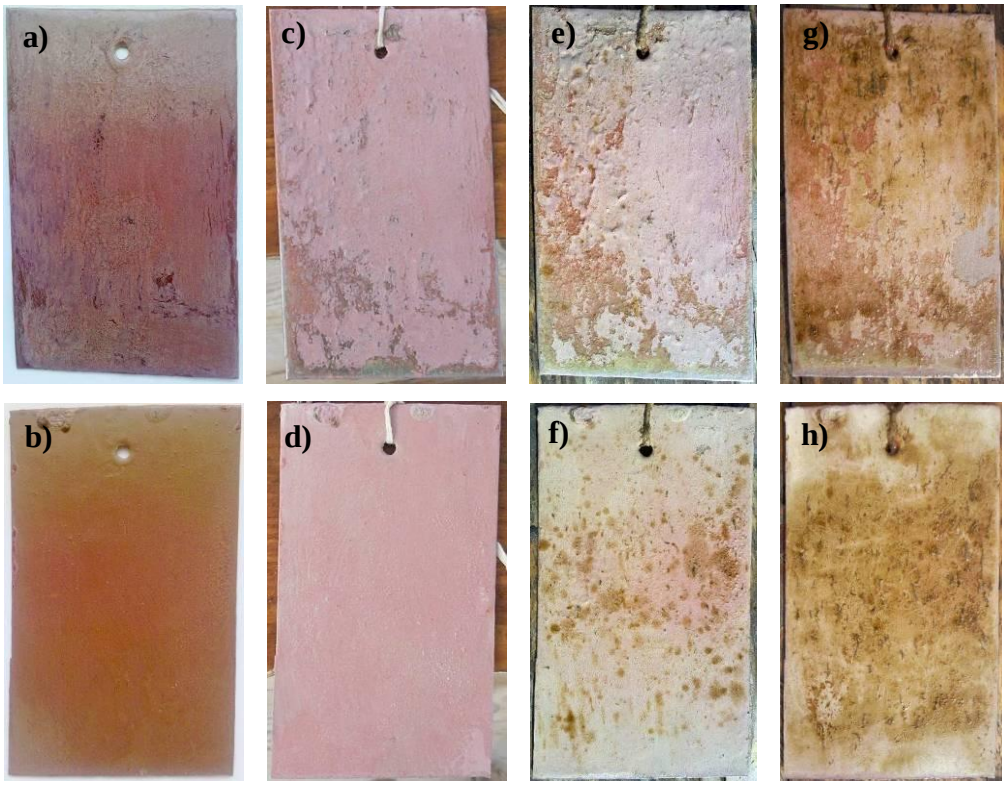

Figure 3.50 Photographs belong to two sides of test plates painted with *Zostera noltii* extract containing antifouling paint before and after immersion for 2 months: a-b) Before immersion, c-d) after 16 days, e-f) after 45 days and g-h) after 60 days (Above: side 1, below: side 2).

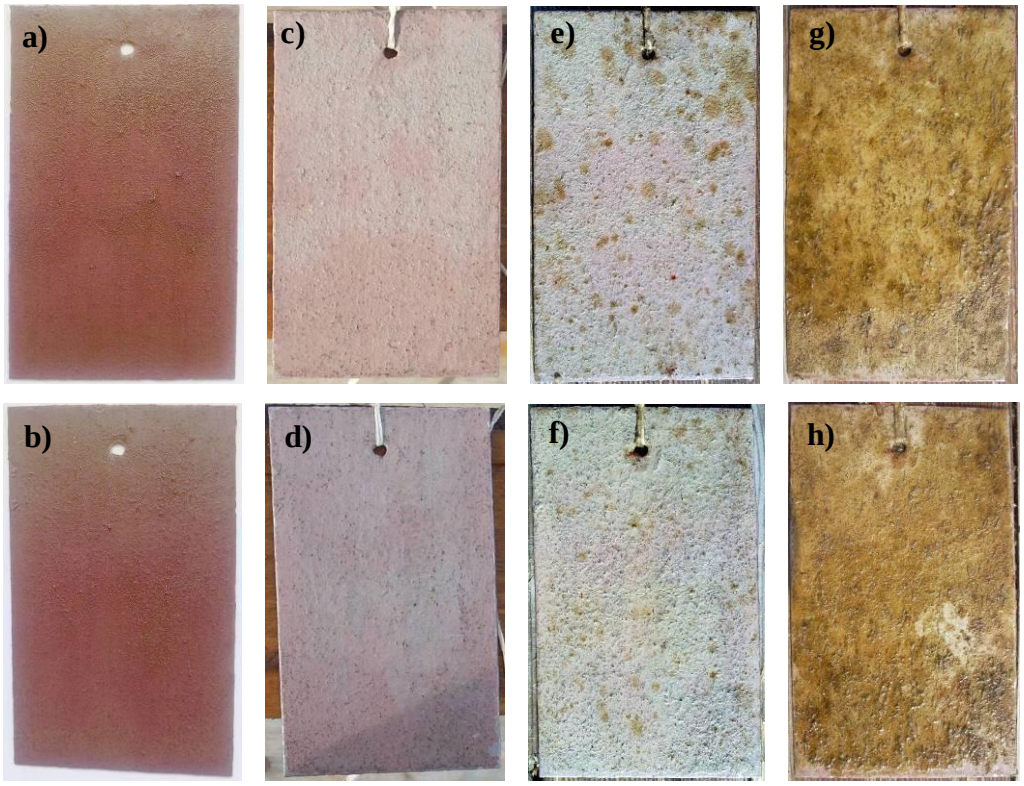

Figure 3.51 Photographs belong to two sides of test plates painted with *Zostera noltii* powder containing antifouling paint before and after immersion for 2 months: a-b) Before immersion, c-d) after 16 days, e-f) after 45 days and g-h) after 60 days (Above: side 1, below: side 2).

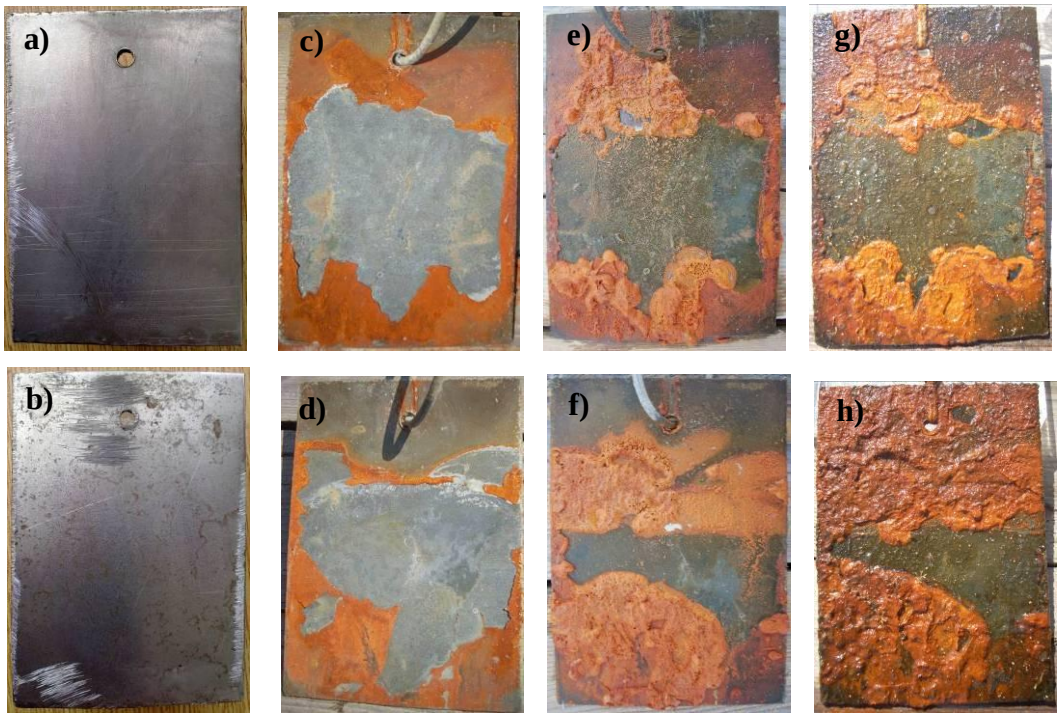

Figure 3.52 Photographs belong to two sides of unpainted test plates before and after immersion for 2 months: a-b) Before immersion, c-d) after 15 days, e-f) after 30 days, and g-h) after 60 days (Above: side 1, below: side 2).

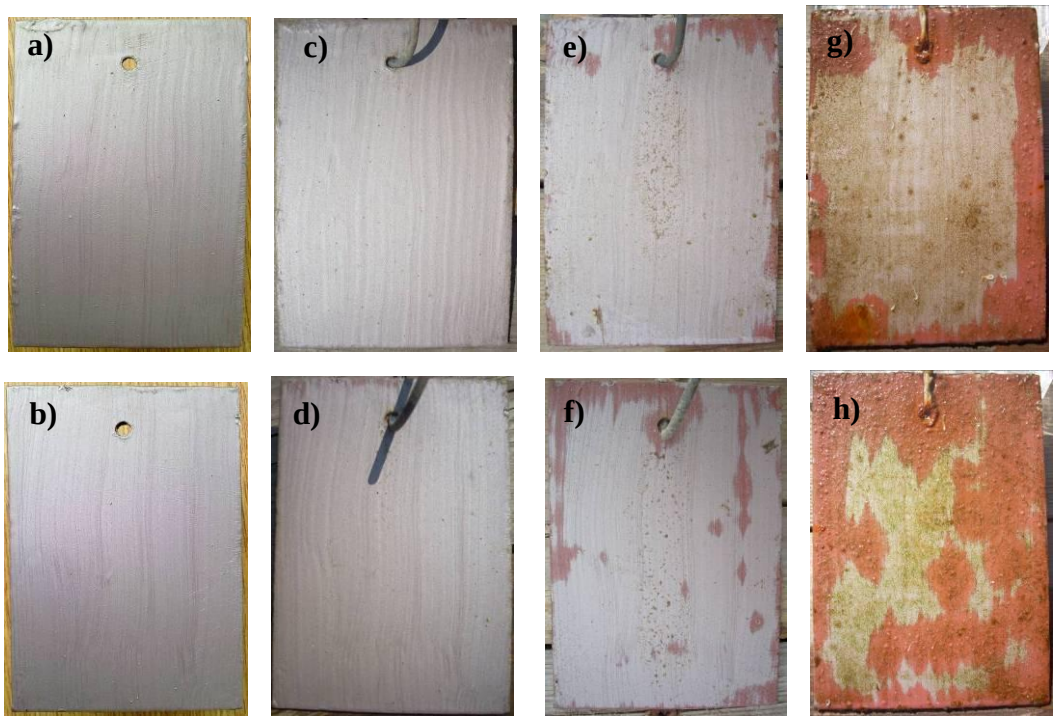

Figure 3.53 Photographs belong to two sides of test plates painted with primer before and after immersion for 2 months: a-b) Before immersion, c-d) after 15 days, e-f) after 30 days, and g-h) after 60 days (Above: side 1, below: side 2).

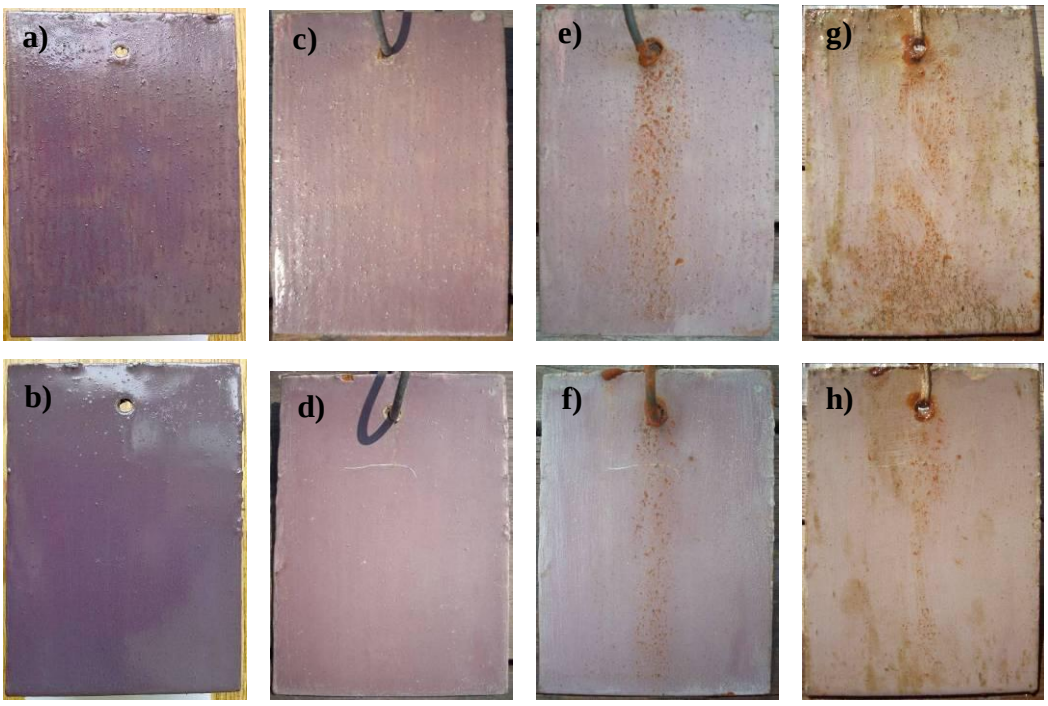

Figure 3.54 Photographs belong to two sides of test plates painted with biocide free paint before and after immersion for 2 months: a-b) Before immersion, c-d) after 15 days, e-f) after 30 days, and g-h) after 60 days (Above: side 1, below: side 2).

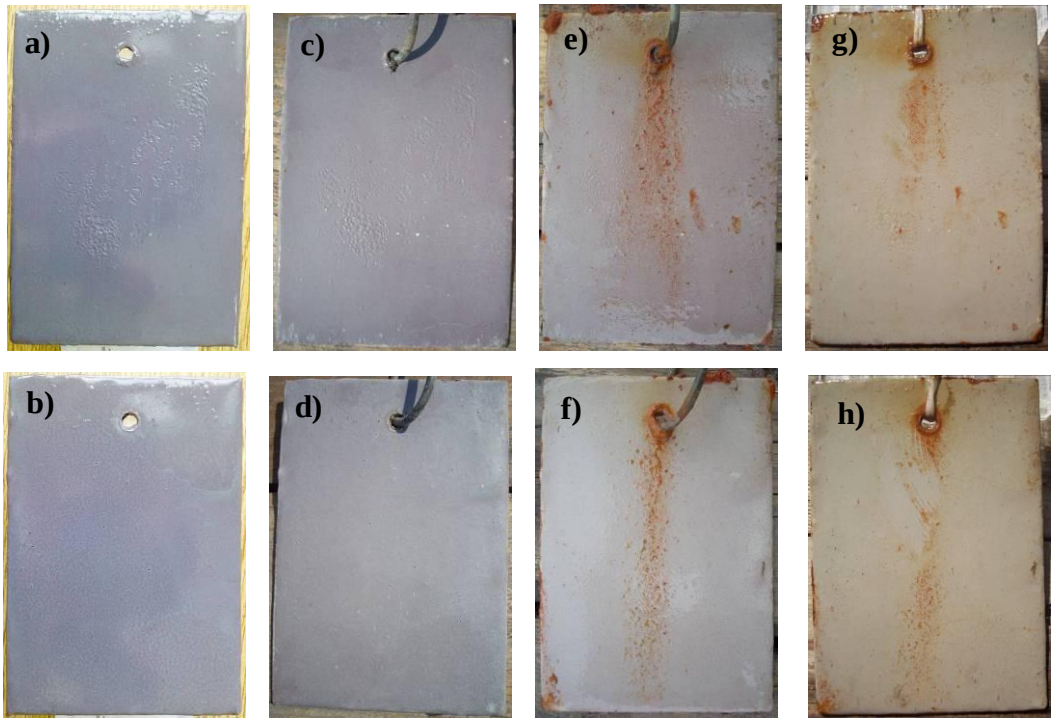

Figure 3.55 Photographs belong to two sides of test plates painted with diuron containing AF paint before and after immersion for 2 months: a-b) Before immersion, c-d) after 15 days, g-h) after 30 days, and g-h) after 60 days (Above: side 1, below: side 2).

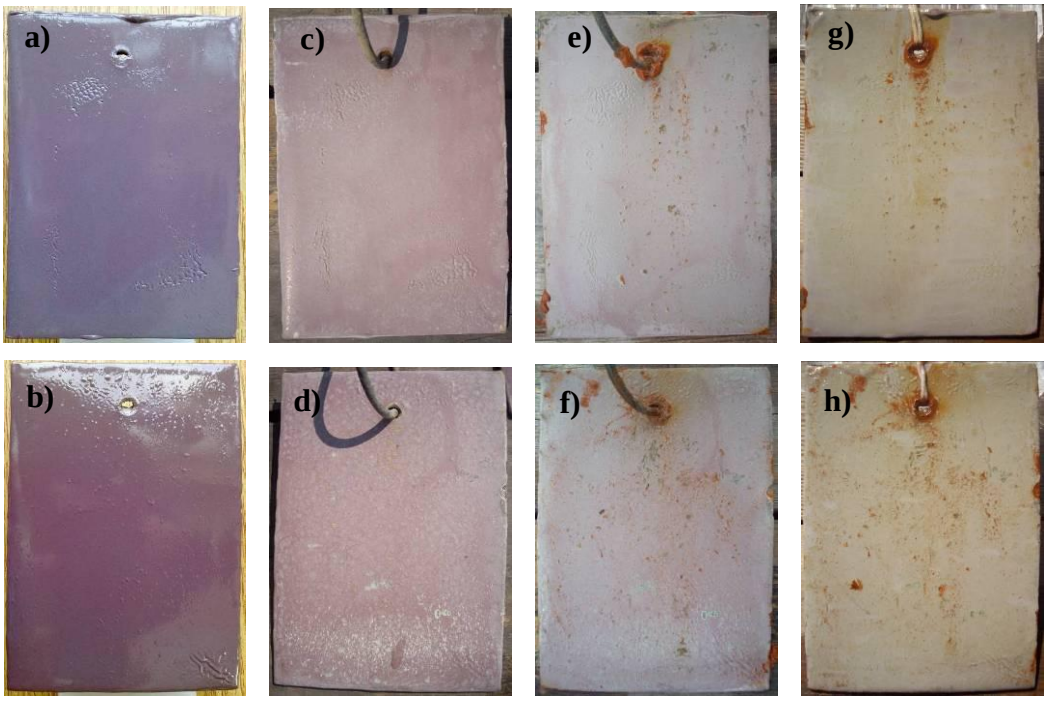

Figure 3.56 Photographs belong to two sides of test plates painted with irgarol containing antifouling paint before and after immersion for 2 months: a-b) Before immersion, c-d) after 15 days, e-f) after 30 days, and g-h) after 60 days (Above: side 1, below: side 2).

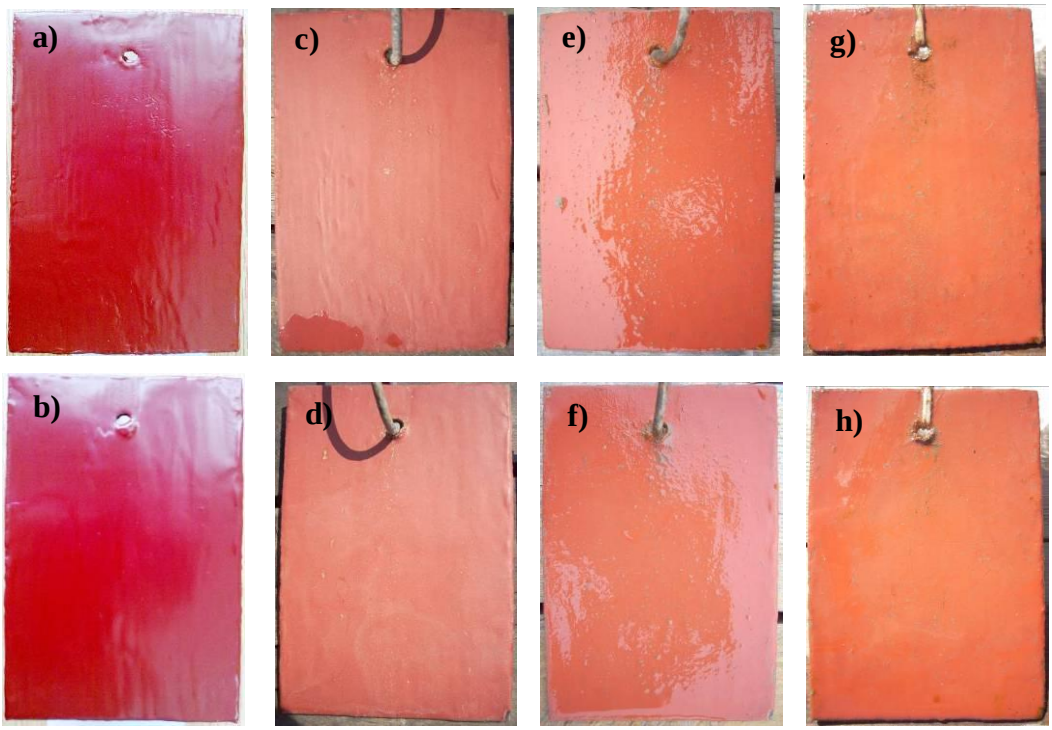

Figure 3.57 Photographs belong to two sides of test plates painted with commercial antifouling paint before and after immersion for 2 months: a-b) Before immersion, c-d) after 15 days, e-f) after 30 days, and g-h) after 60 days (Above: side 1, below: side 2).

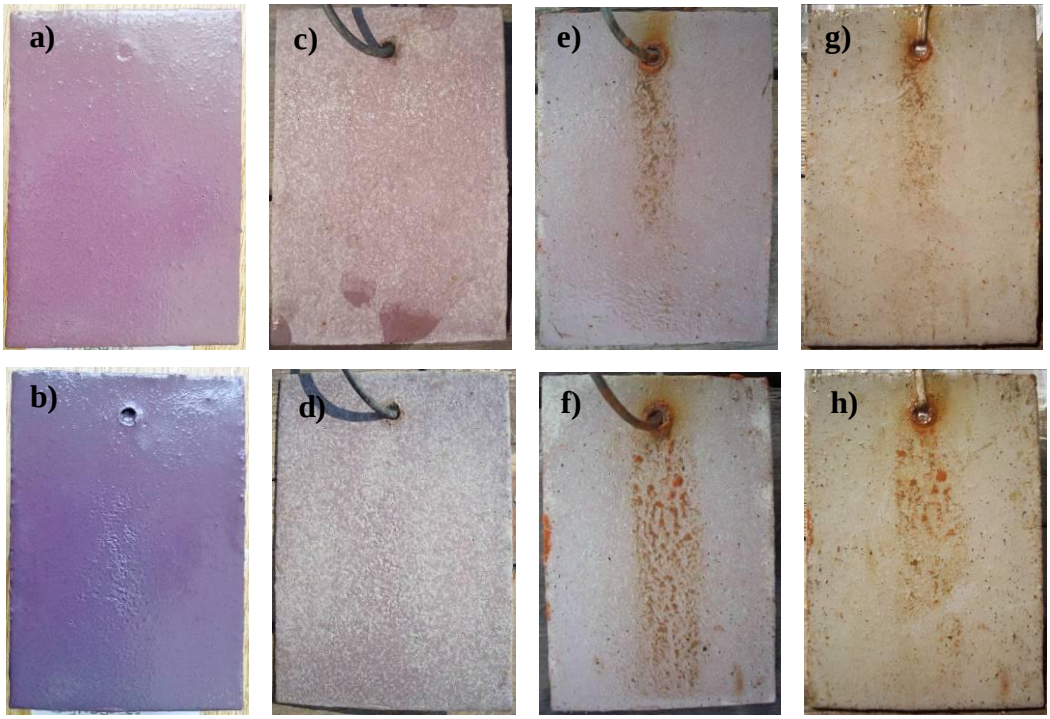

Figure 3.58 Photographs belong to two sides of test plates painted with *Cymodocea nodosa* powder containing antifouling paint before and after immersion for 2 months: a-b) Before immersion, c-d) after 15 days, e-f) after 30 days, and g-h) after 60 days (Above: side 1, below: side 2).

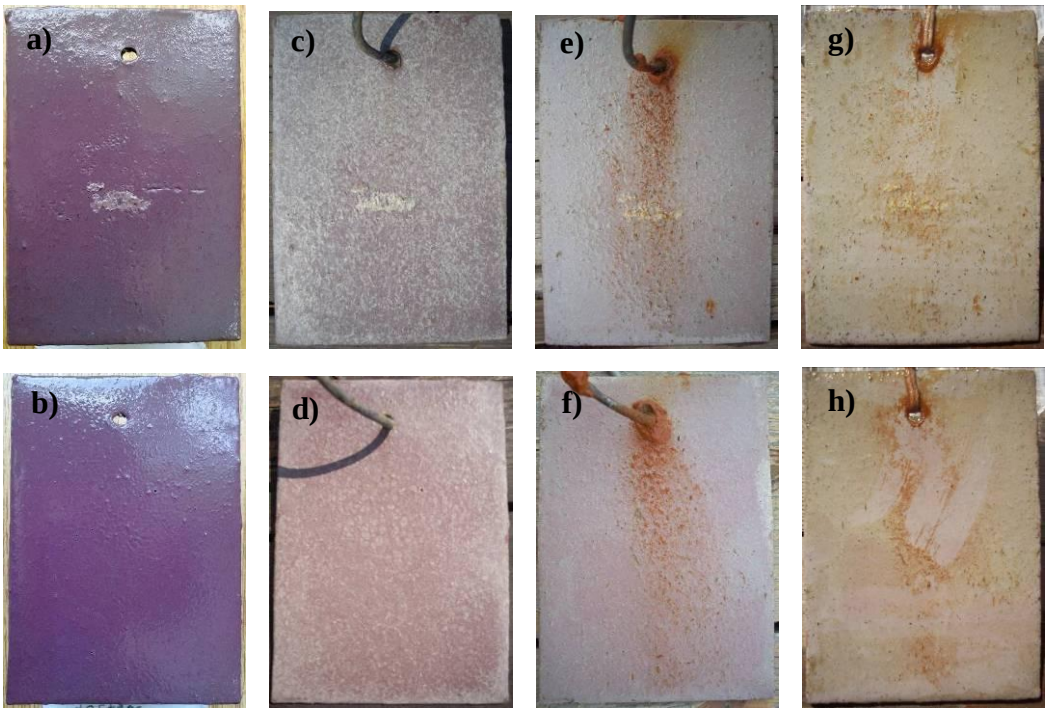

Figure 3.59 Photographs belong to two sides of test plates painted with *Zostera noltii* powder containing antifouling paint before and after immersion for 2 months: a-b) Before immersion, c-d) after 15 days, e-f) after 30 days, and g-h) after 60 days (Above: side 1, below: side 2).

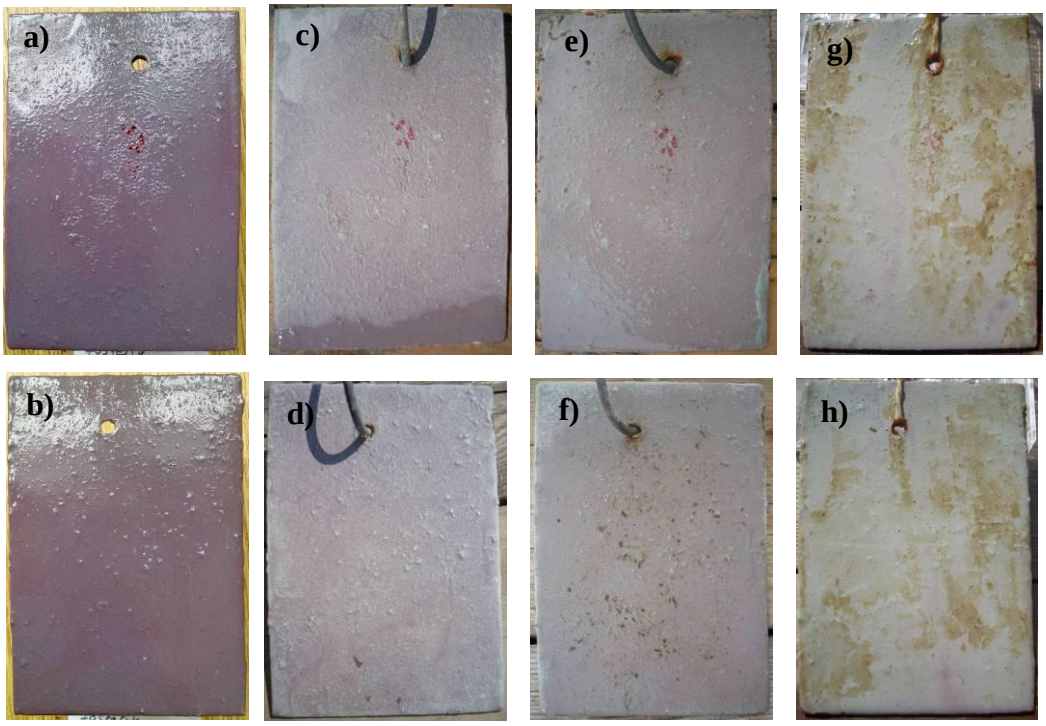

Figure 3.60 Photographs belong to two sides of test plates painted with zosteric acid containing antifouling paint before and after immersion for 2 months: a-b) Before immersion, c-d) after 15 days, e-f) after 30 days, and g-h) after 60 days (Above: side 1, below: side 2).

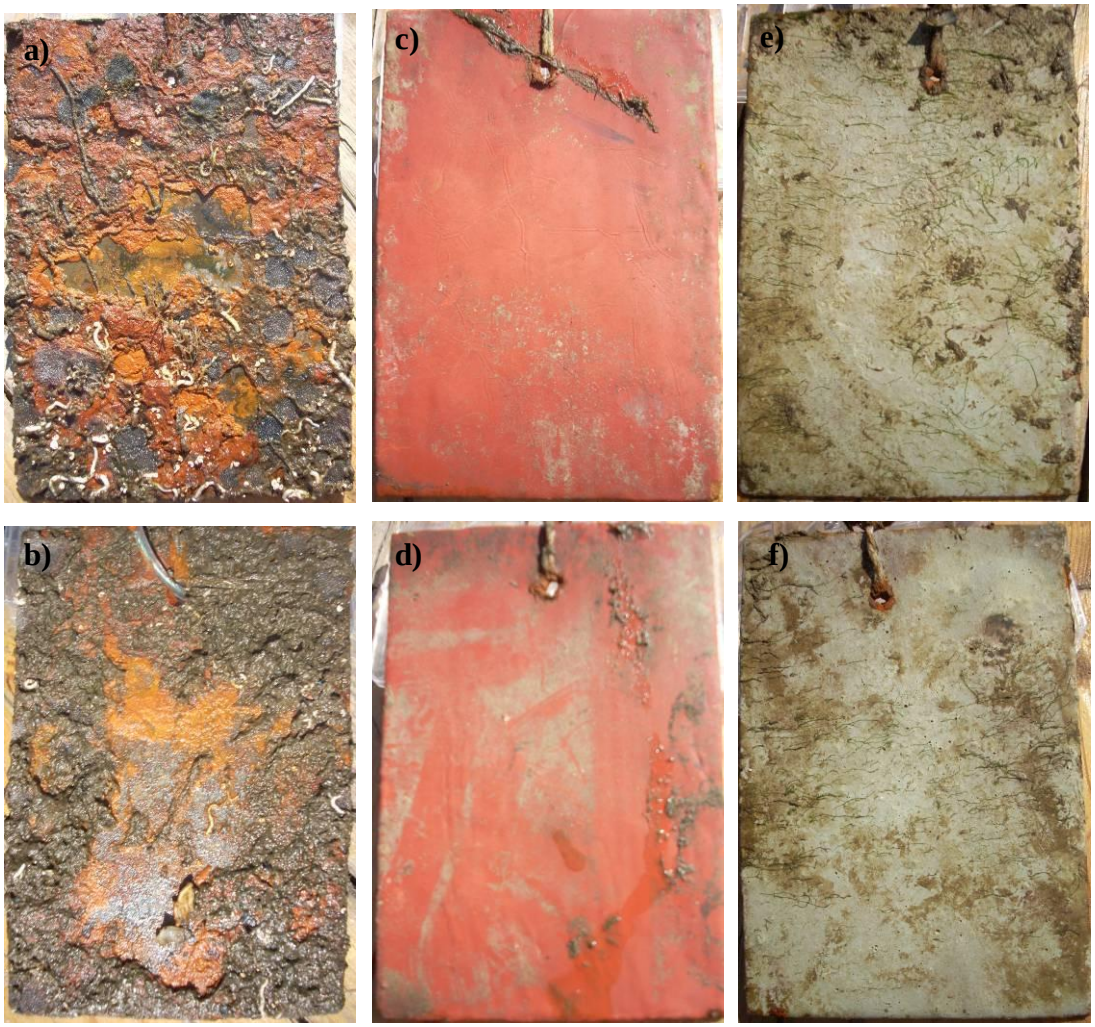

Figure 3.61 Photographs belong to two sides of test plates: a-b) unpainted, c-d) commercial antifouling paint and f-g) zosteric acid containing antifouling paint; after 80 days of immersion.

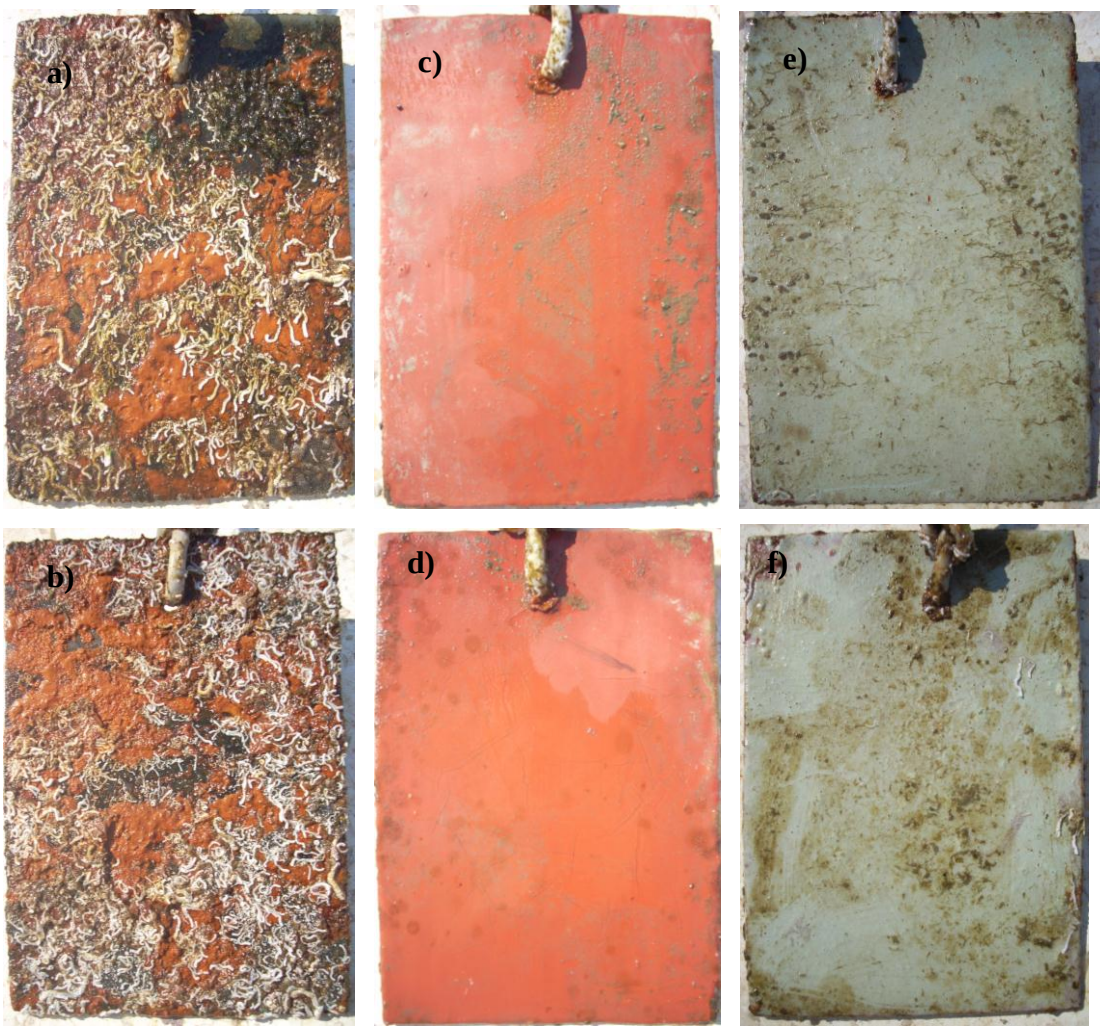

Figure 3.62 Photographs belong to two sides of test plates: a-b) unpainted, c-d) commercial antifouling paint and f-g) zosteric acid containing antifouling paint; after 90 days of immersion.

Table 3.6 Assessment of fouling grades on the surface of antifouling paint test panels.

Plate Name	**Field Test I (60 Days)**		**Field Test II (90 Days)**	
	Side 1	**Side 2**	**Side 1**	**Side 2**
Paint Free Panel	-	-	V	V
Biocide Free Paint	II	II	III	III
Primer Coated Panel	-	-	II	II
Irgarol Containing Paint	II	I	II	II
Diuron Containing Paint	I	I	II	II
Commercial AF Paint	I	I	I	I
C. nodosa Extract Containing Paint	II	I	-	-
C. nodosa Powder Containing Paint	II	II	II	II
Z. noltii Extract Containing Paint	II	II	-	-
Z. noltii Powder Containing Paint	II	II	II	II
Zosteric Acid Containing Paint	-	-	II	II

CHAPTER FOUR
DISCUSSION AND CONCLUSION

Attachment of micro and macro marine organisms onto an artificial surface is called as biofouling. Biofouling is a natural process and it can take place on any substrate surface. However, biofouling is a serious problem for the ships. As fouling organisms cover the hulls of the ships, they cause to increase of weight, reduction of speed, limitations in maneuverability, corrosion and high fuel consumption. In order to prevent biofouling, ship's hulls are painted with special marine paints called as antifouling paints. Tributyltin (TBT) based self-polishing copolymer type antifouling paints were successfully used for prevention of fouling. But application of TBT based antifouling paints were banned in 1 January 2003 and the presence of such paints on the surface of the ships were restricted after 1 January 2008 (IMO, 2001) due to the reports on their harmful effects such as genotoxic and cytotoxic defects on non-target marine organisms (mussels, polychaetes, molluscs, fishes, etc.) (Hagger, Depledge, & Galloway, 2005; Hagger, Fisher, Hill, Depledge, & Jha, 2002 ; Jha, Hagger, & Hill, 2000; Jha, Hagger, Hill, & Depledge, 2000; Lau, Chan, Leung, Luan, Yang, & Qiu, 2007; Micael, Reis-Henriques, Carvalho, & Santos, 2007).

Diuron and irgarol are used as herbicides since their inhibitory activity on D1 protein in photosystem II. These herbicides are also used in antifouling paints as co-biocides to prevent biofouling on ships' hull. However, their negative effects have been reported on several non-target organisms in the literature (Bellas, 2006; Faria, López, Fernández-Sanjuan, Lacorte, & Barata, 2010; Perina, Abessa, Pinho, & Fillmann, 2011; Tsunemasa & Okamura, 2011; Wang, Li, Huang, Xu, & Wang, 2011). The main aim of this thesis was the development of an eco-friendly biocide from secondary metabolite cocktails of marine plants. In this context, extracts of marine plants were prepared and also zosteric acid was synthesized in order to perform acute toxicity tests and antifouling performance tests in comparison with commercial biocides. According to results of acute toxicity tests on *A. salina*, zosteric acid and marine plant extracts were not toxic to nauplii. The acting mechanism of zosteric acid is depended on prevention of attachment rather than

acute toxicity which is contrary to acting mechanism of booster biocides (Geiger et al., 2004). On the other hand, tested booster biocides were even more toxic than potassium dichromate, a reference substance used in acute toxicity tests on *A. salina*.

Embryonic toxicities of booster biocides (diuron, irgarol and copper pyrithione) which were highly toxic to *A. salina* nauplii in acute toxicity tests were investigated with the hatching percentage tests on *A. salina* and morphologic changes on nauplii after hatching period. Irgarol was not effective on the hatching percentage of *A. salina* cysts. Low solubility of irgarol in water (7 mg/L) and its highly hydrophobic nature (Konstantinou & Albanis, 2004) might be some major factors for this observation. On the other hand, diuron was more toxic than irgarol and EC_{50} value of diuron was found as 12.01 mg/L. The effect of diuron on hatching percentage can be explained with higher solubility of diuron in water (35 mg/L) and polar urea skeleton as a main functional group in its structure (Konstantinou & Albanis, 2004). The toxicity of copper pyrithione was higher than diuron and irgarol. More than two fold decreases in hatching percentages at studied concentrations were observed for copper pyrithione. In morphological analysis studies, irgarol and diuron did not change the morphology of larvae, but a major fraction of *A. salina* nauplii in diuron containing medium was unable to break cyst wall. Thus, our suggestion on the mechanism of action for diuron is the possible inhibition of hatching enzyme of *A. salina*.

In characterization studies of acetylcholine esterase from *A. salina*, the optimum conditions found were in parallel to the findings reported in the literature (Fan et al., 2010). The Michaelis-Menten constants were found for the acetylcholine esterase in crude tissue extract of *A. salina*. According to the results obtained from inhibition studies of acetylcholine esterase by booster biocides (irgarol, diuron and zosteric acid), only irgarol decreased AChE enzyme activity up to two folds at studied inhibitor concentrations. The inhibition type of AChE was found as competitive type inhibition from Lineweaver-Burk plots. Inhibition of AChE by irgarol can be attributed to its structural similarity to known AChE inhibitors. Irgarol can be protonated from its nitrogen atoms belong to triazine ring and thus it is also able to form hydrogen bonds with functional amino acid side-chains. In the literature, the

inhibitory effects of triazine derivatives, 7H-thiazolo[3,2-b]-1,2,4-triazin-7-one, on AChE have been reported with enzyme inhibition and molecular docking experiments (Liu, Yi, Shi, Liang, & Gao, 2007). The structure of the irgarol is also similar to known AChE inhibitors and their inhibition constants (K_i) are close to commercial AChE inhibitors such as chlordiazepoxide hydrochloride.

In the literature, the number of studies concerning the toxicity of irgarol on AChE is very limited and there are only two published papers on two estuarine organisms (Key, Chung, Hoguet, Sapozhnikova, & Fulton, 2008; Key et al., 2009). In these published papers, both acute toxicity and AChE levels as a biomarker for sublethal effects of irgarol on a grass shrimp and an estuarine fish were studied. Key et al. (2008) have reported no statistically significant differences in AChE levels in adult shrimp but authors noted a trend for lower AChE levels as irgarol concentrations increased. On the contrary, they reported significantly elevated larval AChE levels at the highest exposure of 2.0 mg L^{-1} (Key et al., 2008). In the second paper, Key et al. (2009) indicated that irgarol significantly changed only lipid peroxidase levels. Key et al. (2009) also stated that AChE levels were not significantly affected by irgarol. Although Key et al. (2008) noted the toxic and sublethal effects of irgarol were only observed at concentrations well above its environmental levels, they also warranted further studies on AChE as a possible indicator of sublethal effects.

Inasmuch as investigations on enzyme inhibition kinetics with Michaelis-Menten and Lineweaver-Burk models give important information on the relationship between enzyme and inhibitor interactions such as inhibition types and also special parameters (K_m, V_{max} and K_i) not only IC_{50} values but also inhibition kinetics on AChE inhibition should be examined in future studies related to marine antifouling co-biocides development. We strongly suggest that the toxic biocides or structures considered as ingredients of antifouling paints should be checked for their AChE inhibition rates before their commercial uses or other applications. Otherwise, possible toxic co-biocides in aquatic ecosystems or closed bays where sea currents are not enough will negatively affect the marine biodiversity by reducing swimming

or locomotor activities that are important physical activities in prey-predators relations and also reproductive activities of marine organisms.

In recent years, computer based animal tracking methods have attracted much attention and especially used for sublethal behavior or movement analysis of fast moving animals. However, accuracy of the algorithms beyond video tracking software could change according to area of use, size and speed of the animal, etc. Therefore, a robust algorithm background is needed for video tracking software specially developed for area of use. Such an area that is prone to suffer greatly from personal errors is acute toxicity tests on microscopic organisms. It is vital to count dead or alive animals after end point of the test. However, the human eye can mistakenly count the animals with errors even under the magnifier or optical microscope. Another area of use for video tracking methods is determination of locomotor behavior in toxicity tests. Since it points out sublethal toxicity of a chemical and most of the determination methods are open to personal errors, video tracking methods have become very important tools for obtaining accurate results. In this respect, an example acute toxicity test method with detection of sublethal behavior was developed using video tracking methods. According to the results, the method was able to accurately detect the number of alive nauplii at acute toxicity end points, the mean velocity of individuals or population and paths traveled by each individual.

The results obtained from field tests showed that marine plant extract containing paints were not durable as long as other paint formulations. However, comparable results were obtained with zosteric acid containing paints when compared to diuron, irgarol and commercial AF paint. In the first antifouling performance evaluation period, only micro-slime layer was observed on most of the tested panels but in the second period tube worms and algal growth was also present. Although it was not better than commercial AF paint, zosteric acid can be used as co-biocide or it can be modified to obtain more effective antifouling agent. Therefore, synthesized zosteric acid could be an eco-friendly alternative to booster biocides like diuron and irgarol. In conclusion, zosteric acid could be used in rosin based self-polishing antifouling

paints not only solely but also as co-biocide or it could be modified to provide prolonged protection from fouling organisms.

REFERENCES

Abarzua, S. & Jakubowski, S. (1995). Biotechnological investigation for the prevention of biofouling. I. Biological and biochemical principles for the prevention of biofouling. *Marine Ecology Progress Series 123*, 301-312.

Advisory Committee on Pesticides. (2000). *In: Minutes of the 278th Meeting of the Advisory Committee on Pesticides*.

Alexandratos, S.D. (1999). Synthesis and purification of zosteric acid. *US Patent* (5990336).

Almeida, E., Diamantino, T.C., & Sousa, O. (2007). Marine paints: the particular case of antifouling paints. *Progress in Organic Coatings 59*, 2-20.

Arimura, H., Hiyoshi, S., Nakamura, N., & Tsuboi, M. (2004). (Poly)oxyalkylene block silyl ester copolymer, antifouling coating composition, antifouling coating formed from antifouling coating composition, antifouling method using antifouling coating composition and hull or underwater structure covered with antifouling coating. *US Patent* (6828030).

Alyuruk, H., Doner, E., Karabay, Z., & Cavas, L. (2010). Antifouling Performances and Acute Toxicities of Eco-Friendly Biocides. *Hacettepe Journal of Biology & Chemistry 38* (4), 277-286.

Alzieu, C. (1991). Environmental problems caused by TBT in France: assessment, regulations, prospects. *Marine Environmental Research 32*, 7–17.

Bailey, S.K. & Davies, I.M. (1991). Continuing impact of TBT, previously used in mariculture, on dogwhelk (*Nucella lapillus* L.) populations in a Scottish Sea Loch. *Marine Environmental Research 32*, 187-196.

Barahona, M.V. & Sánchez-Fortún, S. (1999). Toxicity of carbamates to the brine shrimp *Artemia salina* and the effect of atropine, BW284c51, iso-OMPA and 2-PAM on carbaryl toxicity. *Environmental Pollution 104*, 469-476.

Barbier, P., Guise, S., Huitorel, P., Amade, P., Pesando, D., Briand, C., & Peyrot, V. (2001). Caulerpenyne from *Caulerpa taxifolia* has an antiproliferative activity on tumor cell line SK-N-SH and modifies the microtubule network. *Life Sciences 70*, 415–429.

Bartolomé, M.C. & Sánchez-Fortún, S. (2005). Effects of selected biocides used in the disinfection of cooling towers on toxicity and bioaccumulation in *Artemia* larvae. *Environmental Toxicology and Chemistry 24*, 3137-3142.

Basheer, C., Tan, K.S., & Lee, H.K. (2002). Organotin and Irgarol 1051 contamination in Singapore coastal waters. *Marine Pollution Bulletin 44,* 697-703.

Bellas, J. (2006). Comparative toxicity of alternative antifouling biocides on embryos and larvae of marine invertebrates. *Science of the Total Environment 367*, 573–585.

Bellotti, N., del Amo, B., & Romagnoli, R. (2012). Taratannin a natural product with antifouling coating application. *Progress in Organic Coatings 74* (3), 411-417.

Blustein, G., Pérez, M., García, M., Stupak, M., & Cerruti, C. (2009). Reversible effect of potassium sorbate on *Balanus amphitrite* larvae. Potential use as antifoulant. *Biofouling 25*, 573-580.

Boudouresque, C.F., Lemée, R., Mari, X., & Meinesz, A. (1996). The invasive alga *Caulerpa taxifolia* is not a suitable diet for the sea urchin *Paracentrotus lividus*. *Aquatic Botany 53*, 245-250.

Boxall, A.B.A., Comber S.D., Conrad A.U., Howcroft J., & Zaman N. (2000). Inputs, monitoring and fate modeling of antifouling biocides in UK estuaries. *Marine Pollution Bulletin 40*, 898-905.

Brix, K., Gerdes, R., Adams, W., & Grosell, M. (2006). Effects of Copper, Cadmium, and Zinc on the Hatching Success of Brine Shrimp (*Artemia franciscana*). *Archives of Environmental Contamination and Toxicology 51*, 580-583.

Bryan, G.W., Gibbs, P.E., Burt, G.R., & Hummerstone, L.G. (1987). The effects of tributyl tin (TBT) accumulation on adult dogwhelk, *Nucella lapillus*: Long term field and laboratory experiments. *Journal of Marine Biological Association of the U.K. 67*, 525-544.

Caldwell, G.S., Bentley, M.G., & Olive, P.J.W. (2003). The use of a brine shrimp (*Artemia salina*) bioassay to assess the toxicity of diatom extracts and short chain aldehydes. *Toxicon 42*, 301-306.

Callow, M.E. & Callow, J.A. (1998). Attachment of zoospores of the fouling alga Enteromorpha in the presence of zosteric acid. *Biofouling 13*, 87-95.

Callow, M.E. & Fletcher, R.L. (1994). The influence of low surface energy materials on bioadhesion - a review. *International Biodeterioration & Biodegradation 34*, 333-348.

Castrisi-Catharios J., Bourdaniotis N., & Persoone G. (2007). A new simple method with high precision for determining the toxicity of antifouling paints on brine shrimp larvae (Artemia): First results. *Chemosphere 67*, 1127-1132.

Cavas, L., Baskin, Y., Yurdakoc, K., & Olgun, N. (2006). Antiproliferative and newly attributed apoptotic activities from an invasive marine alga: *Caulerpa racemosa* var. *cylindracea*. *Journal of Experimental Marine Biology and Ecology 339*, 111-119.

Chesworth, J.C., Donkin, M.E., & Brown, M.T. (2004). The interactive effects of the antifouling herbicides Irgarol 1051 and Diuron on the seagrass *Zostera marina* (L.). *Aquatic Toxicology 66*, 293-305.

Chiou, S.Y., Lai, G.W., Tsai, Y.H., Lee, Y.R., Lin, L.Y., & Lin, G.L. (2005). Kinetics and mechanisms of acetylcholinesterase and butyrylcholinesterase inhibition by cardiovascular drugs and benzodiazepines. *Journal of the Chinese Chemical Society 52*, 843-848.

Ciba Geigy. (1995). *Irgarol 1051 Material Safety Data Sheet*, 6389501. Basel, Switzerland: Additives Division.

Clare, A.S. (1996). Marine natural product antifoulants: status and potential. *Biofouling 9*, 211-229.

Clare, A.S., Rittschof, D., Gerhart, D.J., & Maki, J.S. (1992). Molecular approaches to nontoxic antifouling. *Invertebrate Reproduction and Development 22*, 67-76.

dan Hartog, C. & Kuo, J. (2006). Taxonomy and Biogeography of Seagrasses. In A.W.D. Larkum, R.J. Orth, & C.M. Duarte (Eds.). *Seagrasses: Biology, Ecology and Conservation* (1st Ed.) (1-23) Dordrecht, Springer.

Ellman, G.L., Courtney, K.D., Andres, V., & Featherstone, R.M. (1961). A new and rapid colorimetric determination of acetylcholinesterase activity. *Biochemical Pharmacology 7*, 88-95.

Evans S.M., Kerrigan E., & Palmer N. (2000). Causes of imposex in the dogwhelk Nucella lapillus (L.) and its use as a biological indicator of tributyltin contamination. *Marine Pollution Bulletin 40*, 212-219.

Fan, T., Wang, J., Yuan, W., Zhong, Q., Shi, Y., & Cong, R. (2010). Purification and characterization of hatching enzyme from brine shrimp *Artemia salina*. *Acta Biochimica et Biophysica Sinica 42*, 165-171.

Faria, M., López, M.A., Fernández-Sanjuan, M., Lacorte, S., & Barata, C. (2010). Comparative toxicity of single and combined mixtures of selected pollutants among larval stages of the native freshwater mussels (*Unio elongatulus*) and the invasive zebra mussel (*Dreissena polymorpha*). *Science of the Total Environment 408*, 2452–2458.

Finney, DJ. (1971). *Probit Analysis*. (3rd Ed). Cambridge University Press, Cambridge, UK.

Flemming, H.C., Griebe, T., & Schaule, G. (1996). Antifouling strategies in technical systems - a short review. *Water Science and Technology 34*, 517-524.

Fonseca, M.S. & Fisher, J.S. (1986). A comparison of canopy friction and sediment movement between four species of seagrass with reference to their ecology and restoration. *Marine Ecology Progress Series 29*, 15–22.

Fonseca, M.S. (1992). A preliminary evaluation of wave attenuation by four species of seagrass. *Estuarine, Coastal and Shelf Science 35*, 565–576.

Fonseca, M.S., Zieman, J.C., Thayer, G.W., & Fisher, J.S. (1983). The role of current velocity in structuring eelgrass Zostera marina meadows. *Estuarine, Coastal and Shelf Science 17*, 367–380.

Fredette, T.J., Diaz, R., van Montfrans, J.J., & Orth, R.J. (1990). Secondary production within a seagrass bed (*Zostera marina-Ruppia maritima*) in lower Chesapeake Bay. *Estuaries 13*, 431–440.

Gadepalli, R.S.V.S., Rimoldi, J.M., Fronczek, F.R., Nillos, M., Gan, J., & Deng, X. (2007). Synthesis of Fenthion Sulfoxide and Fenoxon Sulfoxide Enantiomers: Effect of Sulfur Chirality on Acetylcholinesterase Activity. *Chemical Research in Toxicology 20*, 257-262.

Galgani, F. & Bocquene, G. (1991). Semiautomated colorimetric and enzymatic assays for aquatic organisms using microplate readers. *Water Research 25*, 147–150.

Geiger, T., Delavy, P., Hany, R., Schleuniger, J., & Zinn, M. (2004). Encapsulated Zosteric Acid Embedded in Poly[3-hydroxyalkanoate] Coatings - Protection against Biofouling. *Polymer Bulletin 52*, 65-72

Gitlitz, M.H. (1981). Recent Developments in Marine Antifouling Coatings. *Journal of Coatings Technology 53*, 46-52.

Hagger J.A., Depledge M.H., & Galloway, T.S. (2005). Toxicity of tributyltin in the marine mollusc *Mytilus edulis*. *Marine Pollution Bulletin 51*, 811-816.

Hagger J.A., Fisher A.S., Hill S.J., Depledge M.H., & Jha A.N. (2002). Genotoxic, cytotoxic and ontogenic effects of tributyltin on the marine worm, *Platynereis dumerilii* (Polychaeta: *Nereidae*). *Aquatic Toxicology 57*, 243–255.

Hall, L.W., Giddings, J.M., Soloman, K.R., & Balcomb, R. (1999). An ecological risk assessment for the use of Irgarol 1051 as an algaecide for antifoulant paints. *Critical Reviews in Toxicology 29*, 367-437.

Hansen, J.W., Udy, J.W., Perry, C.J., Dennison, W.C., & Lomstein, B.A. (2000). Effect of the seagrass *Zostera capricorni* on sediment microbial processes. *Marine Ecology Progress Series 199*, 83–96.

Heiss, W.M., Smith, A.M., & Keith, P.P. (2000). Influence of the small intertidal seagrass *Zostera novazelandica* on linearwater flow and sediment texture. *New Zealand Journal of Marine and Freshwater Research 34*, 689–694.

Hellio, C., De La Broise, D., Dufossé, L., Le Gal, Y., & Bourgougnon, N. (2001). Inhibition of marine bacteria by extracts of macroalgae: potential use for environmentally friendly antifouling paints. *Marine Environmental Research 52*, 231-247.

Holth, T.F. & Tollefsen, K.E. (2012). Acetylcholine esterase inhibitors in effluents from oil production platforms in the North Sea. *Aquatic Toxicology 112-113*, 92-98.

International Maritime Organization (2001). *International conference on the control of armful anti-fouling systems for ships, adoption of the final act of the conference and any instruments, recommendations and resolutions resulting from the work of the conference*, London, UK, pp. 15.

Jha, A.N., Hagger, J.A., & Hill, S.J. (2000). Tributyltin induces cytogenetic damage in the early life stages of the marine mussel, *Mytilus edulis*. *Environmental and Molecular Mutagenesis 35*, 343-350.

Jha, A.N., Hagger, J.A., Hill, S.J., & Depledge, M.H., (2000). Genotoxic, cytotoxic and developmental effects of tributyltin oxide (TBTO): an integrated approach to the evaluation of the relative sensitivities of two marine species. *Marine Environmental Research 50*, 565-573.

Jones, R. (2005). The ecotoxicological effects of Photosystem II herbicides on corals. *Marine Pollution Bulletin* 51, 495-506.

Jung, V., Thibaut, T., Meinesz, A., & Pohnert, G. (2002). Comparison of the wound-activated transformation of Caulerpenyne by invasive and noninvasive *Caulerpa* species of the Mediterranean. *Journal of Chemical Ecology* 28, 2091-2105.

Karabay, Z. (2011). *Antifouling performances of some eco-friendly biocides*, MSc Thesis, Department of Chemistry, The Graduate School of Natural and Applied Sciences, Dokuz Eylül University.

Kanwar, A.S. (2007). Brine shrimp (*Artemia salina*) – a model marine animal for simple and rapid biological assays. *Journal of Chinese Clinical Medicine 21* (4), 236-240.

Katranitsas, A., Castritsi-Catharios, J., & Persoone, G. (2003). The effects of a copper-based antifouling paint on mortality and enzymatic activity of a non-target marine organism. *Marine Pollution Bulletin 46*, 1491-1494.

Kem, I. (1994). Ecotoxicological evaluation of the antifouling compound 2-(tert-butylamino)-4-(cyclopropylamino)-6-(methylthio)-1,3,5-triazine, Irgarol. Supplement 2 – *Aquatic (algae) and higher plant tests*, National Chemicals Inspectorate, Solna, Sweden.

Key, P.B., Chung, K.W., Hoguet, J., Sapozhnikova, Y., & Fulton, M.H. (2008). Effects of the anti-fouling herbicide Irgarol 1051 on two life stages of the grass shrimp, *Palaemonetes pugio*. *Journal of Environmental Science and Health, Part B 43*, 50-55.

Key, P.B., Hoguet, J., Chung, K.W., Venturella, J.J., Pennington, P.L., & Fulton, M.H. (2009). Lethal and sublethal effects of simvastatin, irgarol, and PBDE-47 on the estuarine fish, *Fundulus heteroclitus*, *Journal of Environmental Science and Health, Part B 44*, 379-382.

Kiil, S., Weinell, C.E., Pedersen, M.S., & Dam-Johansen, K. (2001). Analysis of self-polishing antifouling paints using rotary experiments and mathematical modeling. *Industrial & Engineering Chemistry Research 40*, 3906-3920.

Klein, J., & Verlaque, M. (2008). The *Caulerpa racemosa* invasion: A critical review. *Marine Pollution Bulletin 56*, 205-225.

Konstantinou, I.K, & Albanis, T.A. (2004). Worldwide occurrence and effects of antifouling paint booster biocides in the aquatic environment: a review. *Environment International 30*, 235-248.

Kontiza, I., Vagias, C., Jakupovic, J., Moreau, D., Roussakis, C., Roussis, V. (2005). Cymodienol and cymodiene: new cytotoxic diarylheptanoids from the sea grass *Cymodocea nodosa*. *Tetrahedron Letters 46*, 2845-2847.

Koutsaftis, A. & Aoyama, I. (2008). Toxicity of Diuron and copper pyrithione on the brine shrimp, *Artemia franciscana*: The effects of temperature and salinity. *Journal of Environmental Science and Health, Part A 43*, 1581-1585.

Koutsaftis, A., & Aoyama, I. (2007). Toxicity of four antifouling biocides and their mixtures on the brine shrimp *Artemia salina*. *Science of the Total Environment 387*, 166-174.

Lam, K.H., Cai, Z., Wai, H.Y., Tsang, V.W.H., Lam, M.H.W., Cheung, R.Y.H., Yu, H.X. & Lam, P.K.S. (2005). Identification of a new Irgarol-1051 related s-triazine species in coastal waters. *Environmental Pollution 136*, 221-230.

Lamoree, M.H., Swart, S.P., van der Horst, A., & van Hattum, B. (2002). Determination of diuron and the antifouling paint biocide Irgarol 1051 in Dutch marinas and coastal waters. *Journal of Chromatography A 970*, 183 – 190.

Lau, M.C., Chan, K.M., Leung, K.M.Y., Luan, T.G., Yang, M.S., & Qiu, J.W. (2007). Acute and chronic toxicities of tributyltin to various life stages of the marine polychaete *Hydroides elegans*. *Chemosphere 69*, 135-144.

Lewan, L., Anderson, M., & Morales, P.G. (1992). The use of *Artemia salina* in toxicity testing. *Alternatives to Laboratory Animals 20*, 297-301.

Liu, D., Maguire, R.J., Lau, Y.L., Pacepavicius, G.J., Okamura, H., & Aoyama, I. (1997). Transformation of the new antifouling compound Irgarol 1051 by *Phanerochaete chrysosporium*. *Water Research 31* (9), 2363-2369.

Liu, D., Pacepavicius, G.J., Maguire, R.J., Lau, Y.L., Okamura, H., & Aoyama, I. (1999). Mercuric chloride catalyzed hydrolysis of the new antifouling compound Irgarol 1051. *Water Research 33* (1), 155-163.

Liu, H.X., Yi, M.Q., Shi, X.Y., Liang, P., & Gao, X.W. (2007). Substrate specificity of brain acetylcholinesterase and its sensitivity to carbamate insecticides in *Carassius auratus*. *Fish Physiology and Biochemistry* 33, 29-34.

Löschau, M. & Krätke, R. (2005). Efficacy and toxicity of self-polishing biocide-free antifouling paints. *Environmental Pollution 138*, 260-267.

McConnell, O.J., Hughes, P.A., Targett, N.M., & Daley, J. (1982). Effects of secondary metabolites from marine algae on feeding by the sea urchin, *Lytechinus variegates*. *Journal of Chemical Ecology 8*, 1437-1453, 1982.

Micael, J., Reis-Henriques, M.A., Carvalho, A.P., & Santos, M.M. (2007). Genotoxic effects of binary mixtures of xenoandrogens (tributyltin, triphenyltin) and a xenoestrogen (ethinylestradiol) in a partial life-cycle test with Zebrafish (*Danio rerio*). *Environment International 33*, 1035-1039.

Milne, A. & Hails, G. (1977). Marine Paint. *Patent GB* (1 457 590).

Moore, K.A., & Short, F.T. (2006). Zostera: Biology, Ecology, and Management. In A.W.D. Larkum, R.J. Orth, & C.M. Duarte (Eds.). *Seagrasses: Biology, Ecology and Conservation* (1st Ed.) (361-386) Dordrecht, Springer.

Moreland, D.E. (1980). Mechanisms of action of herbicides. *Annual Review of Plant Physiology 31*, 597-638.

Nelson, D.L. & Cox, M.M. (2008). *Lehninger Principles of Biochemistry*. W.H. Freeman and Company, New York, pp. 201-204.

Nicoletti, E., Della Pieta, F., Calderone, V., Bandecchi, P., Pistello, M., Morelli, I., & Cinelli, F. (1999). Antiviral properties of a crude extract from a green alga *Caulerpa taxifolia* (Vahl) C-Agardh. *Phytotherapy Research 13*, 245–247.

Nunes, B.S., Carvalho, F.D., Guilhermino, L.M., & Van Stappen, G. (2006). Use of the genus *Artemia* in ecotoxicity testing. *Environmental Pollution 144*, 453-462.

Okamura, H., Aoyama, I., Liu, D., Maguire, R.J., Pacepavicius, G.J., & Lau, Y.L. (2000). Fate and ecotoxicity of the new antifouling compound Irgarol 1051 in the aquatic environment. *Water Research 34*, 3523-3530.

Okamura, H., Aoyama, I., Liu, D., Maguire, R.J., Pacepavicius, G.J., & Lau, Y.L. (1999). Photodegradation of Irgarol 1051 in water. *Journal of Environmental Science and Health B 34* (2), 225-238

Olsen, S.M. (2009). *Controlled release of environmentally friendly antifouling agents from marine coatings*, Ph.D. Thesis, Department of Chemical and Biochemical Engineering, Technical University of Denmark.

Omae I. (2003a). Organotin antifouling paints and their alternatives. *Applied Organometallic Chemistry 17*, 81–105.

Omae I. (2003b). General aspects of tin-free antifouling paints. *Chemical Reviews 103*, 3431-3448.

Panagoula, B., Panayiota, M., & Iliopoulou-Georgudaki, J. (2002). Acute Toxicity of TBT and Irgarol in *Artemia salina*. *International Journal of Toxicology* 21, 231-233.

Pérez, M., Blustein, G., Garcia, M., Amo, B., & Stupak, M. (2006). Cupric tannate: A low copper content antifouling pigment. *Progress in Organic Coatings 55*, 311-315.

Pérez, M., Garcia, M., Blustein, G. & Stupak, M. (2007). Tannin and tannate from the quebracho tree: an eco-friendly alternative for controlling marine biofouling. *Biofouling 23*, 151-159.

Perina, F.C., Abessa, D.M.S., Pinho, G.L.L., & Fillmann, G. (2011). Comparative toxicity of antifouling compounds on the development of sea urchin. *Ecotoxicology 20*, 1870–1880.

Pietsch, M. & Gutschow, M. (2005). Synthesis of tricyclic 1,3-oxazin-4-ones and kinetic analysis of cholesterol esterase and acetylcholinesterase inhibition. *Journal of Medicinal Chemistry 48*, 8270-8288.

Ram, J.L., Purohit, S., Newby, B.Z., Cutright, T.J. (2012). Evaluation of the natural product antifoulant, zosteric acid, for preventing the attachment of quagga mussels – a preliminary study. *Natural Product Research 26*, 580-584.

Rasmussen, E. (1977). The wasting disease of eelgrass (*Zostera marina*) and its effects on environmental factors and fauna. In: C.P. McRoy & C. Helfferich (Eds.). *Seagrass Ecosystems: A Scientific Perspective* (1–52) Marcel Dekker, New York.

Shim, W.J., Oh, J.R., Kahng, S.H., Shim, J.H., & Lee, S.H. (1998). Accumulation of Tributyl- and Triphenyltin Compounds in Pacific Oyster, *Crassostrea gigas*, from the Chinhae Bay System, Korea. *Archives of Environmental Contamination and Toxicology 35*, 41–47.

Shin, H.W., Smith, C.M., & Haslbeck, E.G. (2001). Minimum effective release rate of antifoulants. 1. Effects of Zosteric acid at Ford Island, Hawai'i (USA). *Journal of Environmental Biology 22*, 243-250.

Short, F.T. (1987). Effects of sediment nutrients on seagrasses: Literature review and mesocosm experiments. *Aquatic Botany 27*, 41–57.

Smyrniotopoulos, V., Abatis, D., Tziveleka, L.A., Tsitsimpikou, C., Roussis, V., Loukis, A., & Vagias, C. (2003). Acetylene Sesquiterpenoid Esters from the Green Alga *Caulerpa prolifera*. *Journal of Natural Products 66*, 21–24.

Stanley, M.S., Callow, M.E., Perry, R., Alberte, R.S., Smith, R., & Callow, J.A. (2002). Inhibition of fungal spore adhesion by zosteric acid as the basis for a novel, nontoxic crop protection technology. *Phytopathology 92*, 378-383.

Stupak, M.E., García, M.T., & Pérez, M.C. (2003). Non-toxic alternative compounds for marine antifouling paints. *International Biodeterioration & Biodegradation 52*, 49-52.

Thomas, K.V., Fileman, T.W., Readman, J.W., & Waldock, M.J. (2001). Antifouling paint booster herbicides in the UK coastal environment and the potential risks of biological effects. *Marine Pollution Bulletin 42*, 677-688.

Thomas, K.V., McHugh, M., Hilton, M., & Waldock, M. (2002). Antifouling paint booster biocides in UK coastal waters: inputs, occurrence and environmental fate. *Science of the Total Environment 293*, 117–127.

Thomas, K.V., McHugh, M., Hilton, M., & Waldock, M. (2003). Increased persistence of antifouling paint biocides when associated with paint particles. *Environmental Pollution 123*, 153 – 61.

Tischer, W., & Strotmann, H. (1977). Relationship between inhibitor binding of chloroplasts and inhibition of photosynthetic electron transport. *Biochimica et Biophysica Acta 460*, 113-125.

Todd, J.S., Zimmerman, R.C., Crews, P., & Alberte, R.S. (1993). The antifouling activity of natural and synthetic phenolic acid sulphate esters. *Phytochemistry 34*, 401-404.

Tsunemasa, N. & Okamura, H. (2011). Effects of Organotin Alternative Antifoulants on Oyster Embryo. *Archives of Environmental Contamination and Toxicology* 61, 128–134.

Villa, F., Albanese, D., Giussani, B., Stewart, P.S., Daffonchio, D., & Cappitelli, F. (2010). Hindering biofilm formation with zosteric acid. *Biofouling 26* (6), 739-752.

Voulvoulis, N., Scrimshaw, M.D. & Lester, J.N. (2002). Partitioning of selected antifouling biocides in the aquatic environment. *Marine Environmental Research 53*, 1-16.

Voulvoulis, N., Scrimshaw, M.D., & Lester, J.N. (1999). Alternative antifouling biocides. *Applied Organometallic Chemistry 13*, 135-143.

Wahl, M. (1989). Marine epibiosis. I. Fouling and antifouling: some basic aspects. *Marine Ecology Progress Series 58*, 175-189.

Wang, H., Li, Y., Huang, H., Xu, X., & Wang, Y. (2011). Toxicity evaluation of single and mixed antifouling biocides using the *Strongylocentrotus intermedius* sea urchin embryo test. *Environmental Toxicology and Chemistry 30*, 692–703.

Yebra, D.M., Kiil, S., & Dam-Johansen, K. (2004). Antifouling technology past, present and future steps towards efficient and environmentally friendly antifouling coatings. *Progress in Organic Coatings 50*, 75-104.

Yonehara, Y. (2000). Recent topics on marine antifouling coatings. *Bulletin of the Society of Sea Water Science, Japan 54*, 7–12.

Zahuranec, B.J. (1991). *The United States Navy and research on bioactive substances from the sea*, In Thompson MF, 1991.

ABBREVIATIONS

^{1}H-NMR - Proton Nuclear Magnetic Resonance Spectroscopy

AChE – Acetylcholine esterase

AF - Antifouling

ATC – S-acetyl thiocholine iodide

AVI - Audio Video Interleave

$CaCO_3$ – Calcium carbonate

CH_2Cl_2 – Dichloromethane

CI – Confidence Interval

CPDU - 1-(3,4-dichlorophenyl)-1,3-dimethylurea

CPE - Caulerpa prolifera extract

CT - Cupric tannate

Cu2O - Copper(I) oxide

CuP – Copper pyrithione

CYN – caulerpenyne

DCPMU - 1-(3,4-dichlorophenyl)urea

DCPU - 1-(3,4-dichlorophenyl)-3-methylurea

DMF – *N,N*-dimethyl formamide

DMSO – Dimethyl sulfoxide

DTNB - 5,5'-Dithiobis(2-nitrobenzoic acid)

EC_{50} – 50% Effective concentration

FT-IR – Fourier Transform Infrared Spectroscopy

HP – Hatching percentage

IC_{50} – 50% Inhibitory concentration

IMO – International Maritime Organisation

J – Coupling constant

K_i – Inhibition constant

K_m – Michaelis constant

KS - Potassium sorbate

MMA – Methyl methacrylate

NaCl – Sodium chloride

$NaHCO_3$ – Sodium bicarbonate

NaOH – Sodium hydroxide

PB – Phosphate buffer

p-CA – Trans-4-hydroxy cinnamic acid (p-coumaric acid)

PDC – Potassium dichromate

$Py{\bullet}SO_3$ – Sulfurtrioxide pyridine complex

QB – Quinone binding site

R_f – Retention factor

SEM - Standard Error of Mean

SPC - Self-polishing copolymer

TA - Tannic acid

TBT - Tributyltin

TBTM – Tributyltin methacrylate

TCMS - 2,3,5,6-tetrachloro-4-(methylsulphonyl)pyridine

TCMTB - 1,3-benzothiazol-2-ylsulfanylmethyl thiocyanate

TLC – Thin layer chromatography

TNB - 5-thio-2-nitrobenzoic acid

V_{max} – Maximum velocity of enzymatic reaction

ZA – Zosteric acid

ZnO – Zinc(II) oxide

ZnP – Zinc pyrithione

δ – Chemical shift